Mississippi Valley Division,
Regional Planning and Environment Division South

South Central Coast Louisiana

Feasibility Study with Integrated Environmental Impact Statement

Hurricane Ike flooding in Delcambre, Louisiana 2008.

Appendix C: Hydraulics, Hydrology & Climate Preparedness and Resilience

June 2021

CONTENTS

TABLES

FIGURES

Section 1
General

This appendix summarizes the preliminary hydrology, hydraulic, and climate change preparedness and resilience technical work completed to support the components of the South Central Coast Louisiana Integrated Feasibility Study. This report includes description of modeling tools, technical criteria, assumptions and results supporting evaluation, and comparison and selection of a recommended measure.

1.1 INTRODUCTION AND HYDRAULIC DESCRIPTION OF PROJECT AREA

The project area, illustrated in Figure C:1-1, intersects five hydrologic basins: Bayou Teche, Vermilion, Atchafalaya, Terrebonne, and Lower Grand. Bayou Teche and Vermilion can be considered two sub-basins in the combined Teche-Vermilion system. The Atchafalaya and Teche-Vermilion Basins contain the dominant hydrologic features of the project area while the western portions of the Lower Grand and Terrebonne Basins are peripherally relevant.

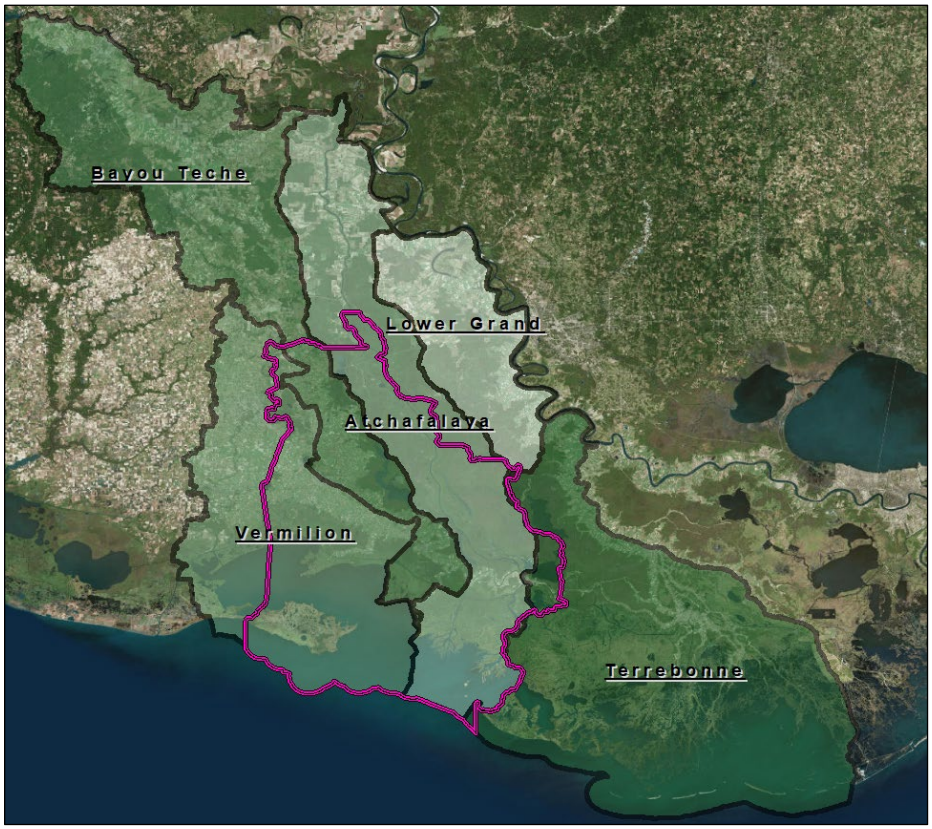

Figure C:1-1. Schematic Delineating the Individual Basin Boundaries Overlaid with the Project Area

1.1.1 Teche-Vermilion Basin

The Teche-Vermilion Basin occupies over 50 percent of the project area. The Teche sub-basin has a drainage area of 2,200 square miles spanning from the west bank of the Red River to Cote Blanche Bay. Bayou Teche (125 miles long) begins in Port Barre and drains into the lower Atchafalaya River. Bayou Teche is an ancient Mississippi River channel and the banks create a natural ridge. Residential and commercial structures largely occur on the natural ridges (Breaux Bridge, New Iberia, Franklin), as they provide natural risk reduction for frequent and low flow events. The density of structures located on the natural ridges was utilized to identify economic damage hot spots for identification of measures. Further details on economic damage hot spots are described in Appendix D: Economics Evaluation.

Inland hydraulic features include Dauterive Lake and Lake Fausse Pointe, which are hydraulically connected to Bayou Teche via the Loreauville Canal. The coastal boundary of this sub-basin includes the Gulf Intercoastal Water Ways (GIWW) until the mouth of the Charenton Drainage and Navigation Canal. The Vermilion sub-basin has a total area of 2,100 square miles that includes the West Cote Blanche and Vermilion Bays, the Vermilion River, and Marsh Island. Much of the coastal area is tidal wetland habitat, transected by the GIWW. Unique to this sub-basin are exposed salt-dome deposits: Cote Blanche Island, Weeks Island, Avery Island, and partially Lake Peigneur.

1.1.2 Atchafalaya Basin

The Atchafalaya Basin contains the Atchafalaya River (137 miles long), a large freshwater body that spans the entire project area (north to south). The basin begins at the Old River Control Structure located upstream of Simmesport and ultimately drains into the Gulf of Mexico (GOM). The Atchafalaya receives 30 percent of the latitudinal flow from the Mississippi River and Red River. Additional flow can be diverted into the Atchafalaya from the Mississippi River through the Morganza spillway. The Atchafalaya floodway, bordered by large Federal river levees, directs flow south towards the Atchafalaya Bay near Morgan City or via the Wax Lake outlet between Centerville and Calumet.

1.1.3 Terrebonne and Lower Grand

While the Terrebonne is a large basin, only the far western portion is considered in the authorization zone. The total area is 3,200 square miles and is made up of mainly tidal wetlands. These range from fresh near Bayou Lafourche to oligohaline towards the GOM. The Lower Grand Basin is contained between the east Atchafalaya levees and the west bank Mississippi levees. The main channels in this basin are the Port Allen Lock waterway and the Avoca Island cutoff. Much of the upper basin is alluvial and is heavily used for agriculture. The main hydrologic contribution of this area is as a catchment area for rainfall.

1.2 OVERVIEW OF ANALYSIS GOALS

The goals of this analysis, to hydraulically analyze major sources of flooding from riverine and storm surge events and to evaluate and compare measures carried forward into third and fourth planning iteration descriptions of measures, are presented in Appendix D: Plan Formulation and Chapter 3 of the Main Feasibility Report. The measures are examined for a range of flooding frequencies for both riverine and surge events combined with the effects of relative sea level rise in the future.

Section 2
Coastal Storm Surge Analysis

2.1 BACKGROUND

While the study area has periodically experienced localized flooding from excessive rainfall events, the primary cause of flooding events has been storm surges from hurricanes and tropical storms. Since the turn of the century, storm surges associated with four Category 2 or higher hurricanes (Lili, Rita, Gustav, and Ike) have greatly impacted the area. Structures have been frequently inundated, resulting in billions of dollars in damages to southwest coastal Louisiana. Additional details on damages from flooding is described in the Main Report, Chapter 2 Inventory and Forecast. Hurricane storm surge also causes significant, permanent damage to wetlands. Hurricane surge has formed ponds in stable, contiguous marsh areas and expanded existing, small ponds, as well as removed material in degrading marshes (Barras, 2009). Fresh and intermediate marshes appear to be more susceptible to surge impacts, as observed in Barras (2006).

2.1.1 Storms of Record

Hurricane Audrey (June 25 - 29, 1957) ranks as the 7th deadliest hurricane to strike the United States and was the deadliest natural disaster in the history of southwest Louisiana in modern record-keeping, with at least 500 deaths

(source: http://www.srh.noaa.gov/lch/?n=audrey; accessed January 7, 2016).

Hurricane Lili (September 23 - October 3, 2002) was originally a Category 4 hurricane and first made landfall near Marsh Island in Iberia Parish with maximum sustained winds of 92 mph. Highest recorded rainfall amount was about 9 inches in some parts of Louisiana.

(source: https://coast.noaa.gov/hes/docs/postStorm/Lili_%20final.pdf; accessed December 15, 2015).

Hurricane Rita (September 24 - 26, 2005), reached its peak intensity southeast of the mouth of the Mississippi River as a Category 5, and first made landfall just west of Johnson's Bayou and east of Sabine Pass at the Texas-Louisiana border as a Category 3 hurricane. Sensors recorded storm-surge water levels over 14 feet above North American Vertical Datum of 1988 (NAVD 88) at Constance Beach (LC11), Creole (LA12), and Grand Chenier (LA11), Louisiana, about 20 miles, 48 miles, and 54 miles, respectively, east of Sabine Pass, Texas. In general, storm-surge water levels increased eastward from the Sabine River into southwest Louisiana. The magnitude of the storm surge was greatest near the coast and decreased inland through the approximate

latitude of I-10, about 35 miles inland from the coast (source: http://pubs.usgs.gov/circ/1306/pdf/c1306_ch7_j.pdf; accessed December 15, 2015).

Hurricane Gustav (August 25 - September 4, 2008) made landfall near Cocodrie, Louisiana on September 1, 2008 as a strong category 2 (based on 110 mph sustained winds) and continued to move northwest, spreading hurricane force wind gusts across portions of Southeast and South Central Louisiana (http://www.srh.noaa.gov/lix/?n=gustavsummary; accessed January 26, 2016). Due to the storm making landfall east of the study area, storm surge values were only 4-5 feet across St. Mary, Iberia, and Vermilion Parishes

(http://www.srh.noaa.gov/images/lch/tropical/HPW1-SUN.pdf; accessed January 26, 2016).

Hurricane Ike (September 1-14, 2008) first made landfall near Galveston, Texas on September 13, 2008 as a Category 2 hurricane with maximum sustained winds of 110 mph

(http://www.srh.noaa.gov/hgx/?n=projects_ike08; accessed December 15, 2015).

Ike was a large hurricane with tropical-storm-force and hurricane-force winds associated at the time of its landfall extending approximately 275 miles and 120 miles from the storm center, respectively. In Louisiana, estimated wind speeds ranged from 80 mph near the Texas-Louisiana border to 50 mph in Vermilion Parish. Storm surge caused flooding in Cameron, Vermilion, and many parishes to the east, with over 9 feet stillwater levels estimated for Lake Charles

(http://www.fema.gov/media-library-data/20130726-1648-20490-1790/757_ch1_final.pdf; accessed December 15, 2015).

2.2 TIDAL PROFILE AND DATUMS

Tidal information for the area was analyzed from two sources, NOAA and CRMS. CRMS is the state funded coastwide reference monitoring system, a set of coast-wide monitoring stations. The location of the gages used are presented in Figure C:2-1. Figure C:2-2 depicts the NOAA datum info.

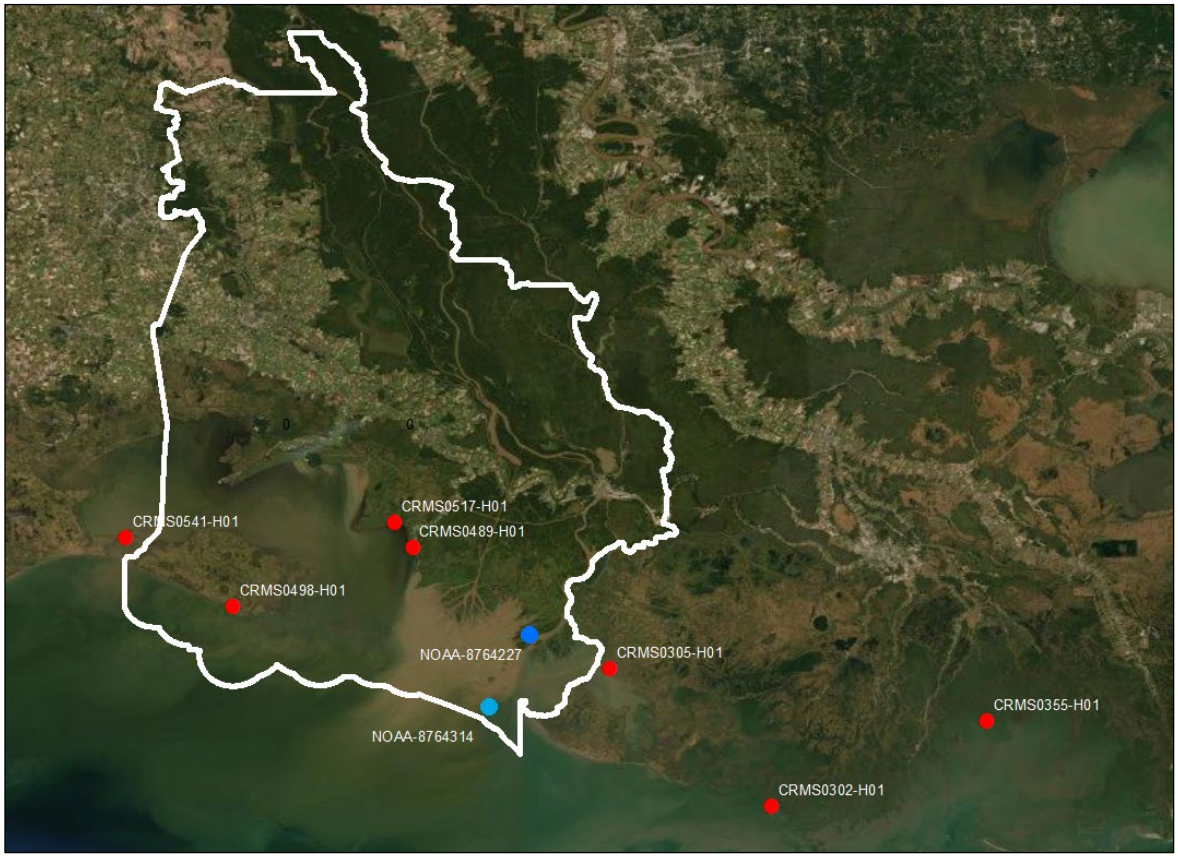

Figure C: 2-1. Locations of nearby Tidal Gages from NOAA (Blue) and CRMS (Red)

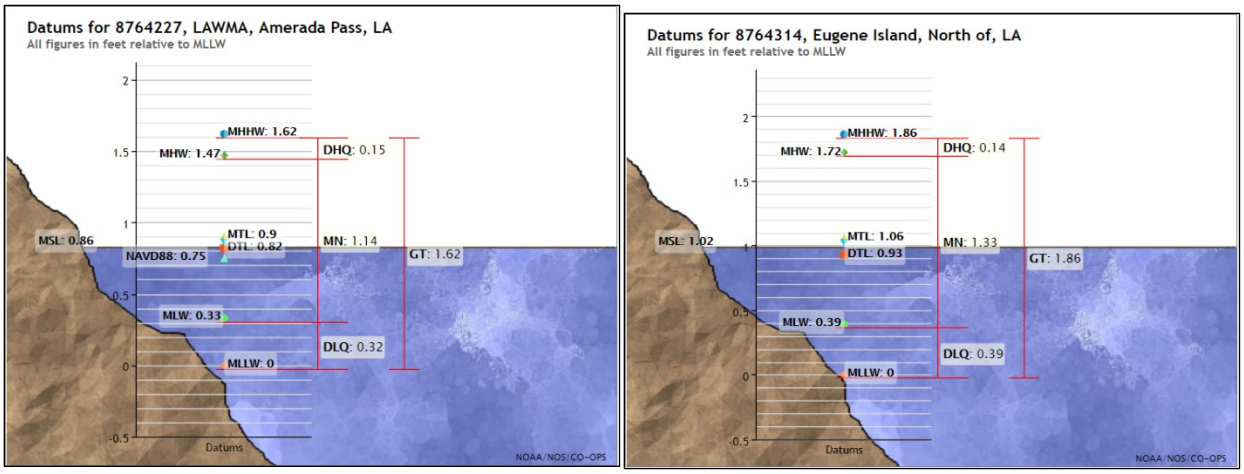

Figure C:2-2. Datum Information for NOAA Gages Relative to MLLW

The mean tidal amplitude for the NOAA gages is 0.67 foot at Eugene and 0.57 foot at Amerada Pass. The average tidal amplitude for the CRMS gages was found to be 0.7 foot. Table C:2-1 includes the locations and average tidal amplitudes of the 7 gages sampled.

Table C:2-1. Average Tidal Amplitude of the CRMS Gages

Station_Id	Lat	Lon	Avg_Amp
CRMS0302-H01	29.14783	-90.917	0.81
CRMS0305-H01	29.38895	-91.198	0.76
CRMS0355-H01	29.29663	-90.5415	0.78
CRMS0489-H01	29.59944	-91.5418	0.44
CRMS0498-H01	29.49783	-91.8543	0.38
CRMS0517-H01	29.64299	-91.573	0.82
CRMS0541-H01	29.61621	-92.0411	0.76

2.3 LACPR ADCIRC MODELING

The first phase of this study utilized the ADCIRC+STWAVE modeling performed statewide for Southern Louisiana for the Louisiana Coastal Protection and Restoration (LACPR) project. The ADCIRC model is a two-dimensional, depth-integrated, barotropic time-dependent long wave, hydrodynamic circulation model that can be used to simulate storm surge response to hurricanes and tropical storms. STWAVE is a steady-state, finite difference, spectral model based on the wave action balance equation. STWAVE is used to model nearshore wind-wave growth and propagation. As a note, after TSP the surge modeling and statistics were updated with 2017 CPRA ADCIRC+SWAN data, further detail is presented in section 2.4. Details of the LACPR model development and results can be found in the LACPR Engineering Report. (https://www.mvn.usace.army.mil/Portals/56/docs/environmental/LaCPR/HydraulicsandHydrology.pdf)

2.3.1 LACPR Statistical Data Processing

The statistics from the LACPR data set included results from 2, 1, 0.25, and 0.2 percent AEP return storms. In order to produce the requested stages for the 50, 20, 10, 5, and 0.5 percent AEP frequencies, linear interpolations were applied using the existing data. For the 0.5 percent AEP stages, the 1 percent and 0.25 percent AEP results were linearly interpolated at each data point. For the higher frequencies of 50, 20, 10, and 5 percent AEP, existing ground elevations were extracted to represent the 100 percent AEP stages. Applying this assumption, the high frequencies are linearly interpolated values between the 2 percent AEP data and the existing ground elevations for each point.

For future conditions, the only directly modeled simulations available were run with a starting Gulf of Mexico (GOM) of +1.15 feet and +5.0 feet NAVD 88 (above 1.2 feet NAVD 88). To estimate the future surge values, a linear interpolation between the +0.0 (Existing) simulations and the +5.0 simulations was applied to produce a +1.8 feet NAVD 88 data set (the intermediate 2075 relative sea level rise (RSLR) scenario). The same process to acquire the 50, 20, 10, 5, and 0.5 percent AEP returns for existing conditions was applied to the future condition data set.

The updated surge statistics from the 2017 CPRA ADCIRC+SWAN model were directly processed for the high frequency returns that were estimated by interpolation for the LACPR (as described previously). Further information on the updated data can be found in section 2.4

2.3.2 LACPR Existing Conditions Results

The existing condition results include direct output for the 2, 1, and 0.2 percent AEP statistics and the interpolated 0.5 percent AEP results, along with the estimated high frequency returns of 50, 20, 10 and 5 percent AEP. Storm sets were run with a starting GOM water surface elevation of 1.2 feet NAVD 88. The data is presented in Figures C:2-3 through C:2-10 for all points contained within the project authorization zone.

2.3.3 LACPR Future Conditions Results

The future condition results include direct output for the 2, 1, and 0.2 percent AEP statistics and the interpolated 0.5 percent AEP results along with the estimated high frequency returns of 50, 20, 10 and 5 percent AEP. The set was interpolated from the existing conditions and the +5.0 NAVD 88 output for the intermediate RSLR of +1.8 feet NAVD 88. The data is presented in Figures C:2-11 through C:2-18 for all points contained within the project authorization zone.

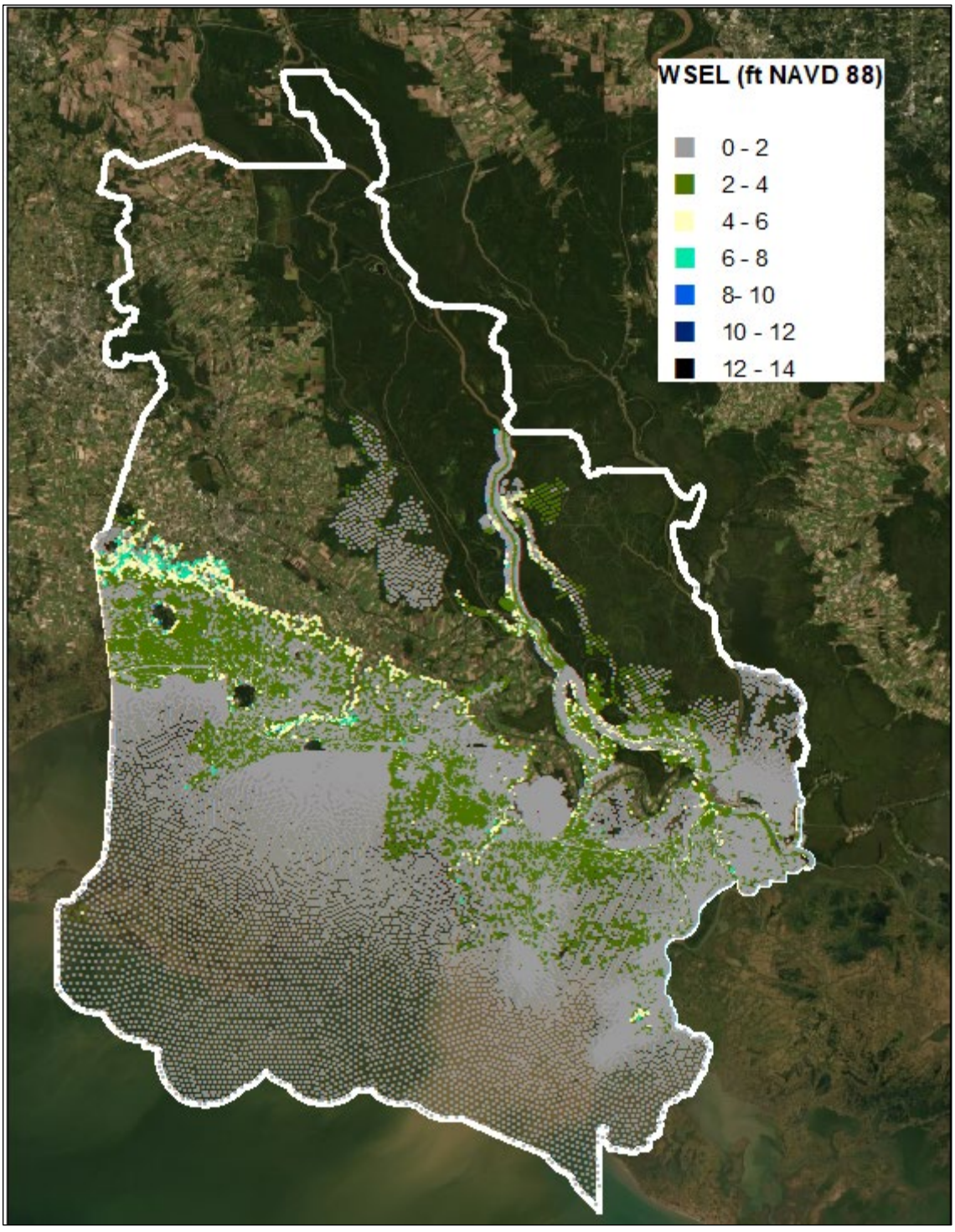

Figure C:2-3. 50% AEP Storm Existing Conditions Water Surface Elevations (ft NAVD 88)

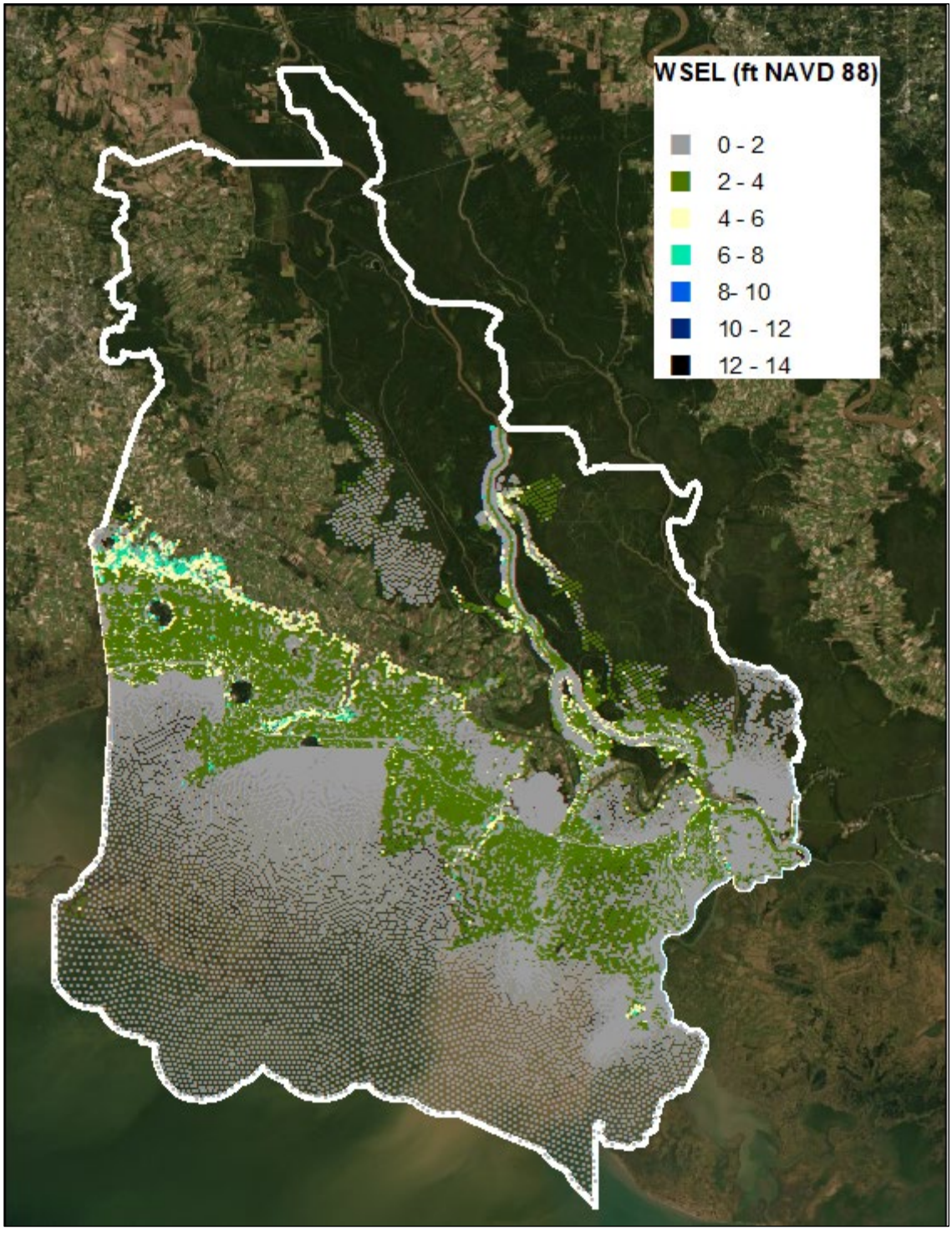

Figure C:2-4. 20% AEP Storm Existing Conditions Water Surface Elevations (ft NAVD 88)

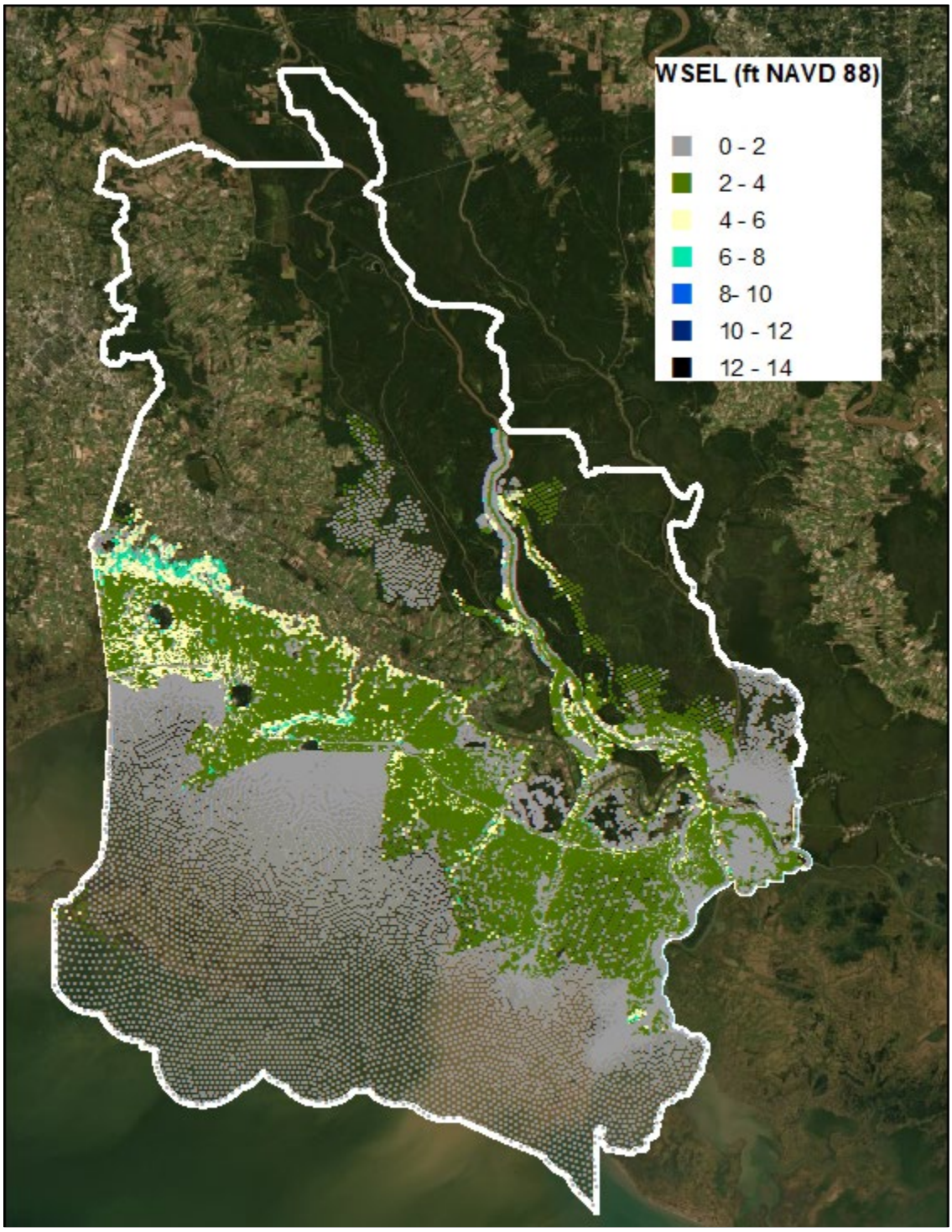

Figure C:2-5. 10% AEP Storm Existing Conditions Water Surface Elevations (ft NAVD 88)

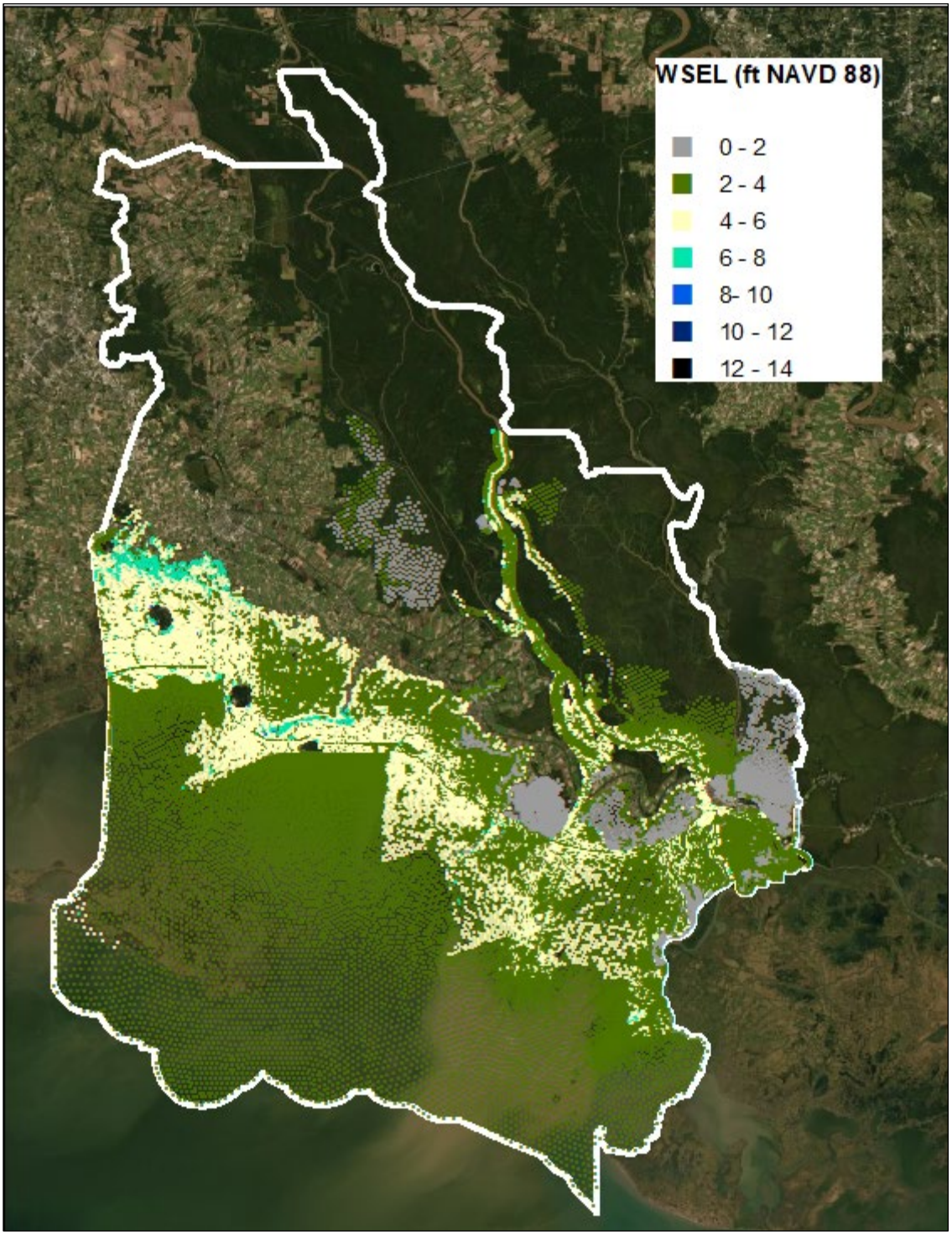

Figure C:2-6. 5% AEP Storm Existing Conditions Water Surface Elevations (ft NAVD 88)

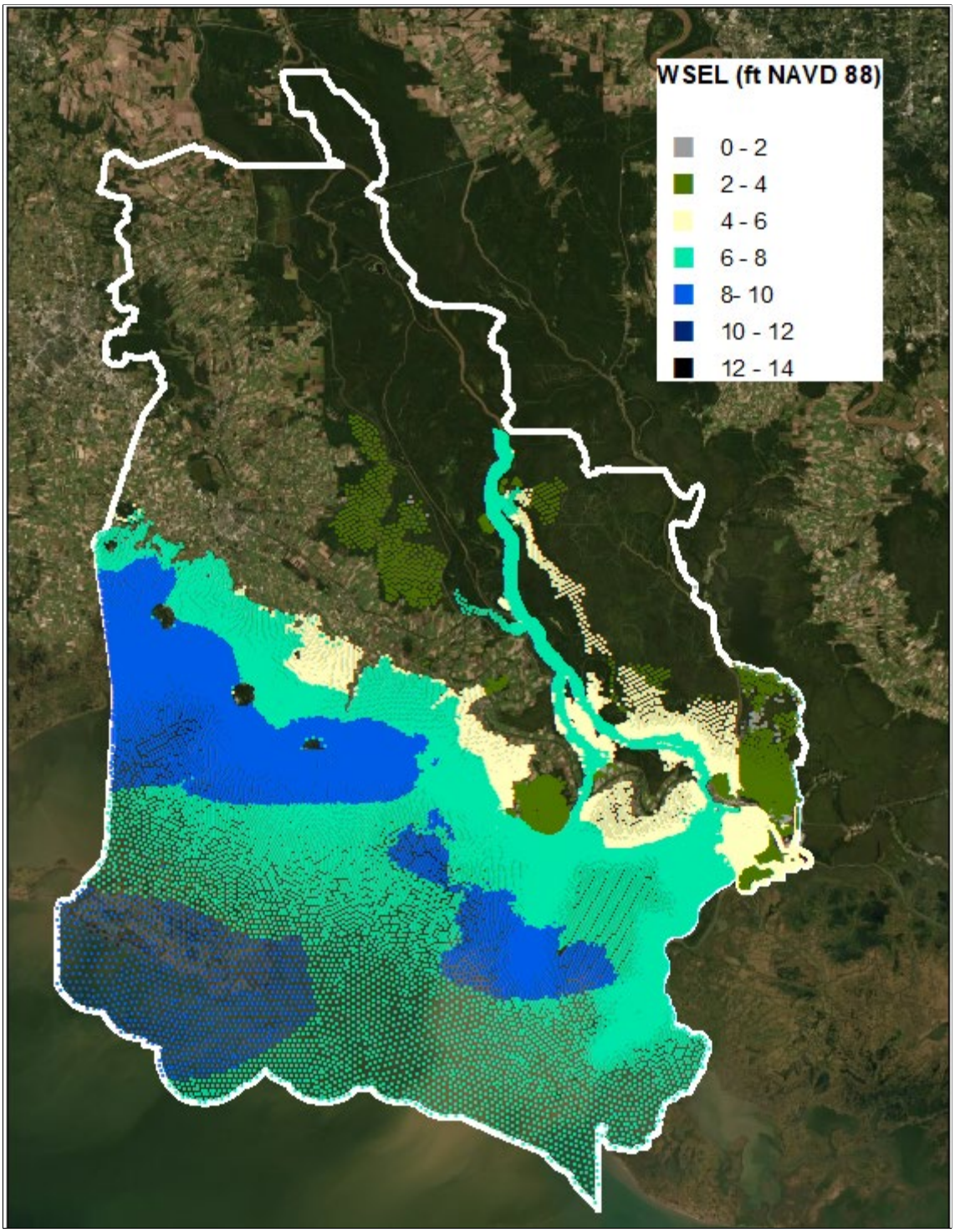

Figure C:2-7. 2% AEP Storm Existing Conditions Water Surface Elevations (ft NAVD 88)

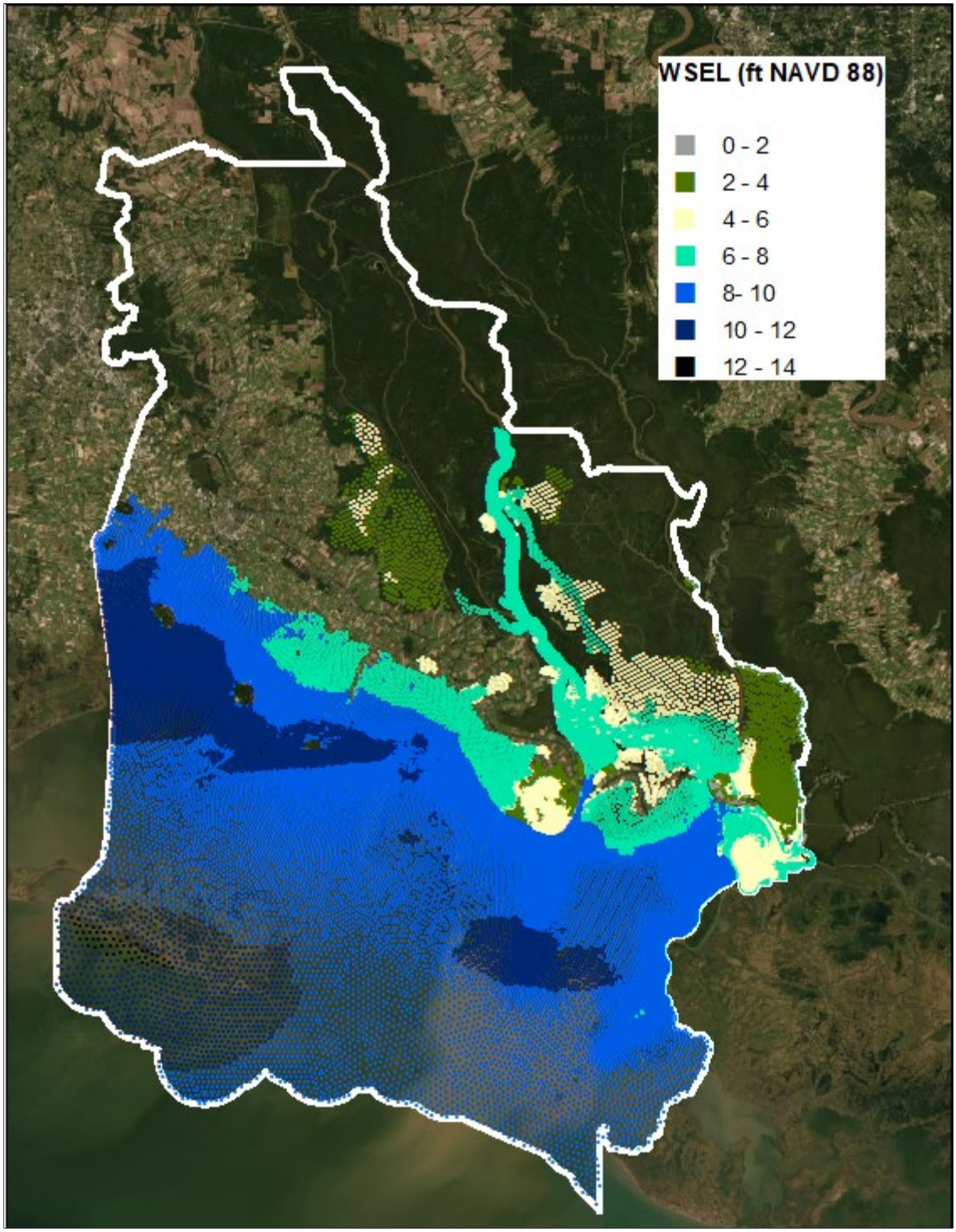

Figure C:2-8. 1% AEP Storm Existing Conditions Water Surface Elevations (ft NAVD 88)

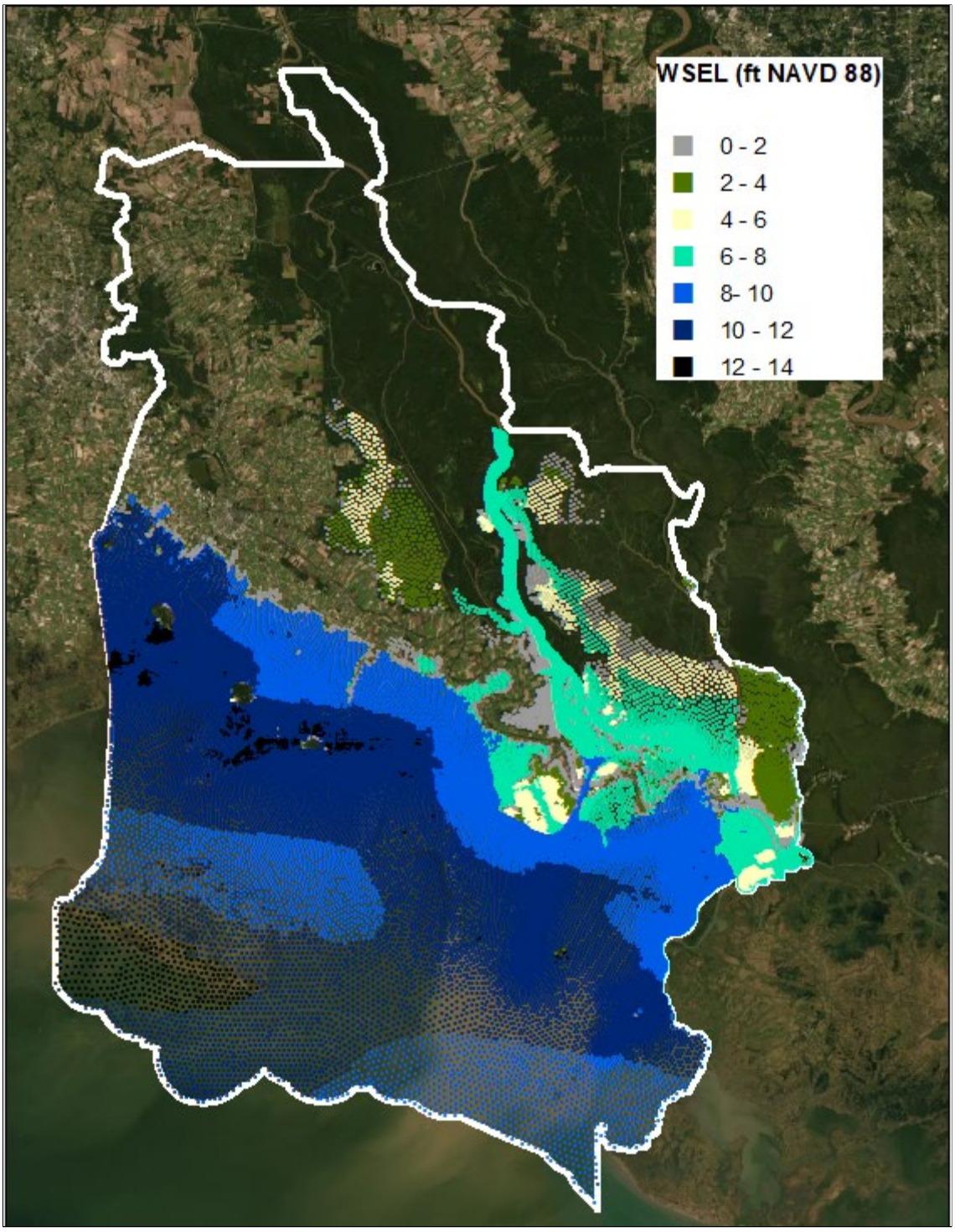

Figure 2. 0.5% AEP Storm Existing Conditions Water Surface Elevations (ft NAVD 88)

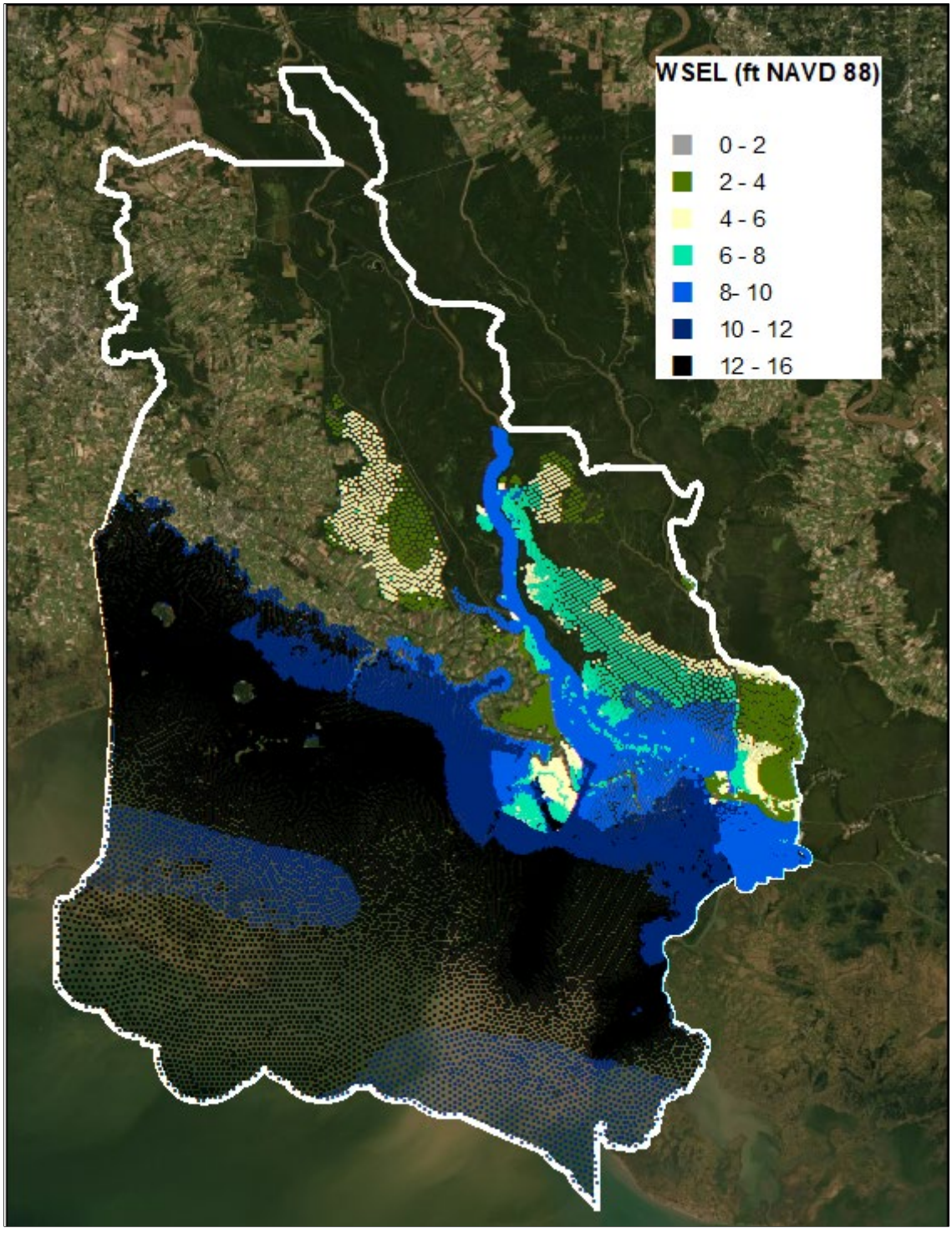

Figure C:2-10. 0.2% AEP Storm Existing Conditions Water Surface Elevations (ft NAVD 88)

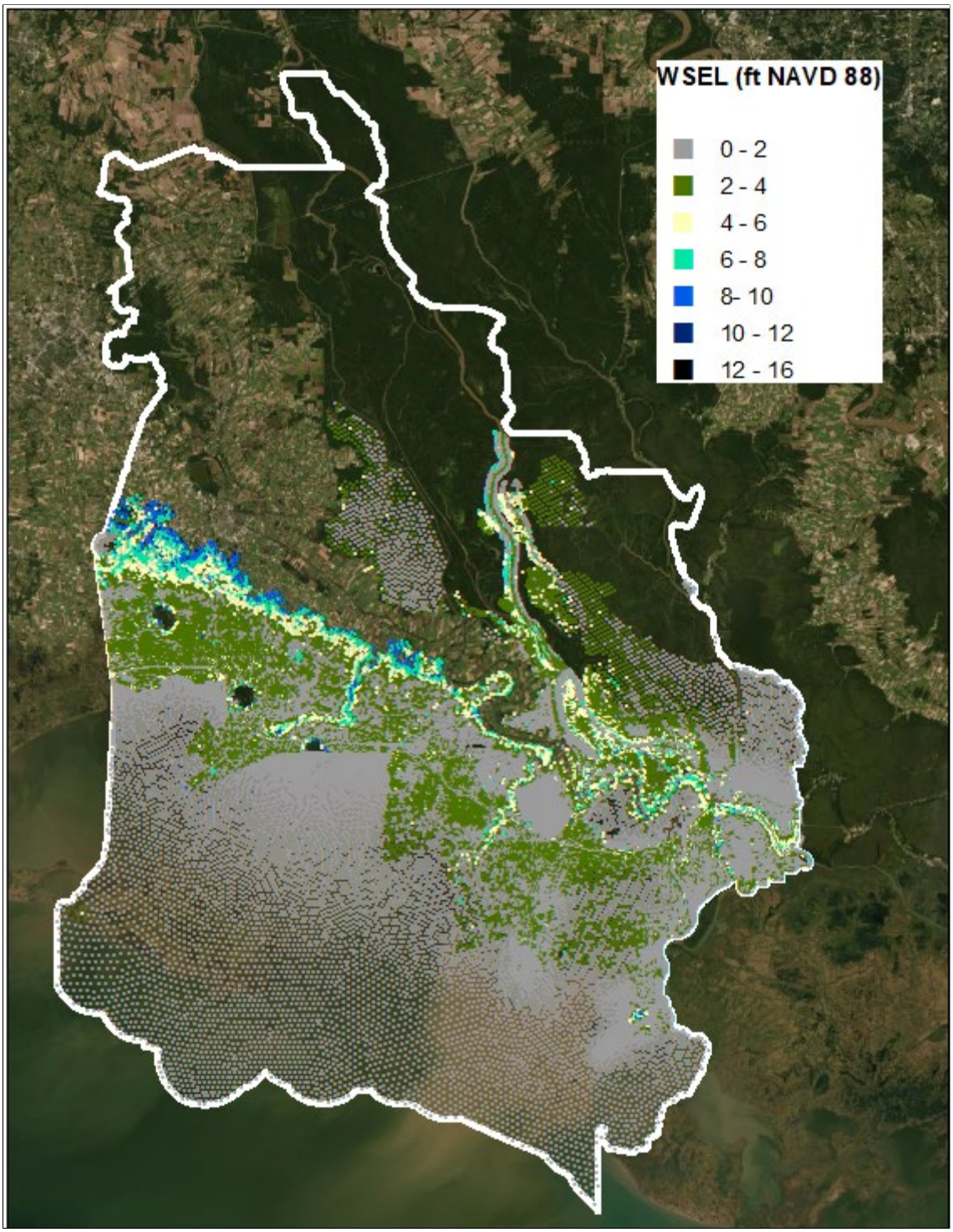

Figure C:2-11. 50% AEP Storm Future Conditions Water Surface Elevations (ft NAVD 88)

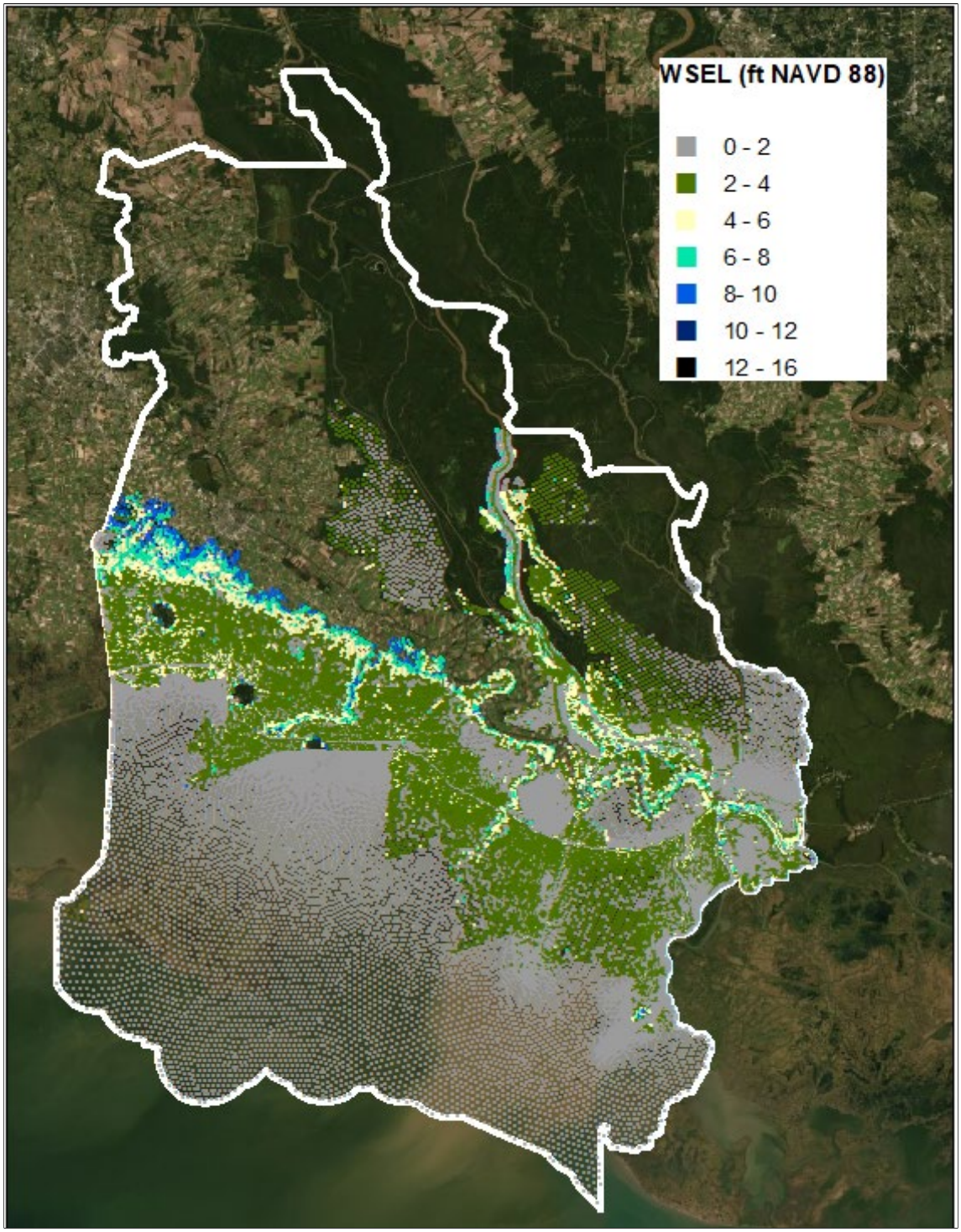

Figure C:2-12. 20% AEP Storm Future Conditions Water Surface Elevations (ft NAVD 88)

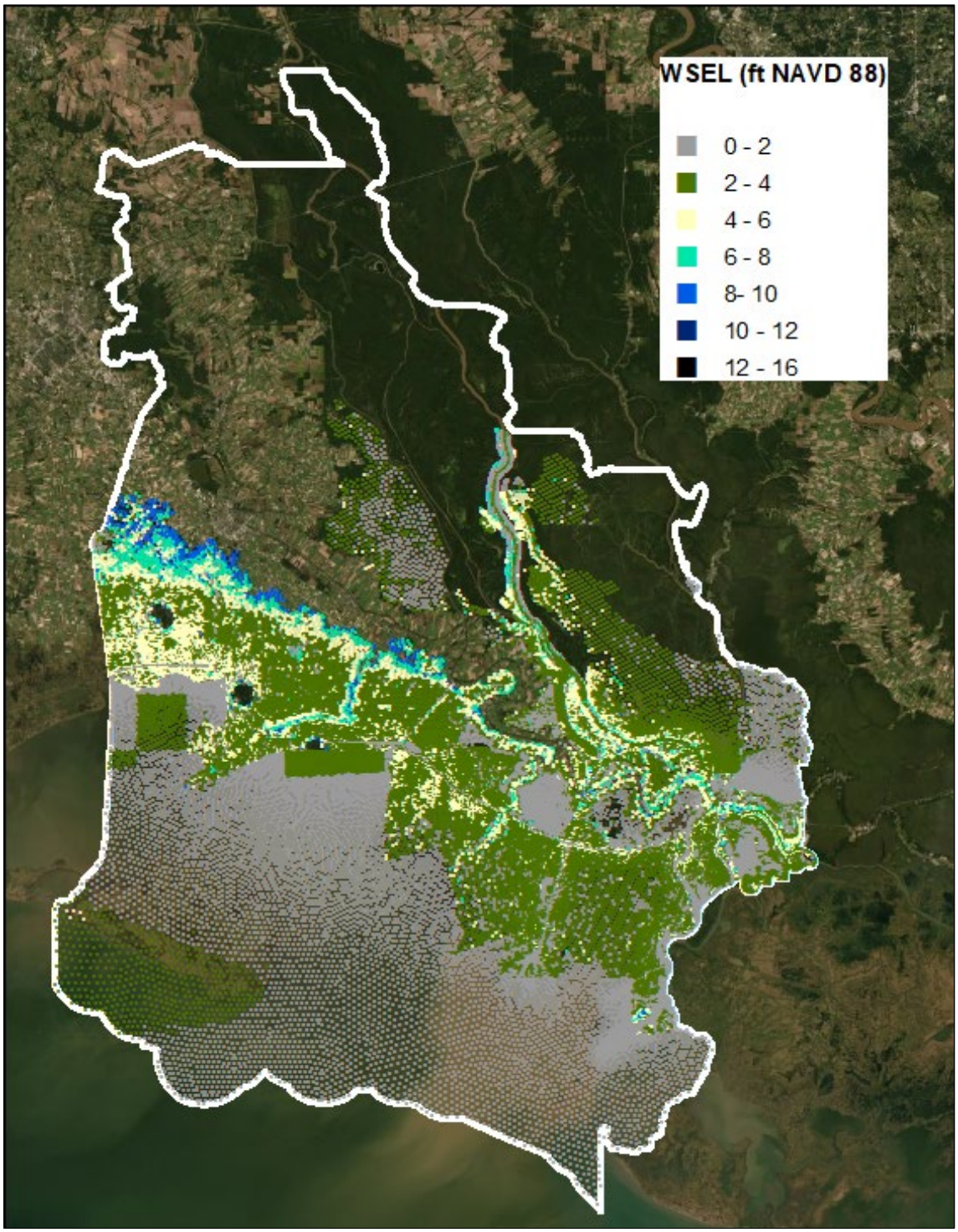

Figure C:2-13. 10% AEP Storm Future Conditions Water Surface Elevations (ft NAVD 88)

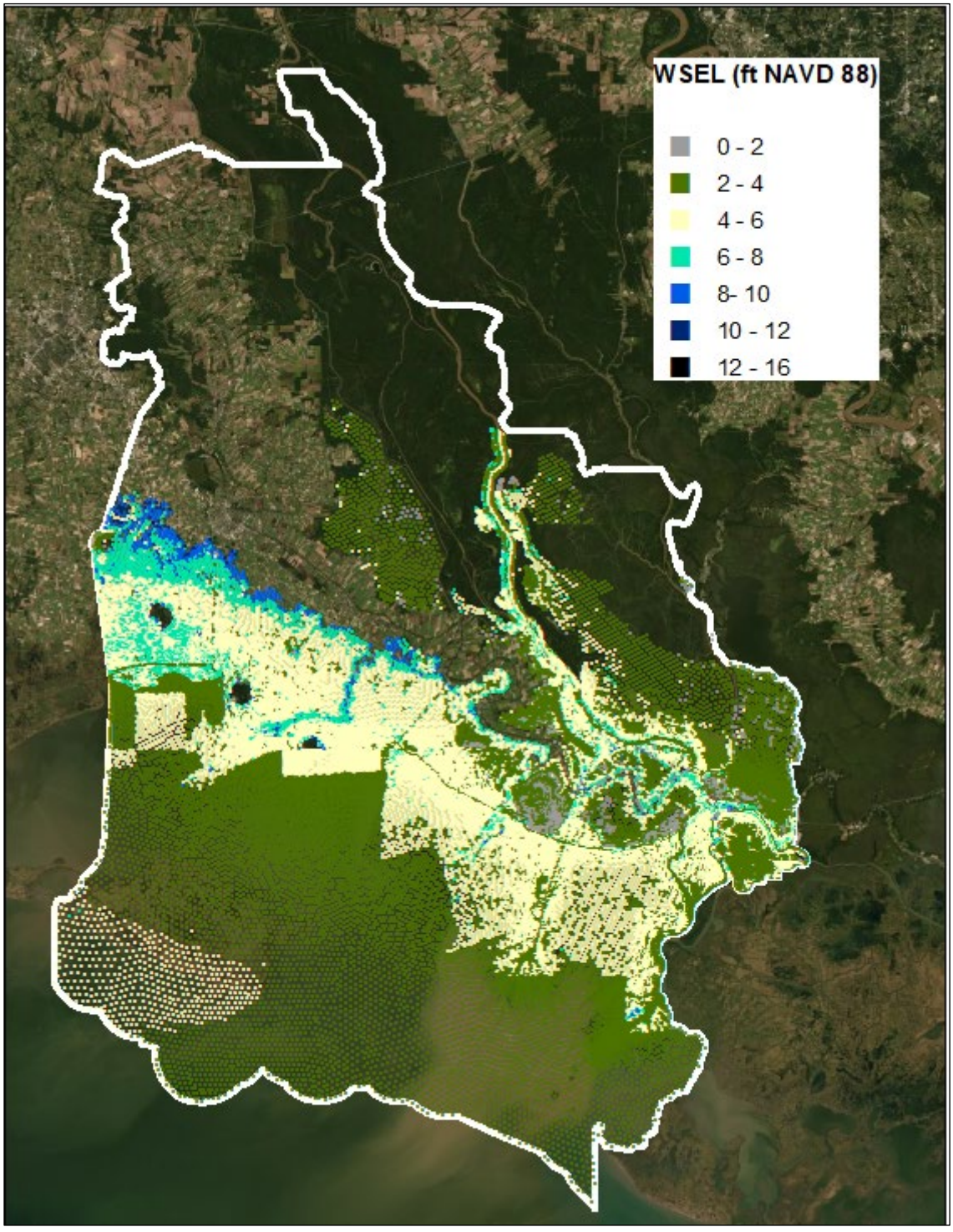

Figure C:2-14. 5% AEP Storm Future Conditions Water Surface Elevations (ft NAVD 88)

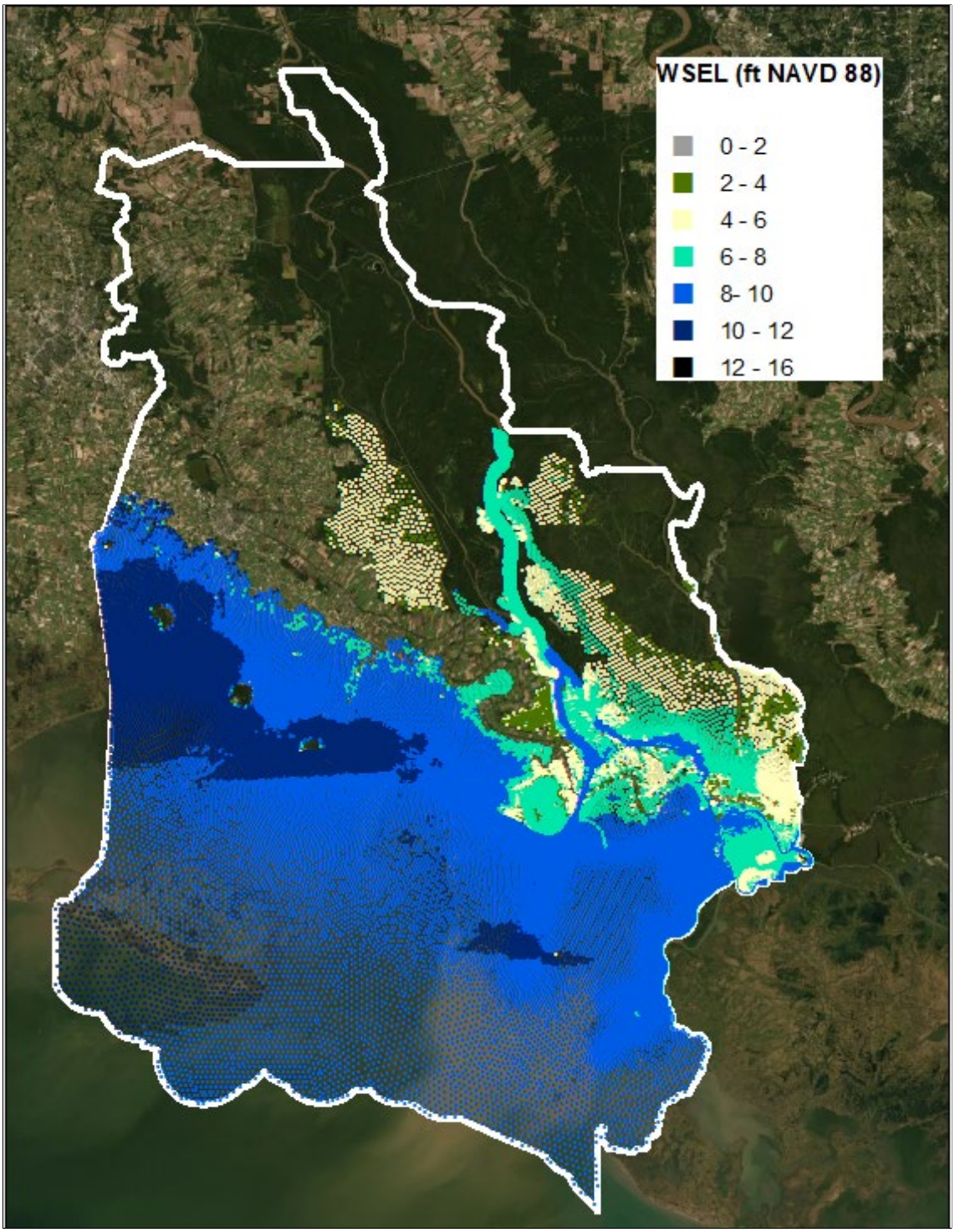

Figure C:2-15. 2% AEP Storm Future Conditions Water Surface Elevations (ft NAVD 88)

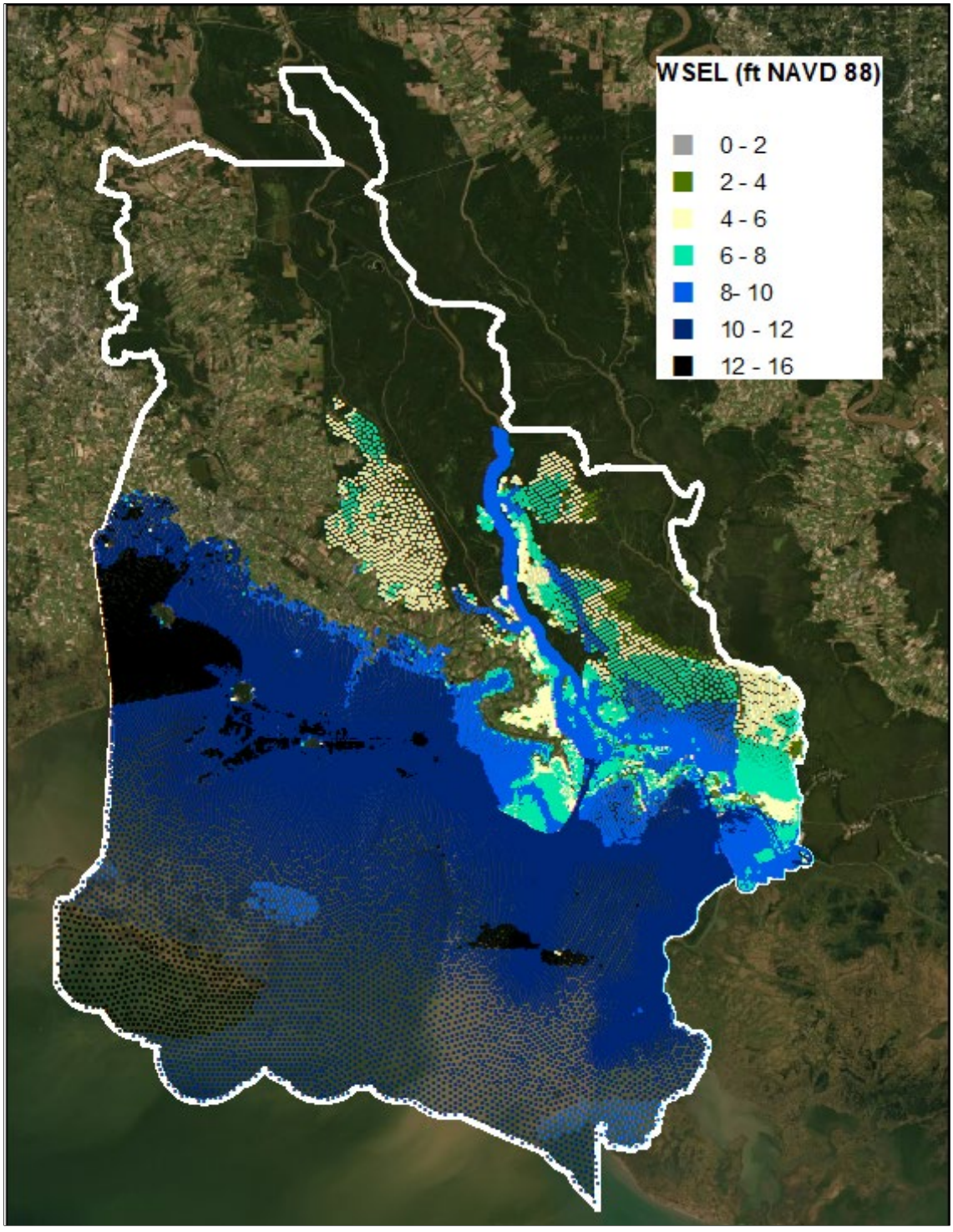

Figure 3. 1% AEP Storm Future Conditions Water Surface Elevations (ft NAVD 88)

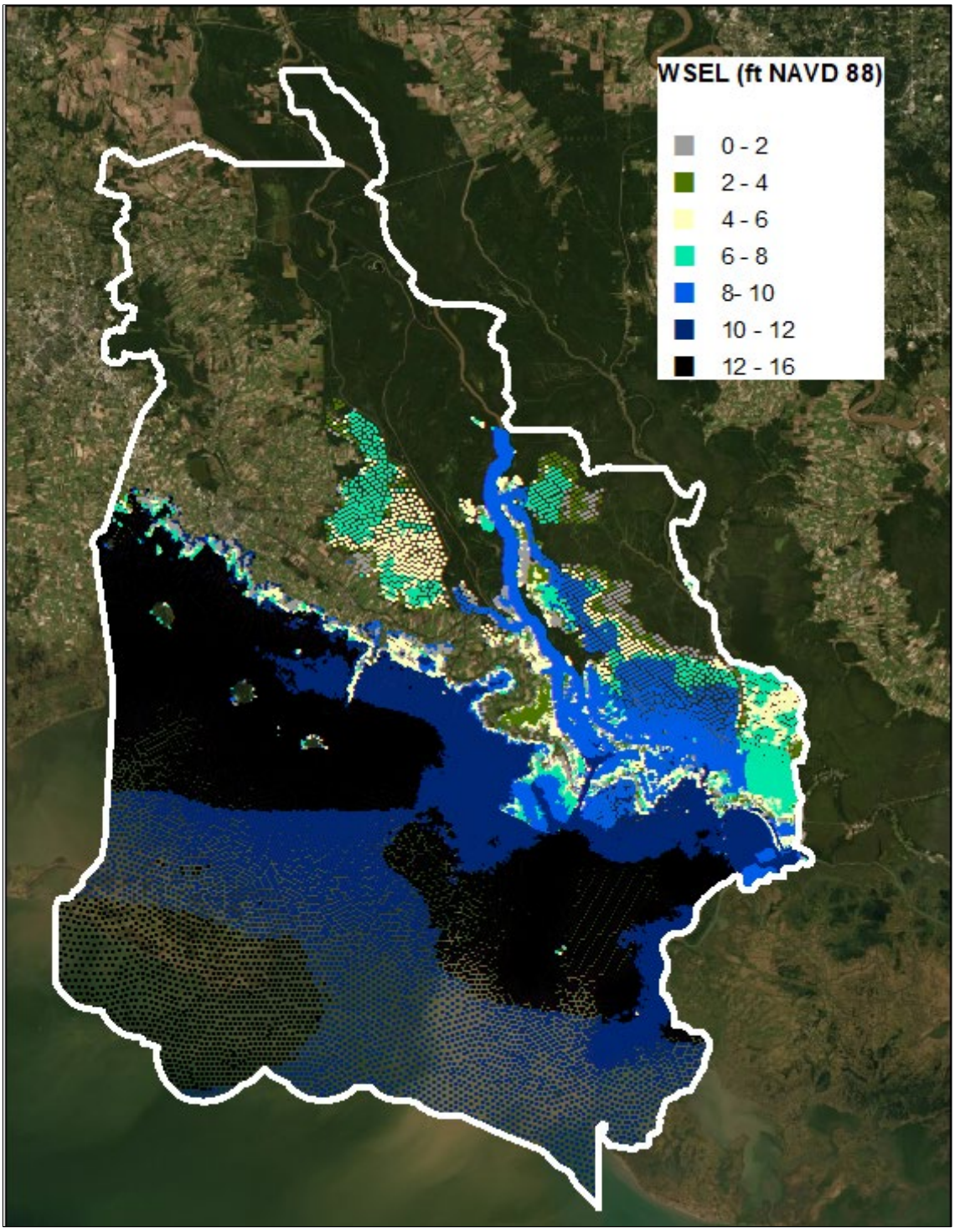

Figure C:2-17. 0.5% AEP Storm Future Conditions Water Surface Elevations (ft NAVD 88)

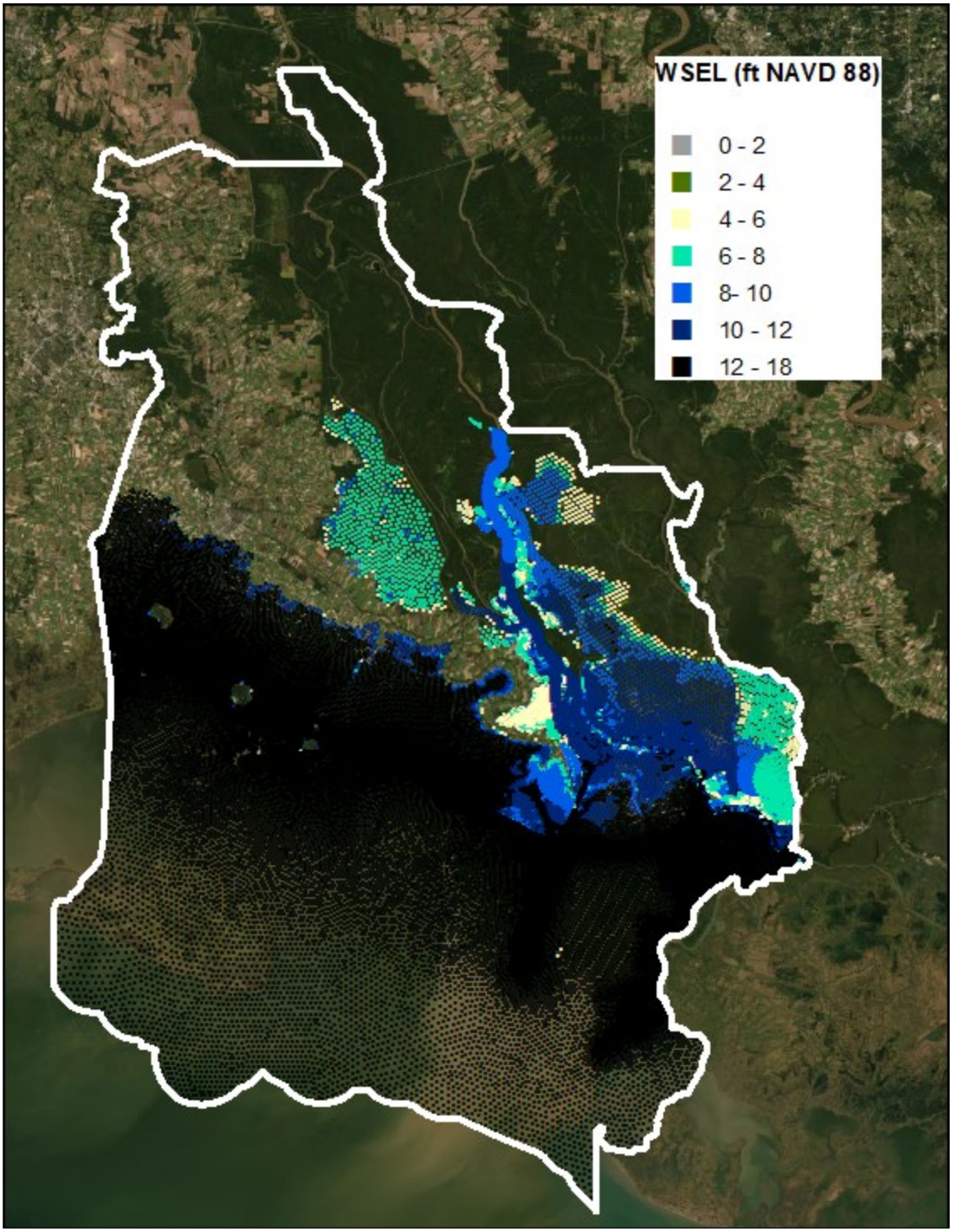

Figure C:2-18. 0.2% AEP Storm Future Conditions Water Surface Elevations (ft NAVD 88)

2.4 SURGE DATA UPDATED WITH 2017 CPRA MODELING

The surge data was updated with the ADCIRC surge hazard dataset from the 2017 CPRA master plan. These data consist of two subsets of 152 synthetic storms (304 total) that vary by tracks, forwards speed, intensities, and diameter. The subsets were constructed for the east and west side of coastal Louisiana. The synthetic storms tracks, along with the historical storm tracks, are presented in Figure C:2-19. The wind speeds are presented in Figure C:2-20.

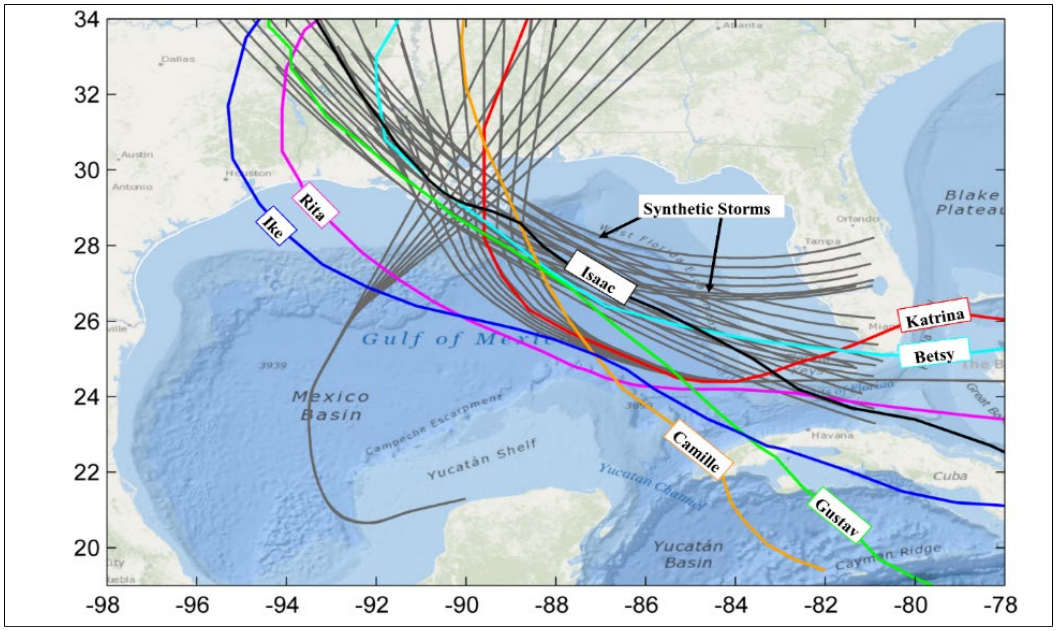

Figure C:2-19. Storm Tracks for JPM-OS Synthetic Events and Historical Storms of Significance

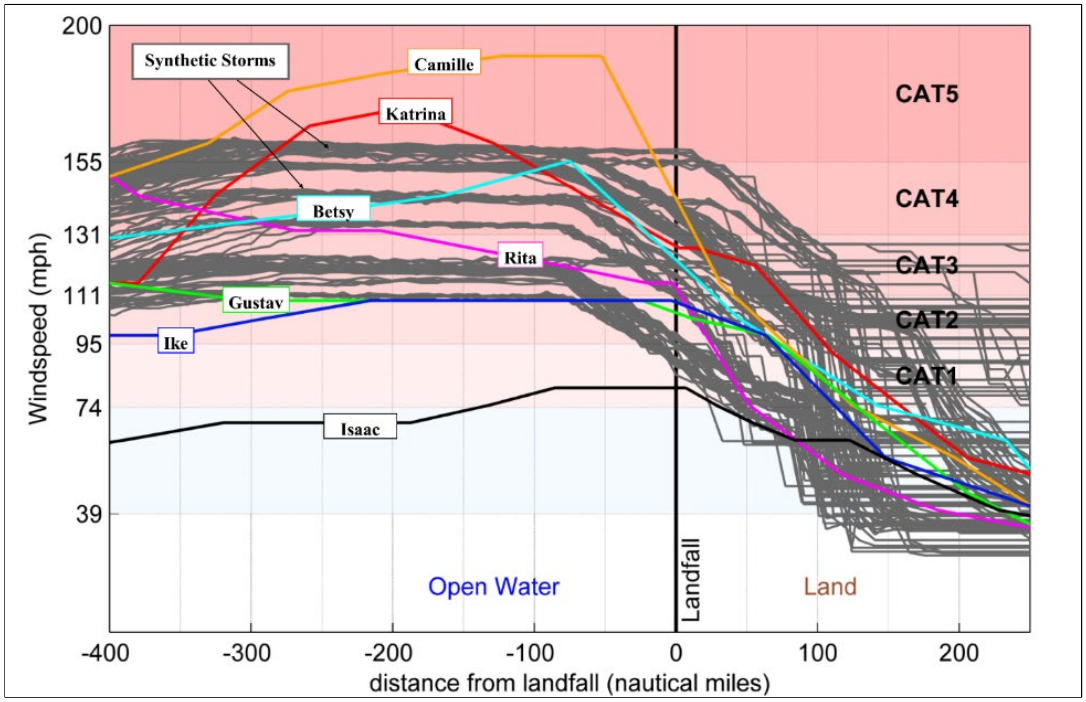

Figure C:2-20. Storm Wind-Speeds for JPM-OS Synthetic Events and Historical Storms of Significance

The updated CPRA ADCIRC was coupled with a SWAN model that provided improved wave data for the entire coast. Surge heights, significant wave heights, and peak wave periods outputs from the storm suite was statistically processed using the ERDC JPM-OS code. This process combines the meteorological probability and the peak surge elevation of every storm to produce stage-frequency surfaces for 0.1, 0.2, 0.5, 1.0, 2.0, 5.0, and 10.0 percent ACE. This procedure was also performed for the wave characteristics.

As a future condition, the ADCIRC+SWAN simulations applied at +1.5 feet eustatic sea level rise to the existing conditions water level of 1.2 feet NAVD 88. The three eustatic sea level rise rates for USACE are 0.3 foot, 0.8 foot, and 2.4 feet over the course of 50 years for low, intermediate, and high. To estimate these scenarios using the existing and future (+1.5 feet) simulations, a linear interpolation/extrapolation was applied to approximate the +0.3 foot, +0.8 foot, and +2.4 feet cases for the entire coast. For the relative sea level rise in the SCCL project area, the local subsidence rate was combined with the eustatic to produce the RSLR. The average subsidence rate of the project area is 1 foot over the 50 year period. This resulted in an estimated RSLR of +1.3, +1.8, and +3.4 for the low, intermediate, and high cases. These projections are depicted in Figure C:2-21, which displays the average low, intermediate, and high projections along with the projections of each gage. Further detail on these rates can be found in section 6.1 of the climate change chapter.

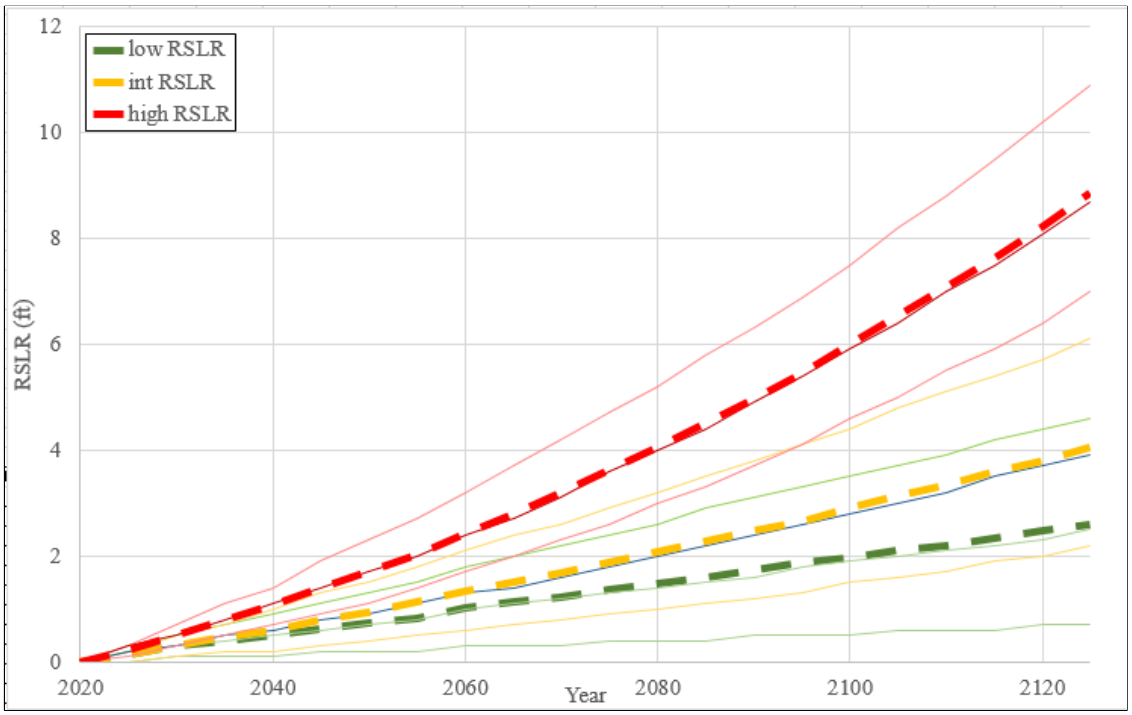

Figure C:2-21. Relative Sea Level Rise for the South Central Coastal Project Area Average rates from gages (dotted); individual rates from gages (solid)

Figures C:2-22 through C:2-29 present the 10-year to 1000-year existing conditions surge and wave elevations. The future condition is presented in Figures C:2-30 through C:2-37 for surge and waves. In general, the waves in the inland region (roughly >5 miles from coast) do not exceed 2 feet for significant wave height. This is observed for both existing and future conditions. The surge elevations contain the effect of wave induced setup as the ADCIRC-SWAN module is two-way coupled.

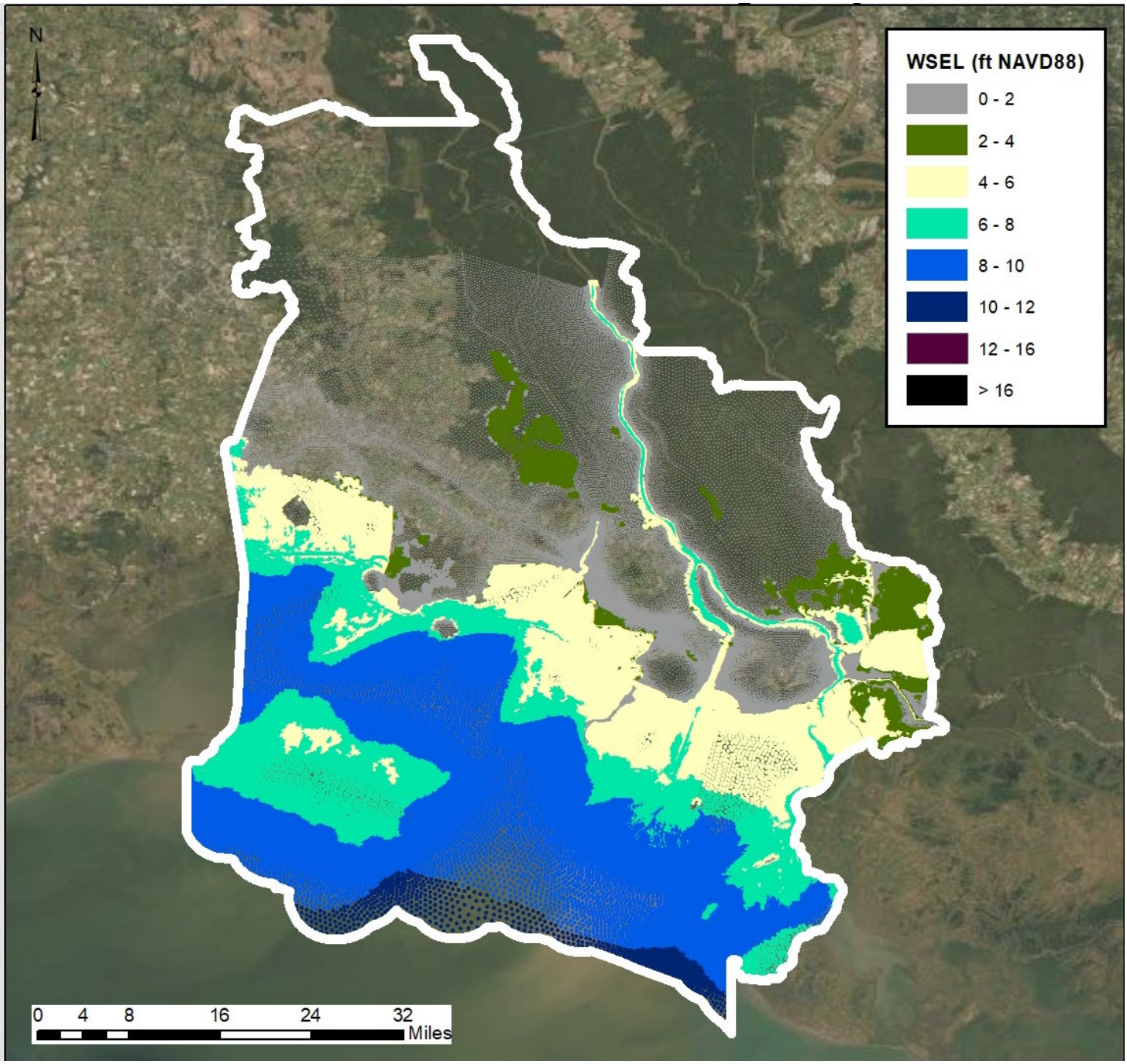

Figure C:2-22.10% AEP; 2025 Existing Conditions; Surge plus Wave Elevations (ft NAVD88) for the SCCL

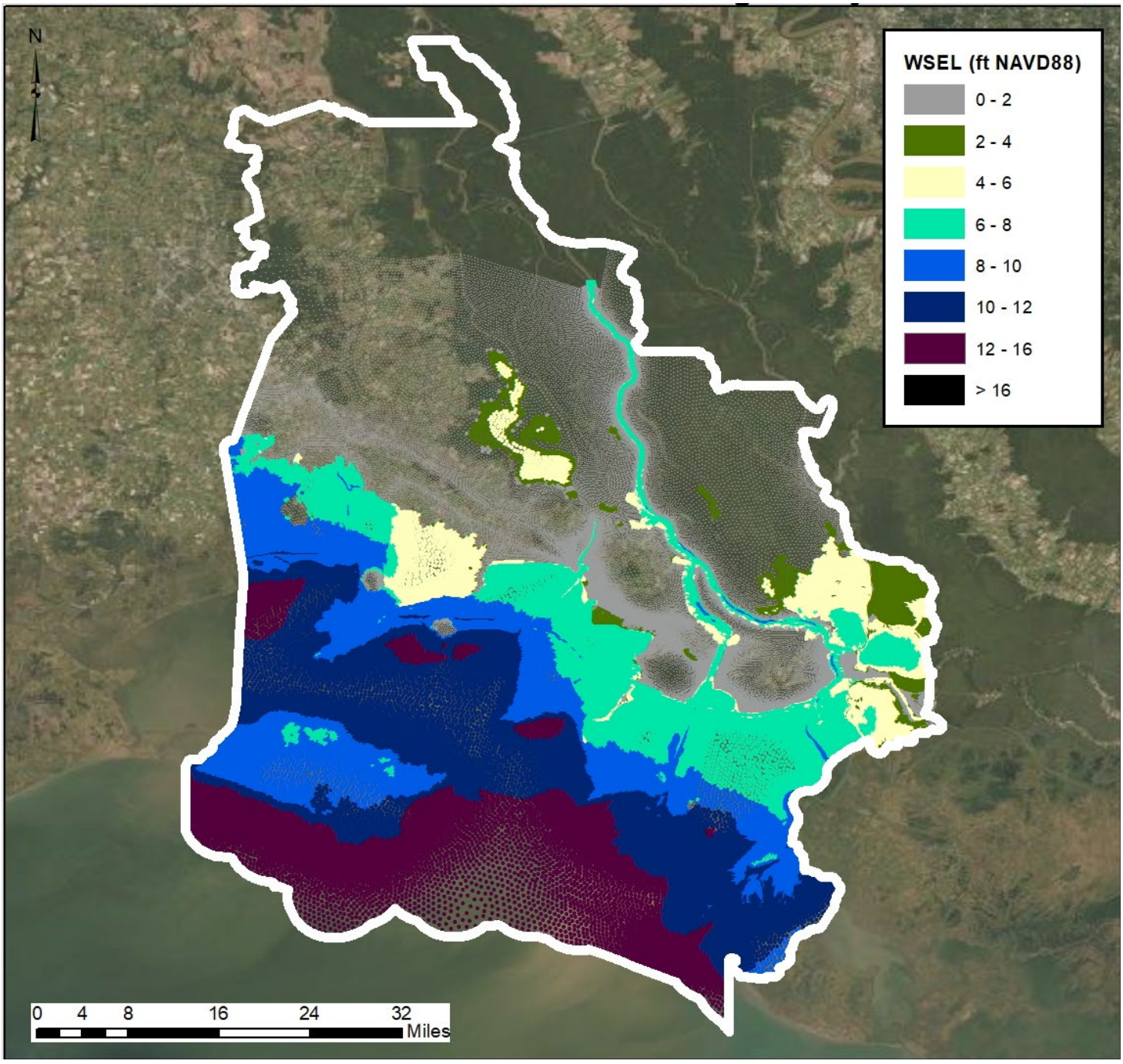

Figure C:2-23. 5% AEP; 2025 Existing Conditions; Surge plus Wave Elevations (ft NAVD88) for the SCCL

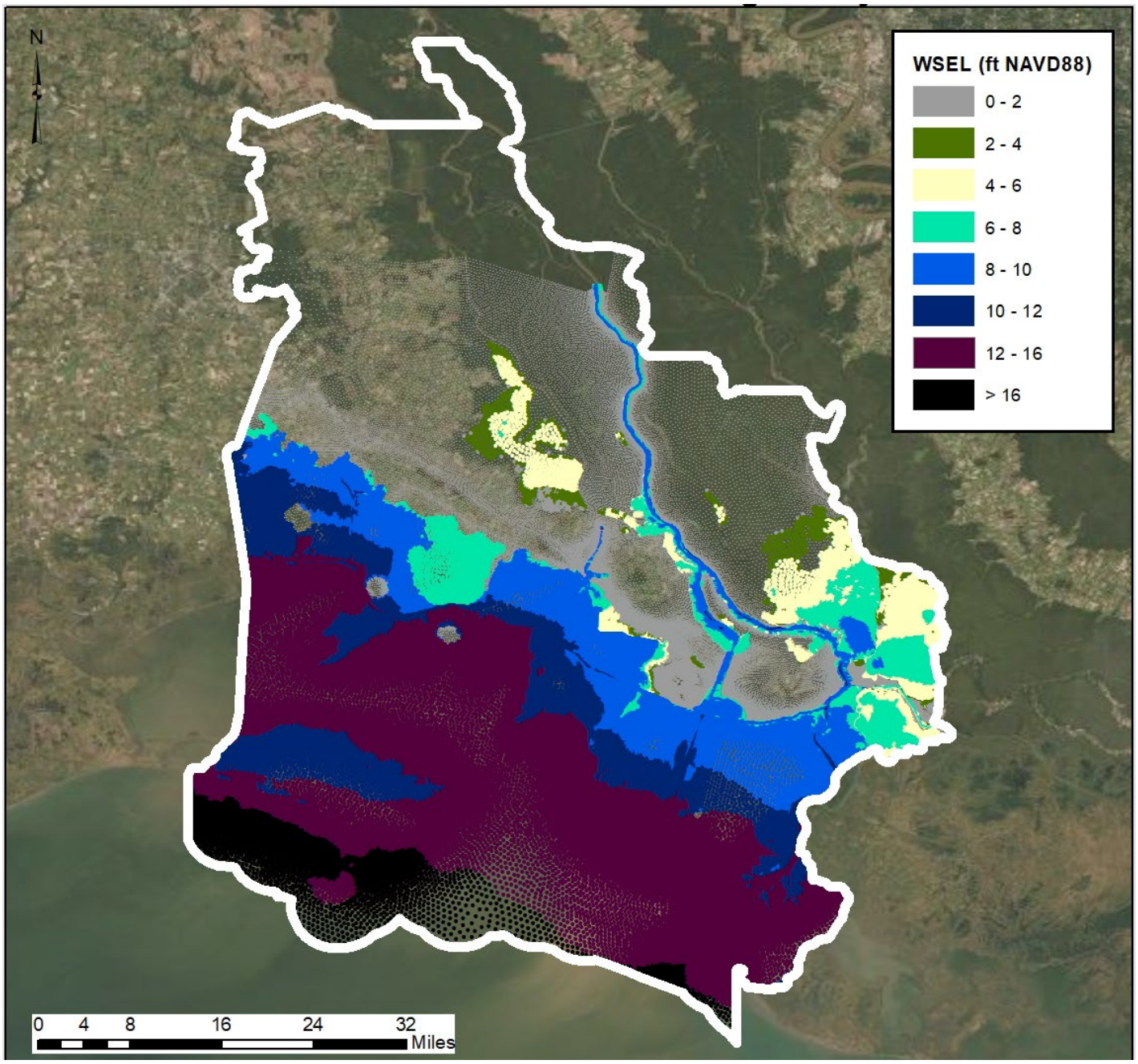

Figure C:2-24. 2% AEP; 2025 Existing Conditions; Surge plus Wave Elevations (ft NAVD88) for the SCCL

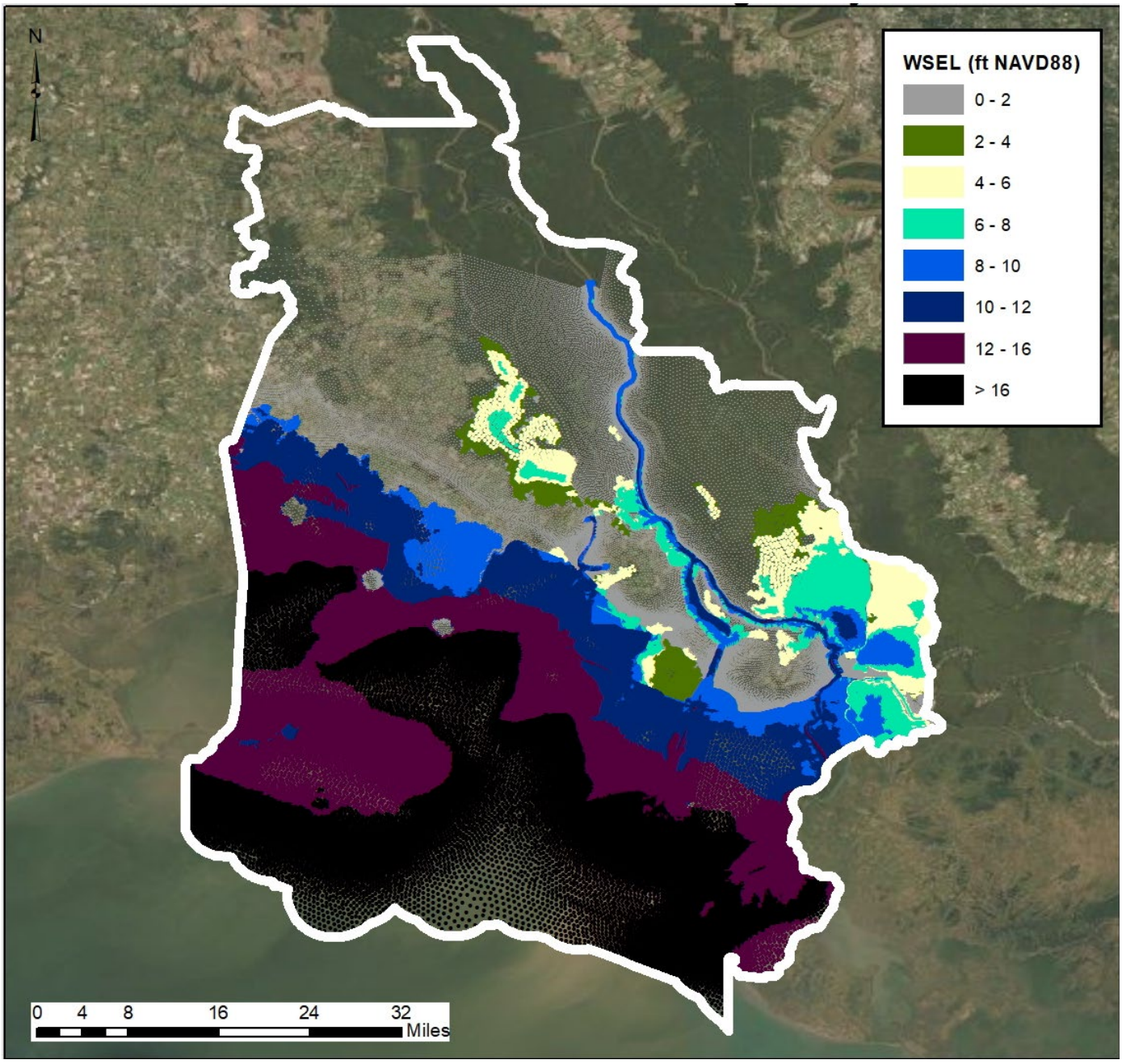

Figure C:2-25. 1% AEP; 2025 Existing Conditions; Surge plus Wave Elevations (ft NAVD88) for the SCCL

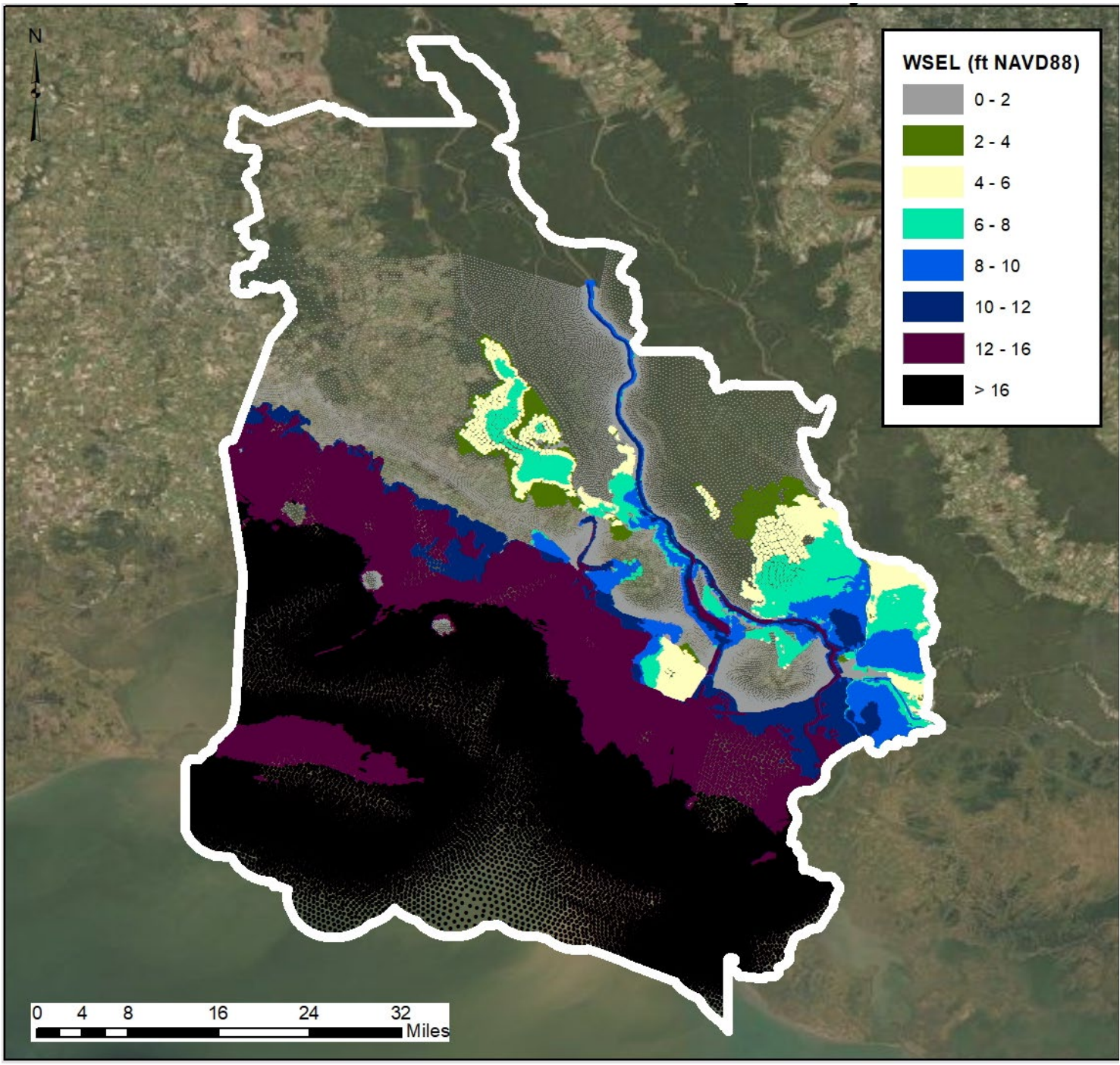

Figure C:2-26. 0.5% AEP; 2025 Existing Conditions; Surge plus Wave Elevations (ft NAVD88) for the SCCL

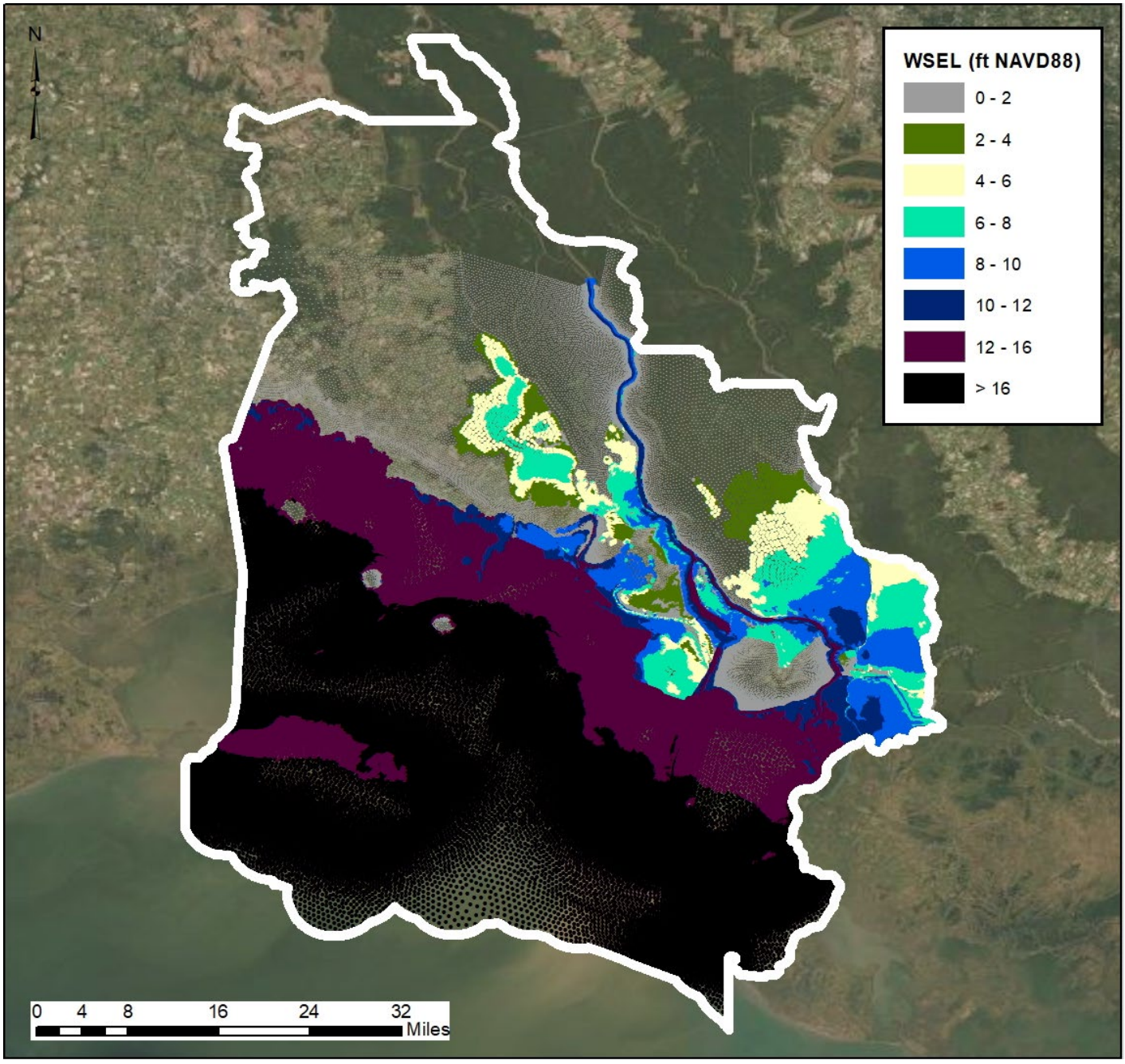

Figure C:2-27. 0.4% AEP; 2025 Existing Conditions; Surge plus Wave Elevations (ft NAVD88) for the SCCL

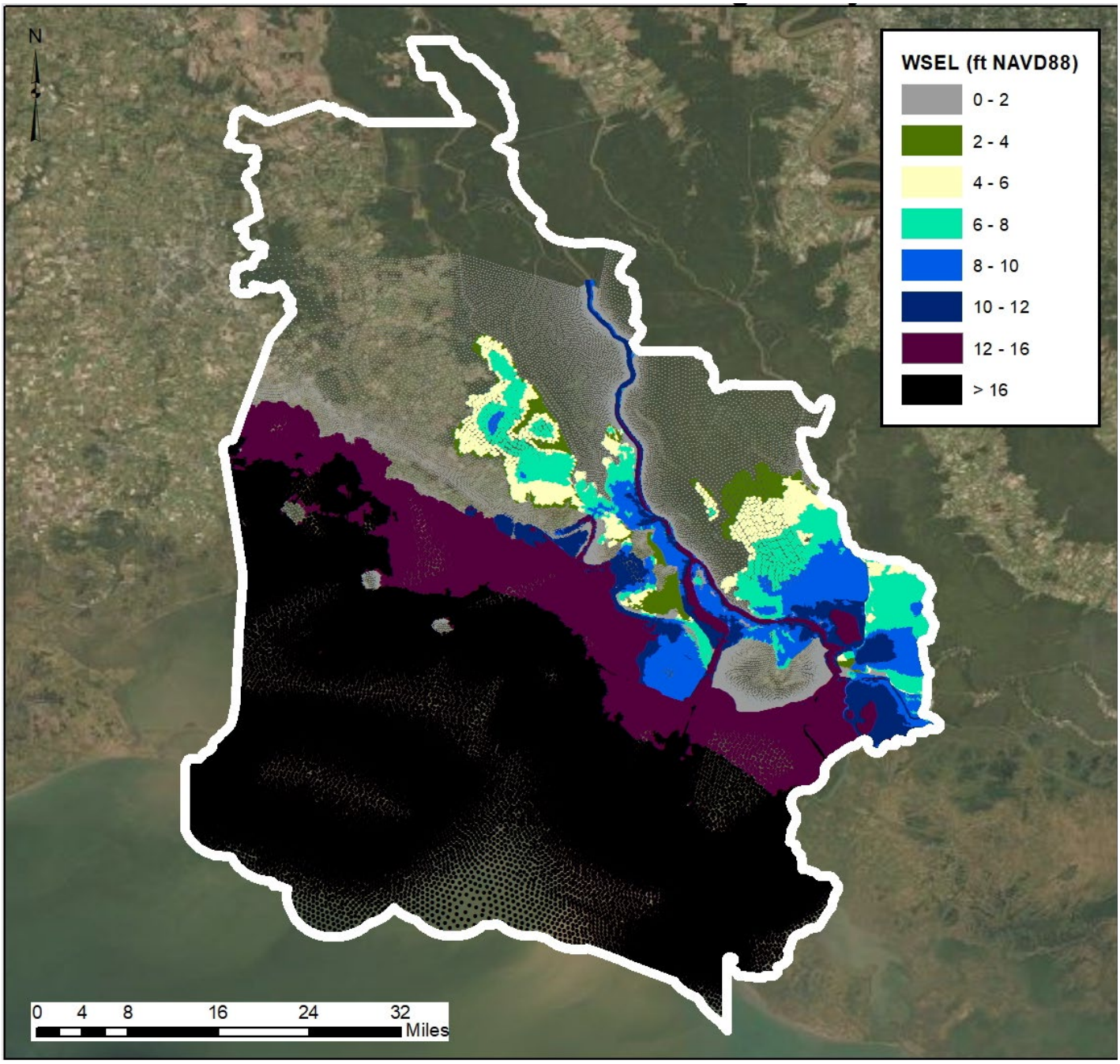

Figure C:2-28. 0.2% AEP; 2025 Existing Conditions; Surge plus Wave Elevations (ft NAVD88) for the SCCL

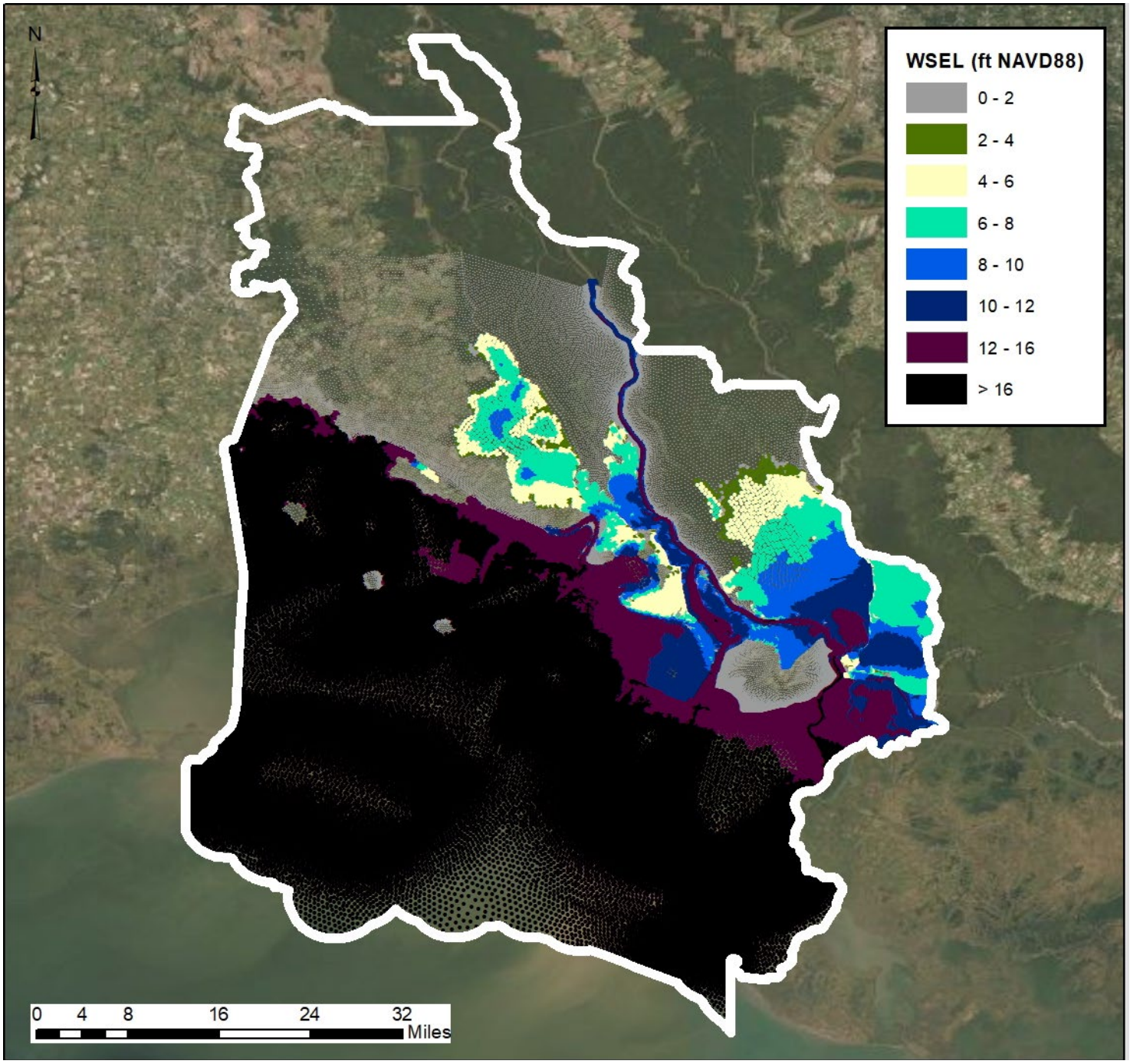

Figure C:2-29. 0.1% AEP ;2025 Existing Conditions; Surge plus Wave Elevations (ft NAVD88) for the SCCL

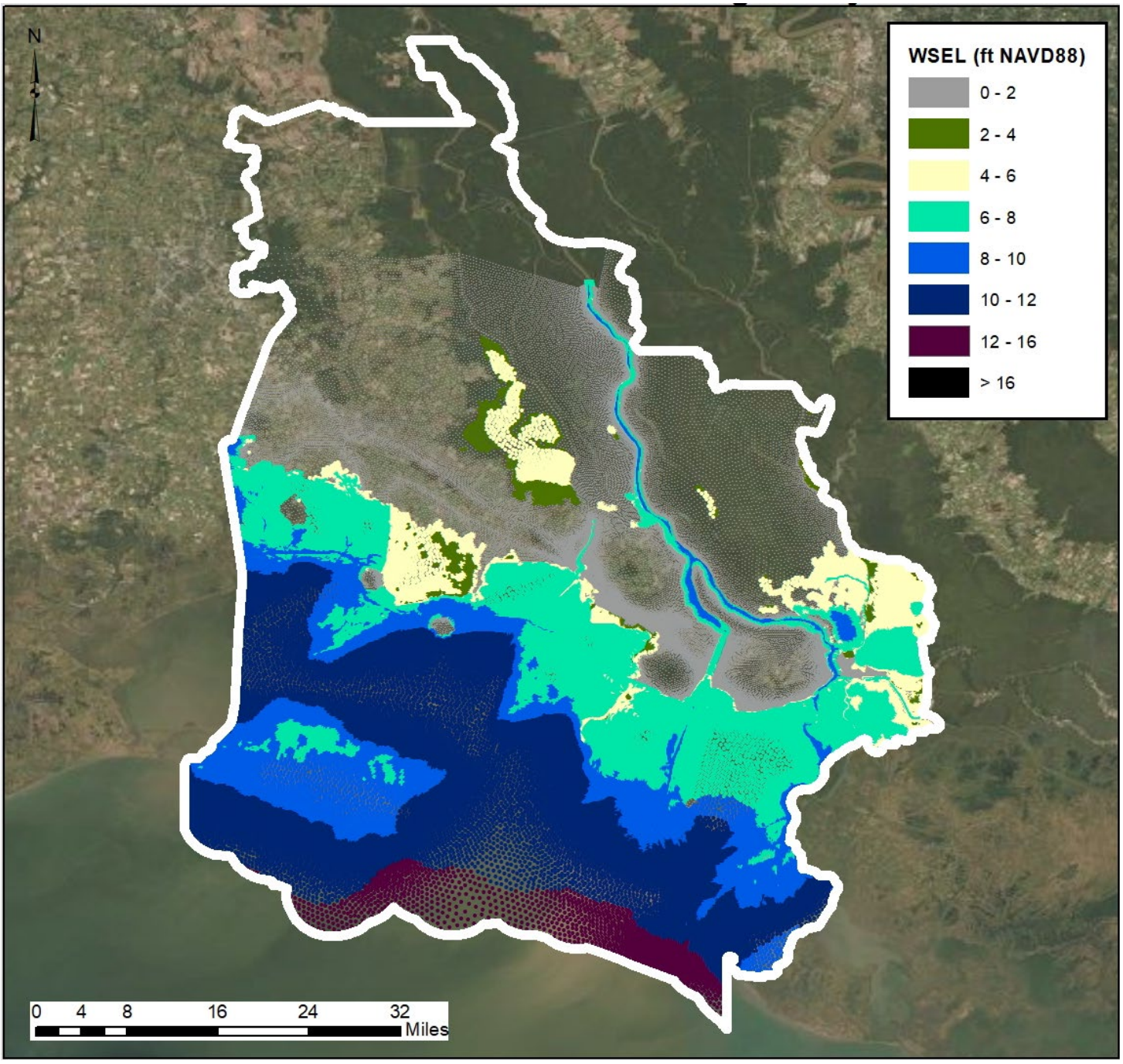

Figure C:2-30. 10% AEP; 2075 Future Conditions; Surge plus Wave Elevations (ft NAVD88) for the SCCL

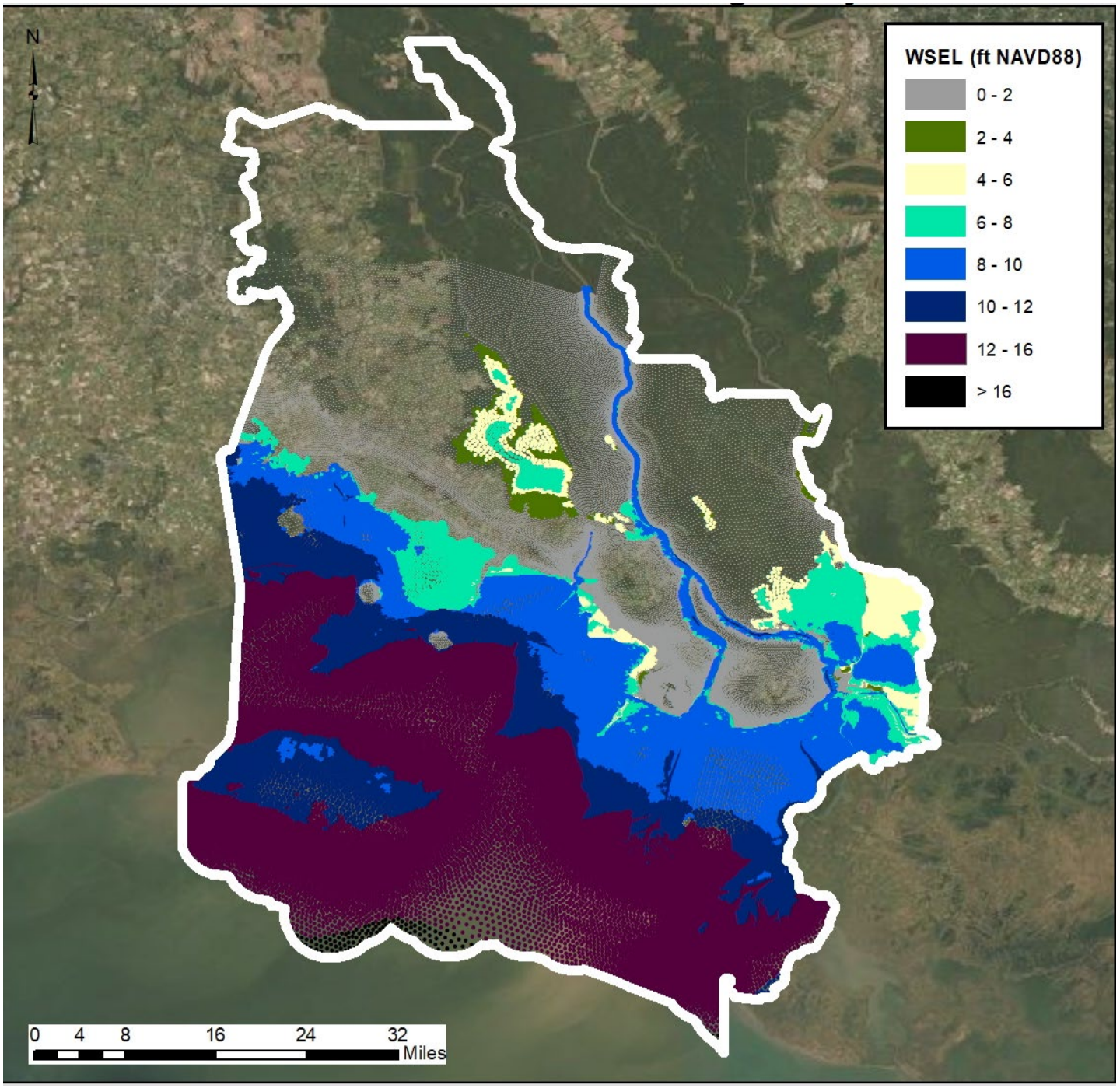

Figure C:2-31. 5% AEP; 2075 Future Conditions; Surge plus Wave Elevations (ft NAVD88) for the SCCL

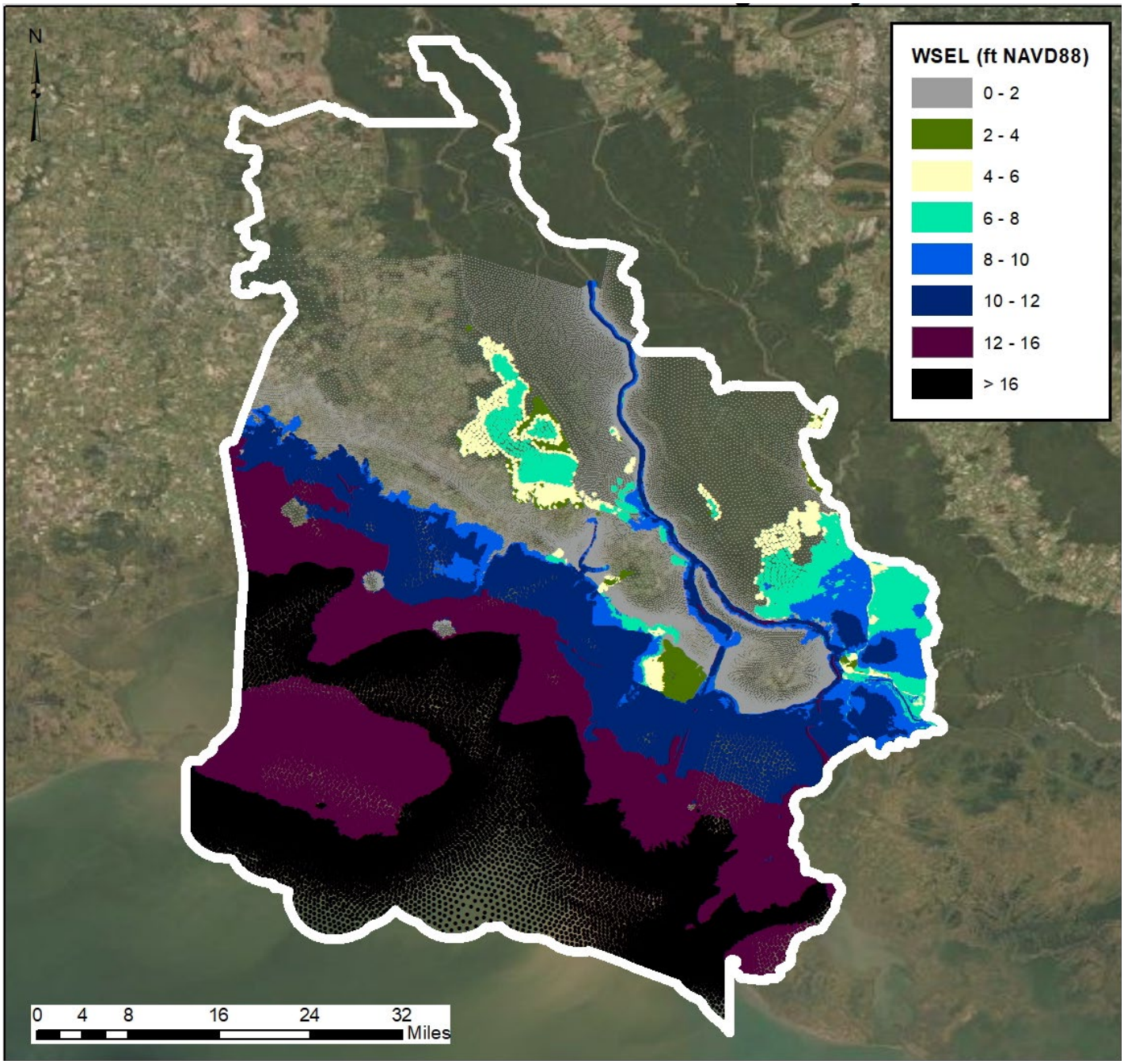

Figure C:2-32. 2% AEP; 2075 Future Conditions; Surge plus Wave Elevations (ft NAVD88) for the SCCL

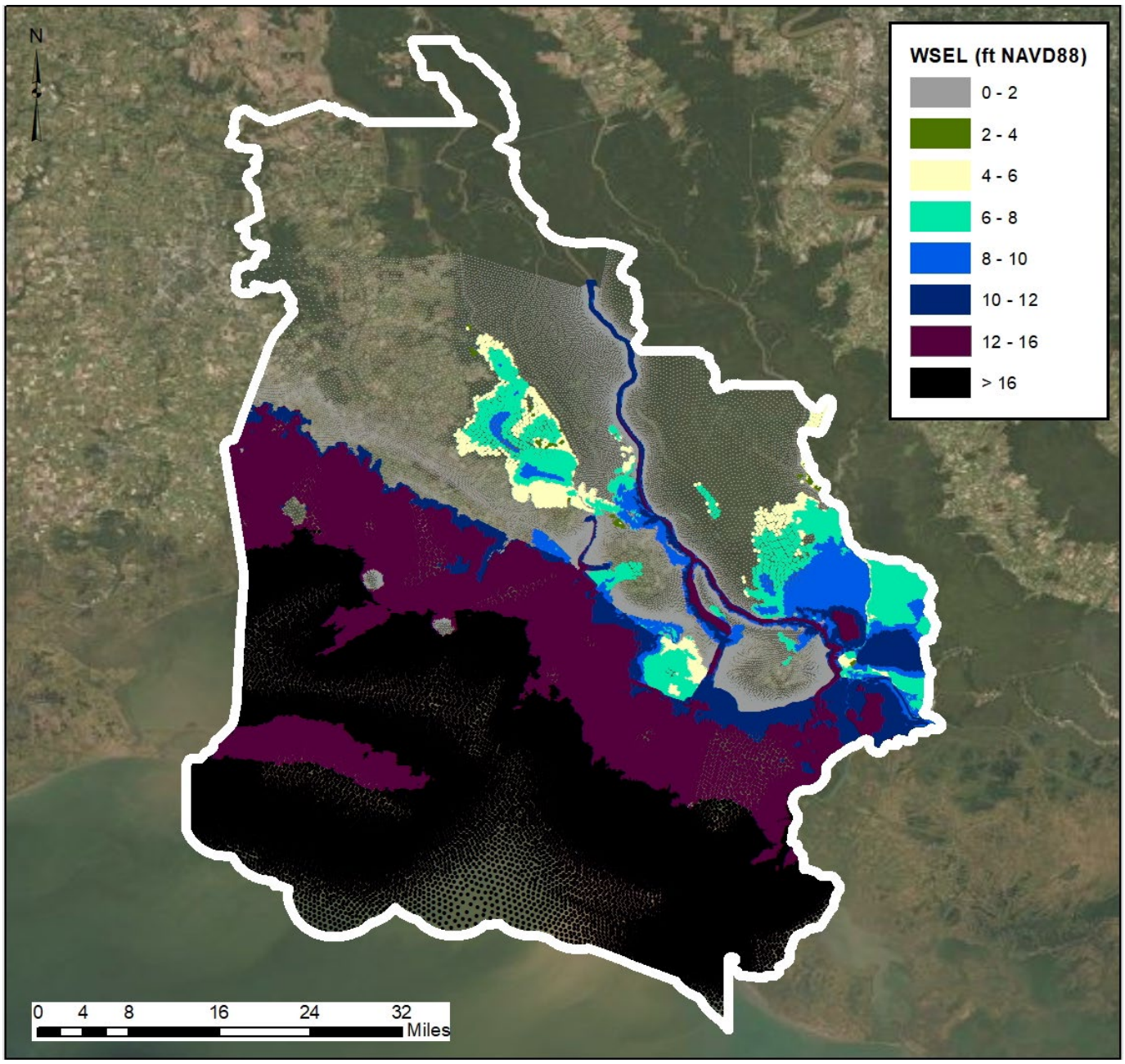

Figure C:2-33. 1% AEP; 2075 Future Conditions; Surge plus Wave Elevations (ft NAVD88) for the SCCL

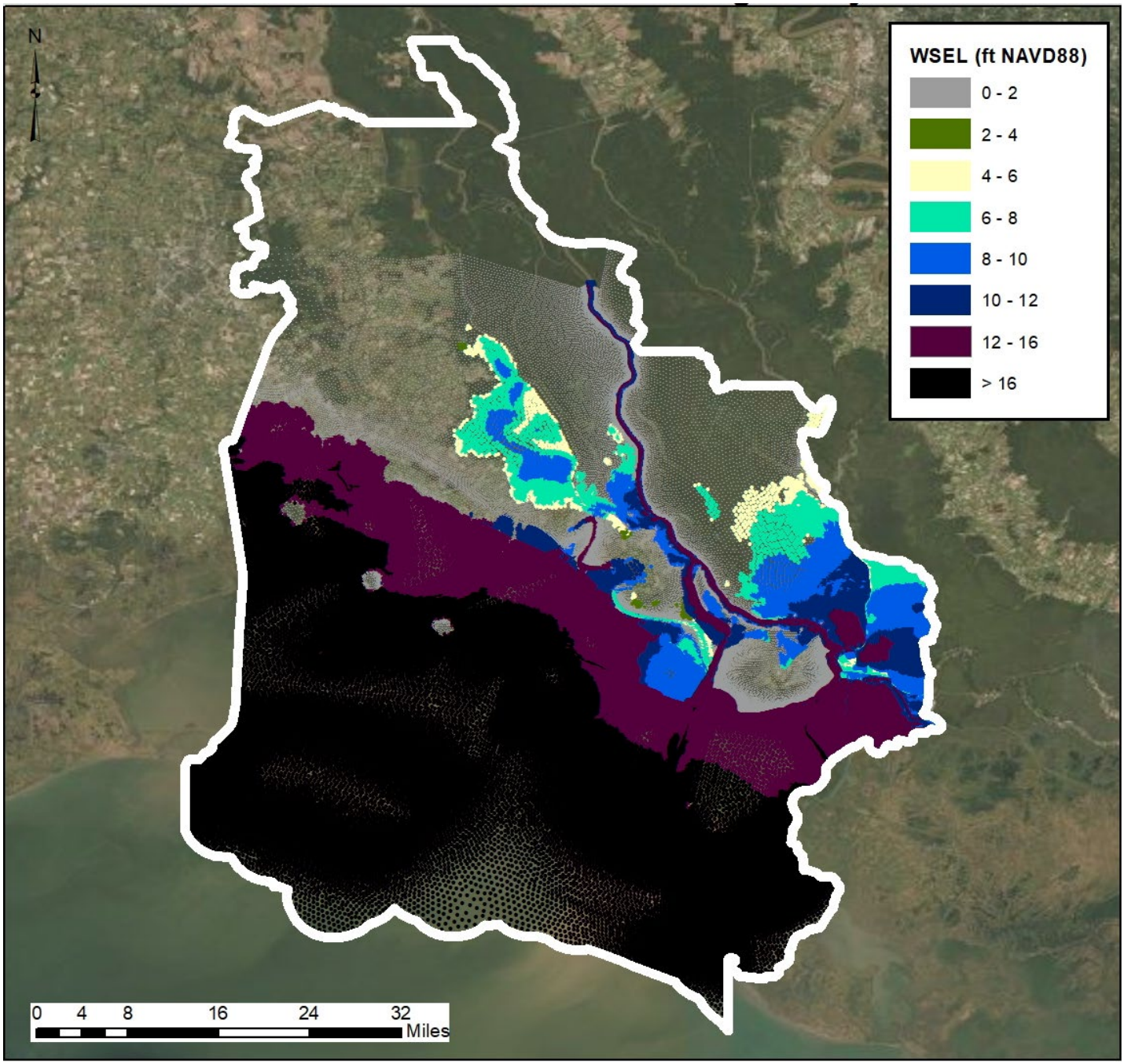

Figure C:2-34. 0.5% AEP; 2075 Future Conditions; Surge plus Wave Elevations (ft NAVD88) for the SCCL

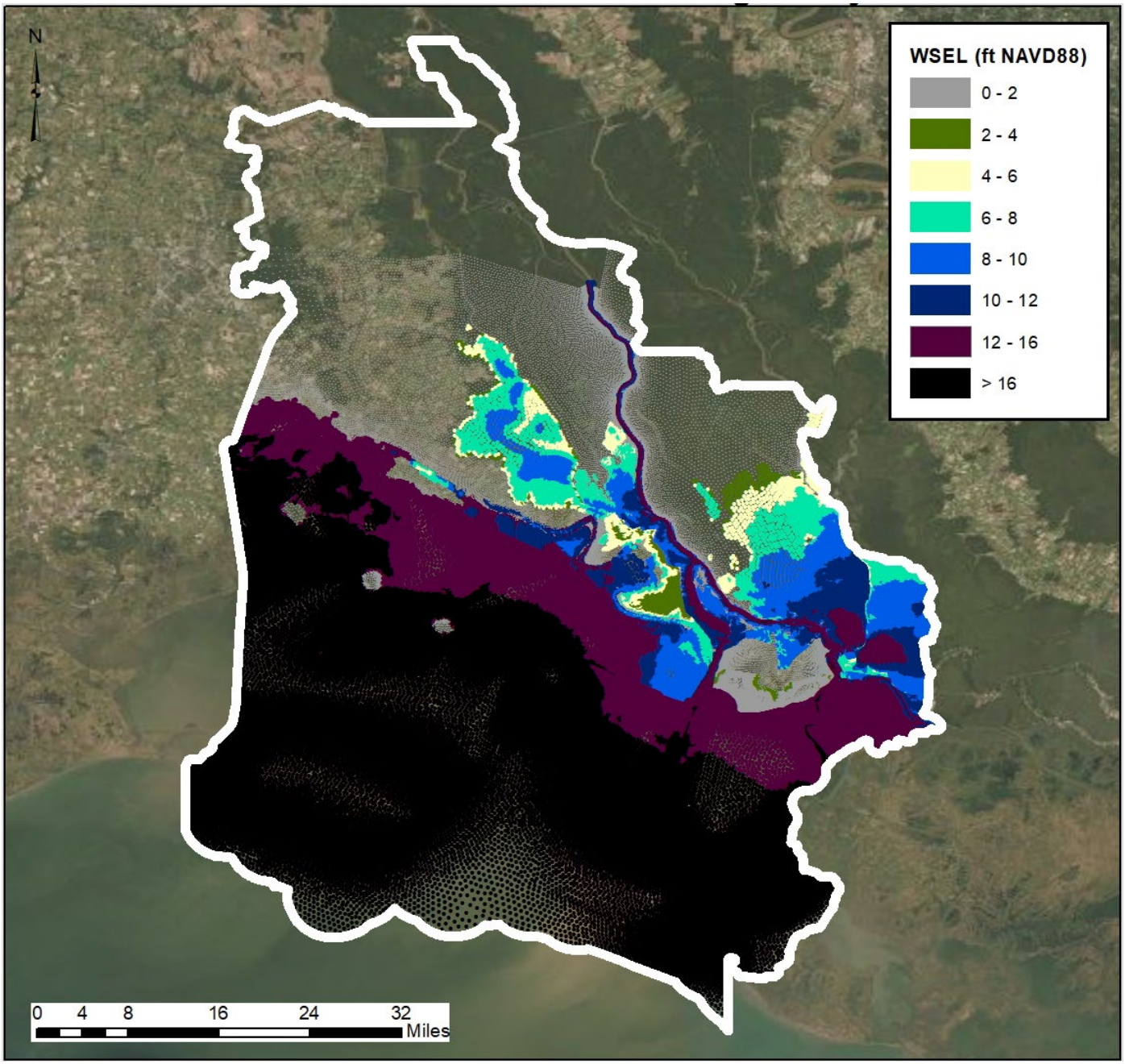

Figure C:2-35. 0.4% AEP; 2075 Future Conditions; Surge plus Wave Elevations (ft NAVD88) for the SCCL

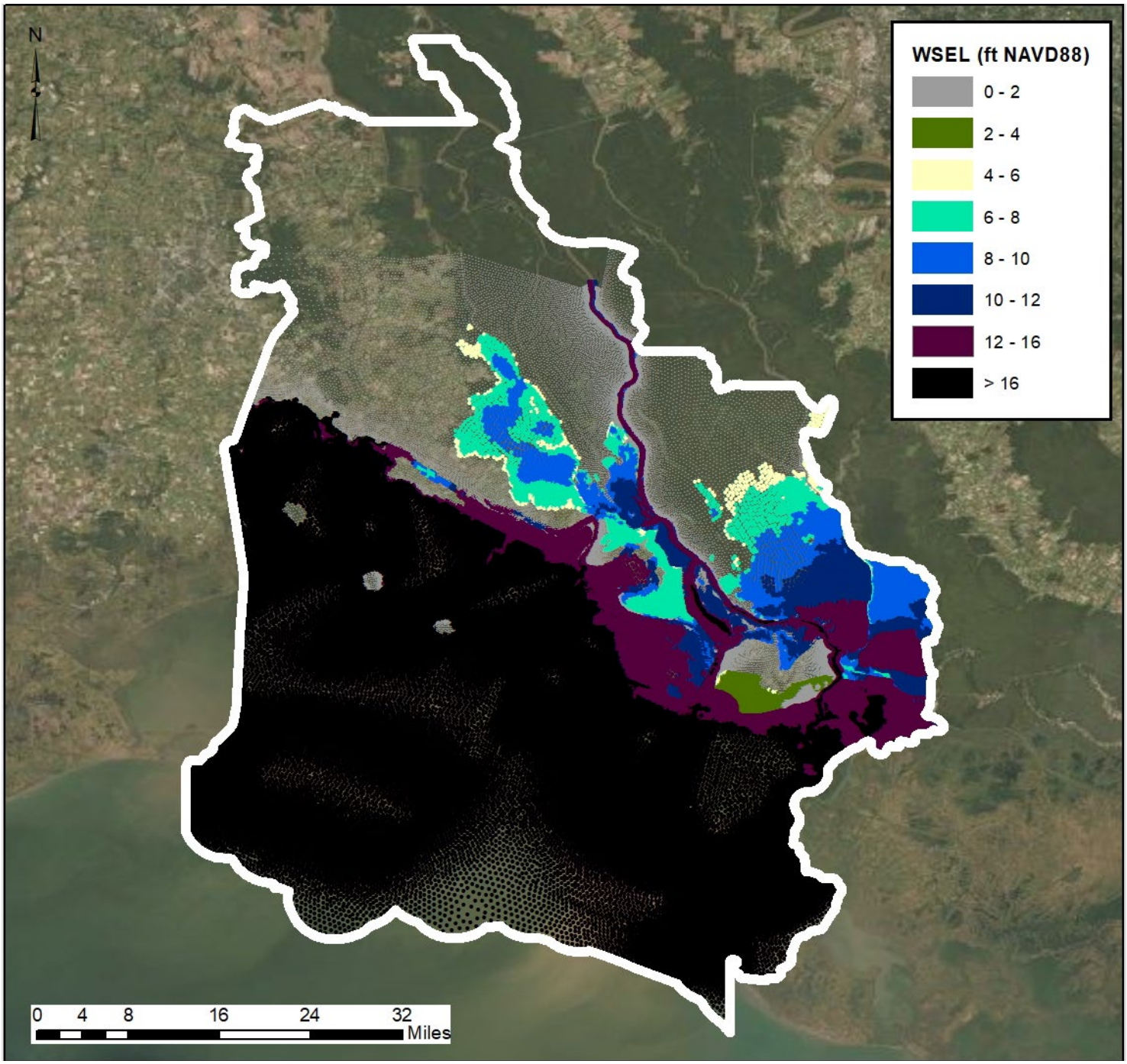

Figure C:2-36. 0.2% AEP; 2075 Future Conditions; Surge plus Wave Elevations (ft NAVD88) for the SCCL

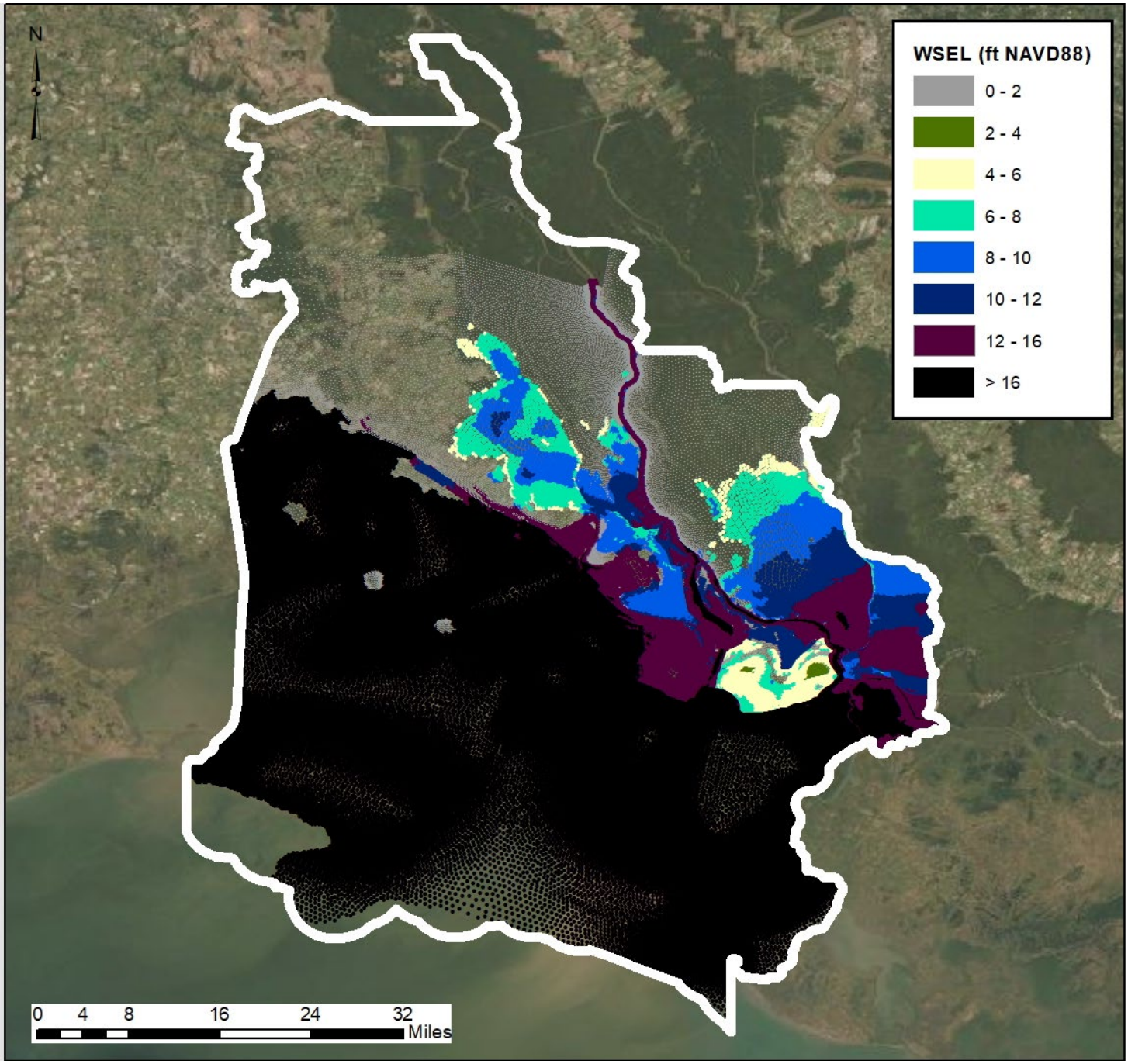

Figure C:2-37. 0.1% AEP; 2075 Future Conditions; Surge plus Wave Elevations (ft NAVD88) for the SCCL

The SWAN portion of the simulation provides the benefit of having high resolution spatially varying wave characteristics for the entire project area. SWAN is a spectral wave model that takes in wind, current, and depth to provide properties of waves and their transformation and transport throughout time. SWAN is capable of producing wave heights as it relates to wave breaking, which is important for this coastal model as wind and surge propagate from offshore to an onshore environment.

For a non-structural designs, wave heights are still important for structural reasons not related to overtopping, but impact on raised infrastructure and housing. For this reason, the stage-frequency data was provided with and without the wave effects included. The wave transformation processes, such as shoaling and breaking, are incorporated in the wave data for the region via SWAN. For raised structures that are in the inundation region, the waves are assumed to not be impeded (they pass underneath the structure) unless the wave is high enough to make impact. Therefore, the 1 percent AEP with waves effects included is the 1 percent surge elevation (with wave setup) + 1 percent significant wave height.

2.5 DISCUSSION OF SHELL REEF MEASURE

The Shell Reef restoration measure involves construction of large, submerged, sectional breakwaters spanning from the eastern boundary of Marsh Island to the Wax Lake Delta. The intent is to restore and reinforce old oyster reefs to assist in reduction energy during surge events. Using engineering judgment, it was determined that the Cote Blanche bay would remain largely hydraulically connected to the GOM, allowing transmission of surge inland. Although local wave reduction would occur near the structures, there remains enough fetch behind the structure for the wave energy to be built up en route to landfall. Additionally, the volume of water behind the breakwaters would likely succumb to seiche during high-wind surge events. The primary aim of this study is to reduce storm surge risk and damage to structures.

Section 3
Riverine Flood Analysis

3.1 MODEL SETUP

This model was expanded from the 2017 Atchafalaya flowline, as shown in Figure C:3-1. The domain now extends east the Mississippi River and Bayou Lafourche, and west to the Vermilion River. This modeling analysis only included riverine impacts; the rainfall impacts were provided by the state contracted Arcadis report (2017). The hydrologic impact of the Atchafalaya River on the project area was modeled using a combined 1-D:2-D domain in HEC-RAS version 5.0.7. The terrain was built from the datasets in Table C:3-1. The 2-D area Manning's n values were mapped using the NCLD 2011 landcover dataset in Figure C:3-2. Table C:3-2 presents the Manning's n values attributed to the project area using the landcover data.

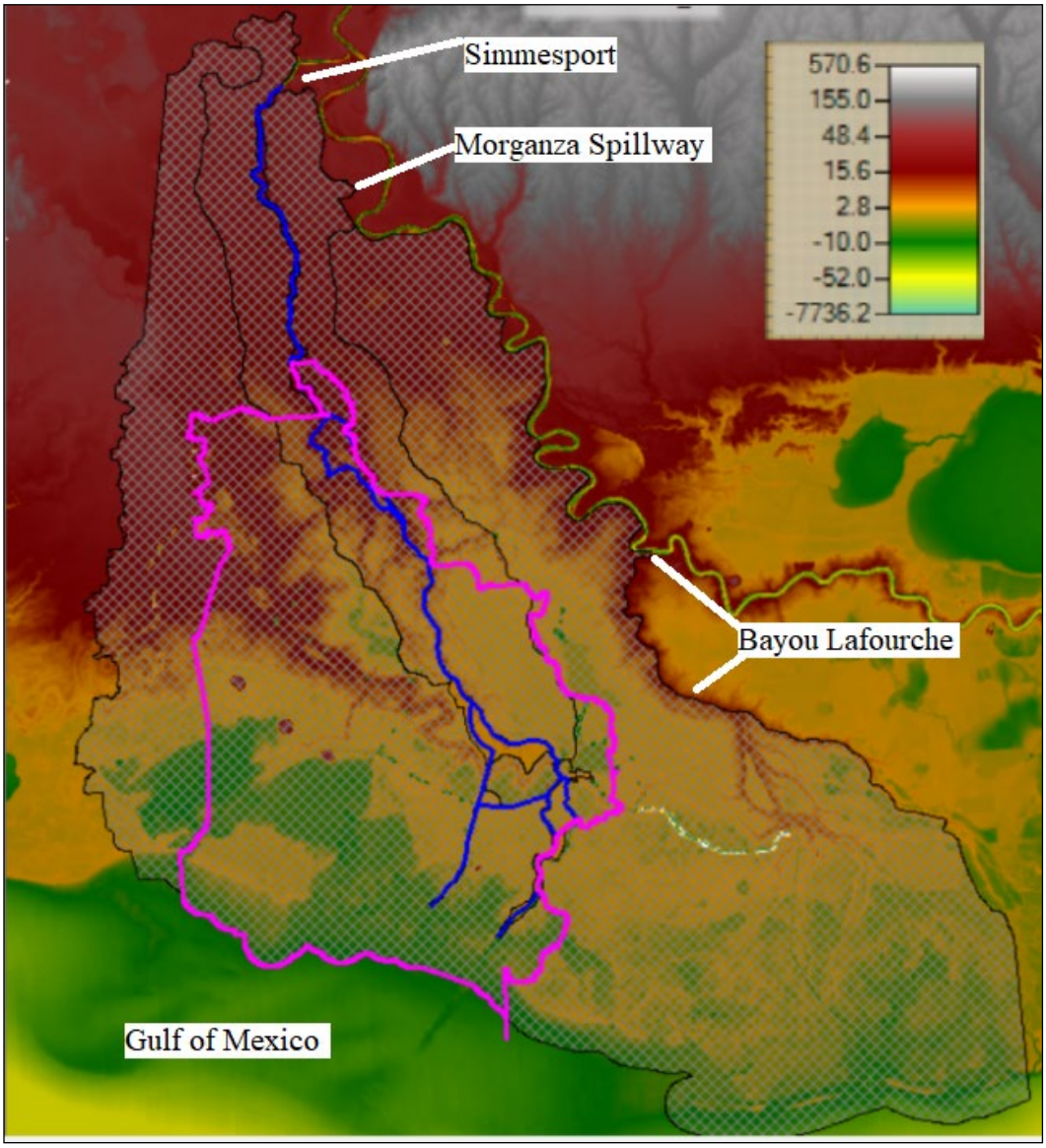

Figure C:3-1. The Computational Domain Superimposed onto the Terrain with Project Features

Table C:3-1. Terrain Dataset Sources and Resolution

Terrain Data	Source	Spatial Resolution
Atchafalaya River Multibean SONAR 2010	USACE-MVN	2ft
Atchafalaya River Levee Lidar 2007	USACE-MVN	1ft
Atchafalaya LIDAR 2013	Northrop Grumman, Advanced GEOINT Solutions Operating Unit	1m
Northern G.O.M. Topobathy	Coastal National Elevation Dataset	1m-3m

USGS Topography	USGS	20ft

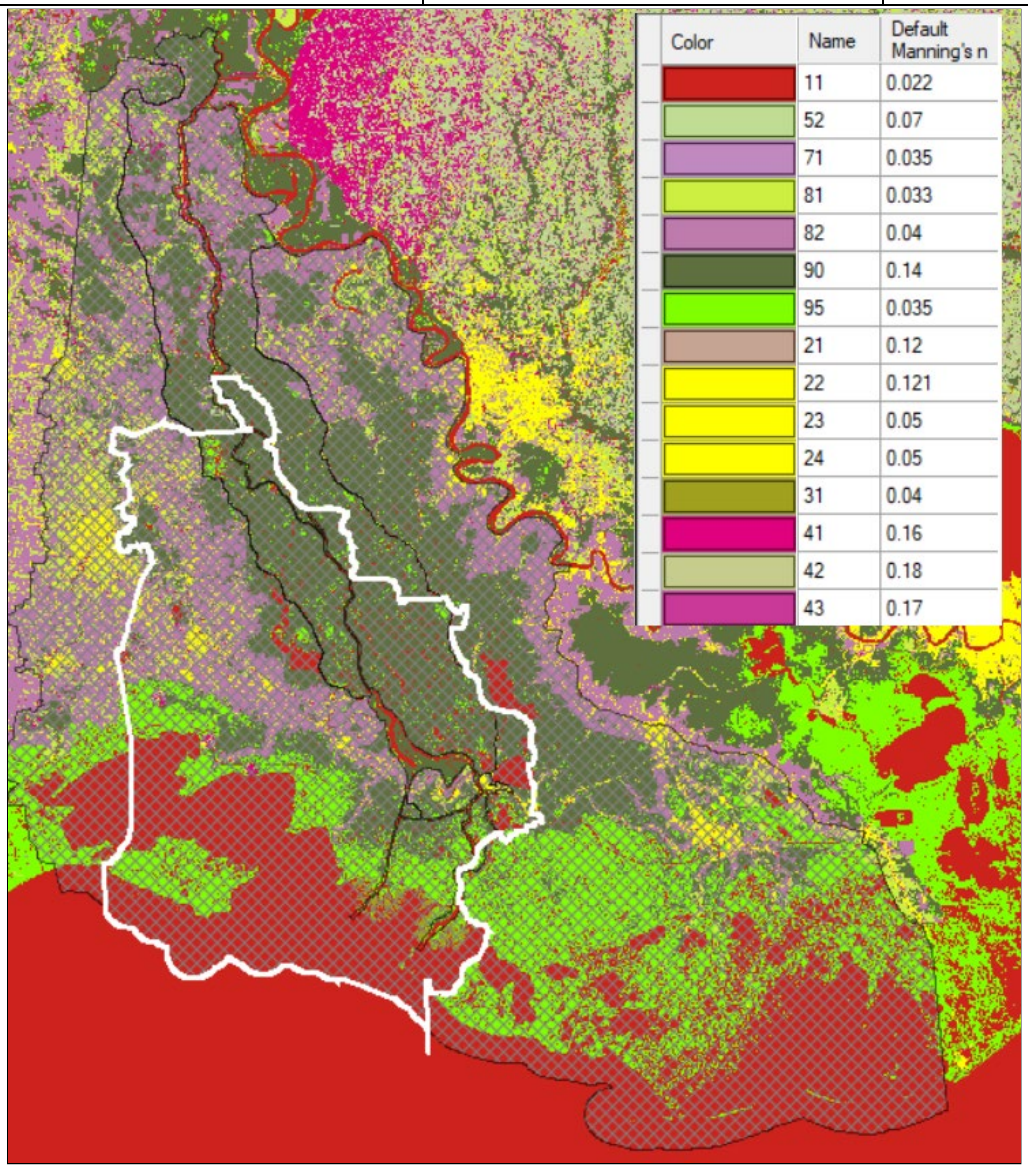

Figure C:3-2. Project Area Superimposed on to Land Cover

Table C:3-2. Manning's n Values Applied to HEC-RAS 2D Model

ID	Description	n-value
11	Open Water	0.022
21	Developed, Open Space	0.12
22	Developed, Low Intensity	0.121
23	Developed, Medium Intensity	0.05
24	Developed, High Intensity	0.05
31	Barren Land	0.04
41	Deciduous Forest	0.16
42	Evergreen Forest	0.18
43	Mixed Forest	0.17
52	Shrub/Scrub	0.07
71	Grassland/Herbaceous	0.035
81	Pasture/Hay	0.033
82	Cultivated Crops	0.04
90	Woody Wetlands	0.14
95	Emergent Herbaceous Wetlands	0.035

The model consists of two flow boundaries. The Atchafalaya main stem is placed at Simmesport with the other boundary located at the Morganza spillway to account for any further contribution from the Mississippi River. The tail water is a stage boundary located in the Gulf of Mexico. The flow rates assigned to the boundary conditions are the predicted 30 percent latitude flow based on the Mississippi River and Red River placed at Simmesport flows. HEC-SSP was used to calculate the flow-frequency data. The method involved fitting a three parameter log Pearson III distribution to annual peak flow data, which returned quantities of annual discharge exceedance probability. The data range for peaks flows was restricted to 1962-2012 and used a regional skew of -0.1 and regional skew mean squared error of 0.302. These values were extracted from the generalized skew map on Plate 1 in bulletin 17-B (U.S. Interagency Advisory Committee on Water Data, 1982). The predicted flow frequency table and graph are presented in Table C:3-3 and Figure C:3-3 with the given confidence intervals and observed events.

Table C:3-3. Flow Frequency Chart For 30% Latitude Flow into the Atchafalaya River; values in 1000 cfs

HEC-SSP 2.0 - 30 Percent of Total Latitude Flow

Frequency Curve for: 30% Latitude Flow-TOTAL-FLOW

Percent Chance Exceedance	Computed Curve Flow in cfs	Expected Prob. Flow in cfs	Confidence Limits Flow in cfs	
			0.05	0.95
0.1	862.0	900.7	988.4	779.2
0.2	823.6	854.1	936.5	748.8
0.3333	795.0	820.1	898.2	726.0
0.5	771.9	793.4	867.7	707.5
0.6667	755.5	774.4	845.9	694.2
1.0	732.0	747.8	815.1	675.2
1.25	718.9	733.1	798.1	664.5
2.0	690.9	702.0	761.8	641.5
5.0	633.9	640.2	689.2	594.1
10.0	587.6	591.2	631.5	554.7
20.0	536.3	538.1	569.6	509.8
50.0	451.4	451.4	473.3	430.5
80.0	381.1	379.9	400.9	358.7
90.0	349.1	347.1	369.7	325.0
95.0	325.0	322.0	346.5	299.3
99.0	284.5	279.0	307.8	256.3

System Statistics

Log Transform: Flow

Statistic	Value
Mean	2.655
Standard Dev	0.088
Station Skew	0.116
Regional Skew	-0.100
Weighted Skew	0.059
Adopted Skew	0.059

Number of Events

Event	Number
Historic Events	0
High Outliers	0
Low Outliers	0
Zero Or Missing	0
Systematic Events	51
Historic Period	

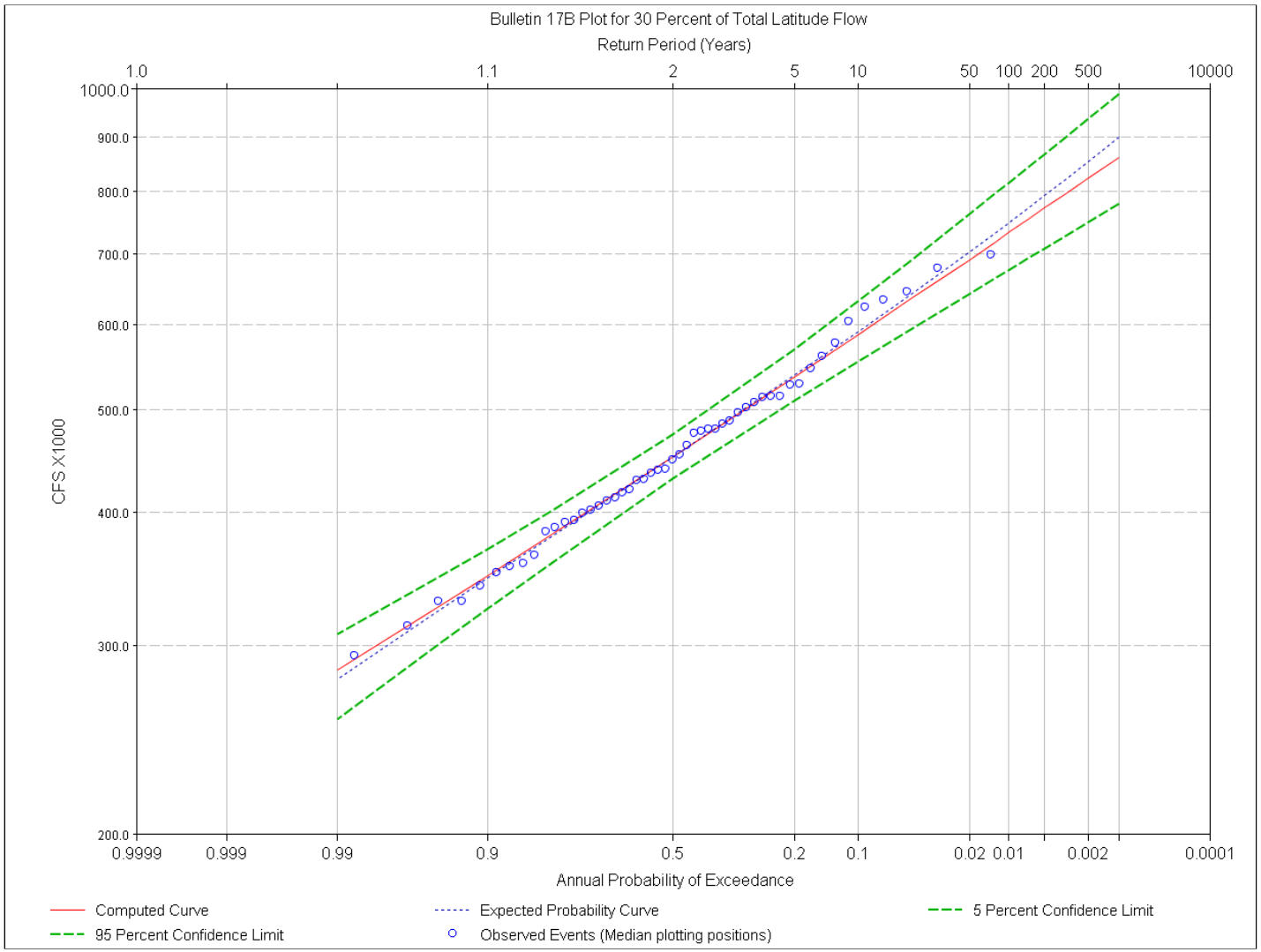

Figure C:3-3. Graphical Representation of the Estimated Flow Frequency Relationship at Simmesport (30% Latitudinal Flow)

The contribution from the Morganza spillway is based on the 70 percent flow estimated to still be in the Mississippi River. The Morganza spillway is primarily operated using a flow rate trigger point of 1.5 million cfs downstream of the Old River Control Structure (ORCS). The boundary is assigned a flow calculated by subtracting 1.5 million cfs from the 70 percent latitude flow, as long as it is a positive value. This results in Morganza only being operated for all frequencies of 2 percent AEP or less.

Sixteen simulations were run for the riverine analysis of the project area. The eight existing condition runs used a downstream gulf boundary stage of 1.2 feet NAVD 88, while the eight future condition runs used a downstream gulf stage boundary of 3.0 feet. NAVD 88 to account for the +1.8 feet intermediate sea level rise scenario (see section 6.1). The 50, 20, 10, 5 percent AEP frequencies were run with the Atchafalaya flow only. The 2, 1, 0.5, and 0.2 percent AEP frequencies included the contribution from the Morganza spillway. All were run for 2 months, allowing enough duration for the system to achieve steady state. The riverine bathymetry is considered to be static for all runs, assuming no scour or accretion in the channel. The steady state scenarios are presented graphically in Figure C:3-4 and tabulated in Table C:3-4. Existing conditions results are presented in Figures C:3-5 through C:3-12 and the future conditions are presented in Figures C:3-13 through C:3-20.

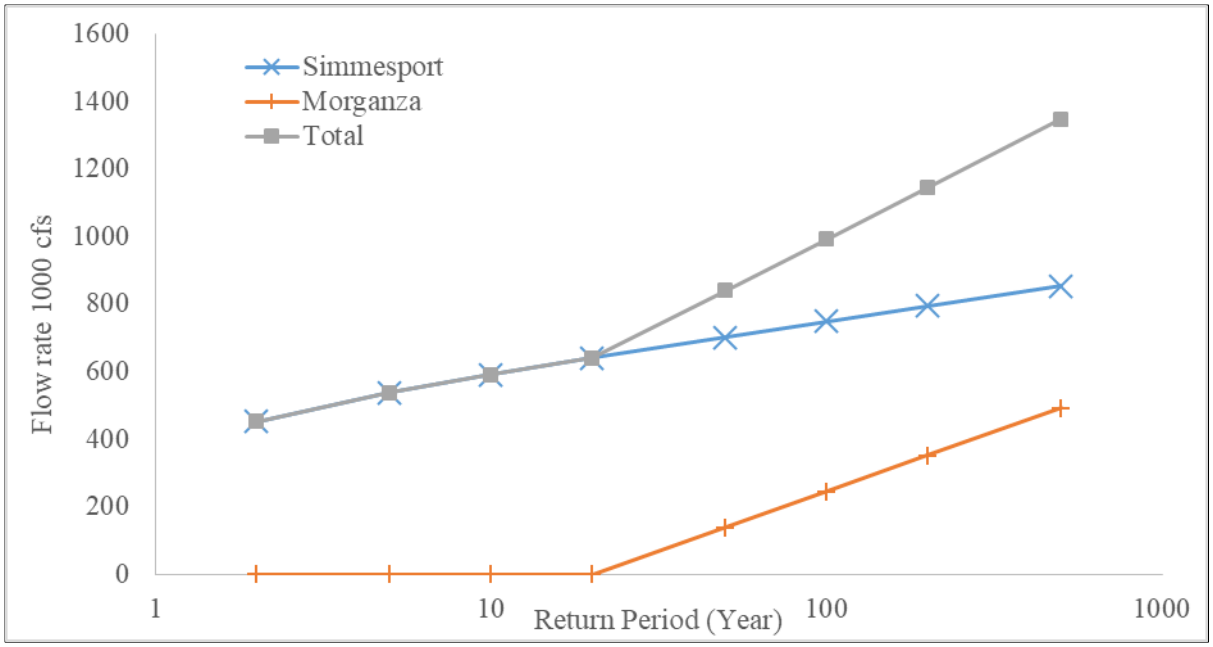

Figure C:3-4. Flow Rates vs Return Period for Riverine Boundaries at Simmesport and Morganza

Table C:3-4. Boundary Conditions for 16 Modeled Scenarios for Riverine Analysis

Return (% AEP)	Simmesport (x1000 cfs)	Morganza (x1000 cfs)	Gulf stage (ft NAVD88)
0.2	854.1	492.9	1.2
0.5	793.4	351.3	1.2
1	747.8	244.9	1.2
2	702	138.0	1.2
50	640.2	0.0	1.2
10	591.2	0.0	1.2
20	538.1	0.0	1.2
5	451.4	0.0	1.2
0.2	854.1	492.9	3.0
0.5	793.4	351.3	3.0
1	747.8	244.9	3.0
2	702	138.0	3.0
25	640.2	0.0	3.0
10	591.2	0.0	3.0
20	538.1	0.0	3.0
50	451.4	0.0	3.0

3.2 EXISTING CONDITIONS RESULTS

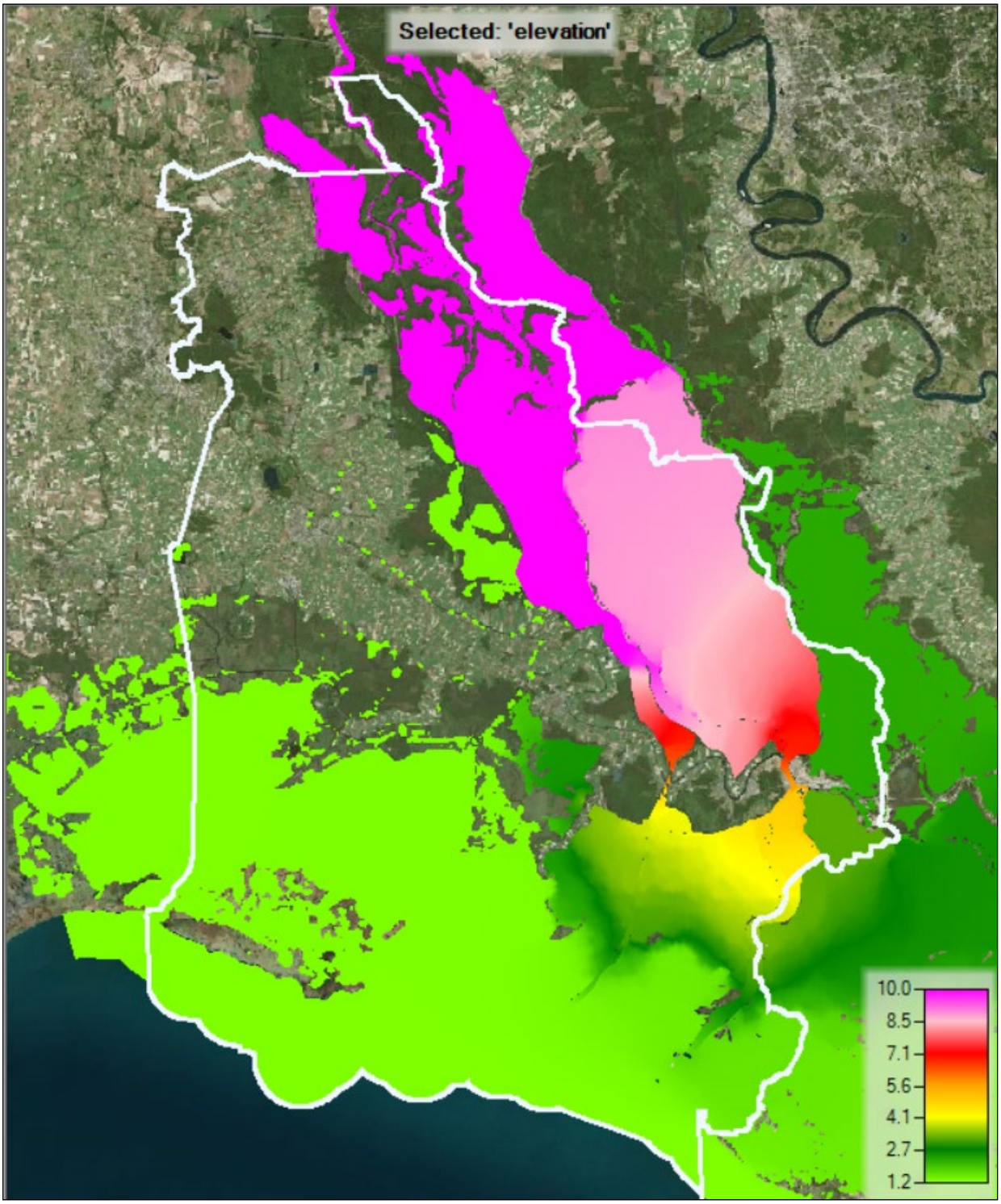

Figure 4. 50% AEP Existing Conditions Max Steady State Riverine Water Levels in ft NAVD 88

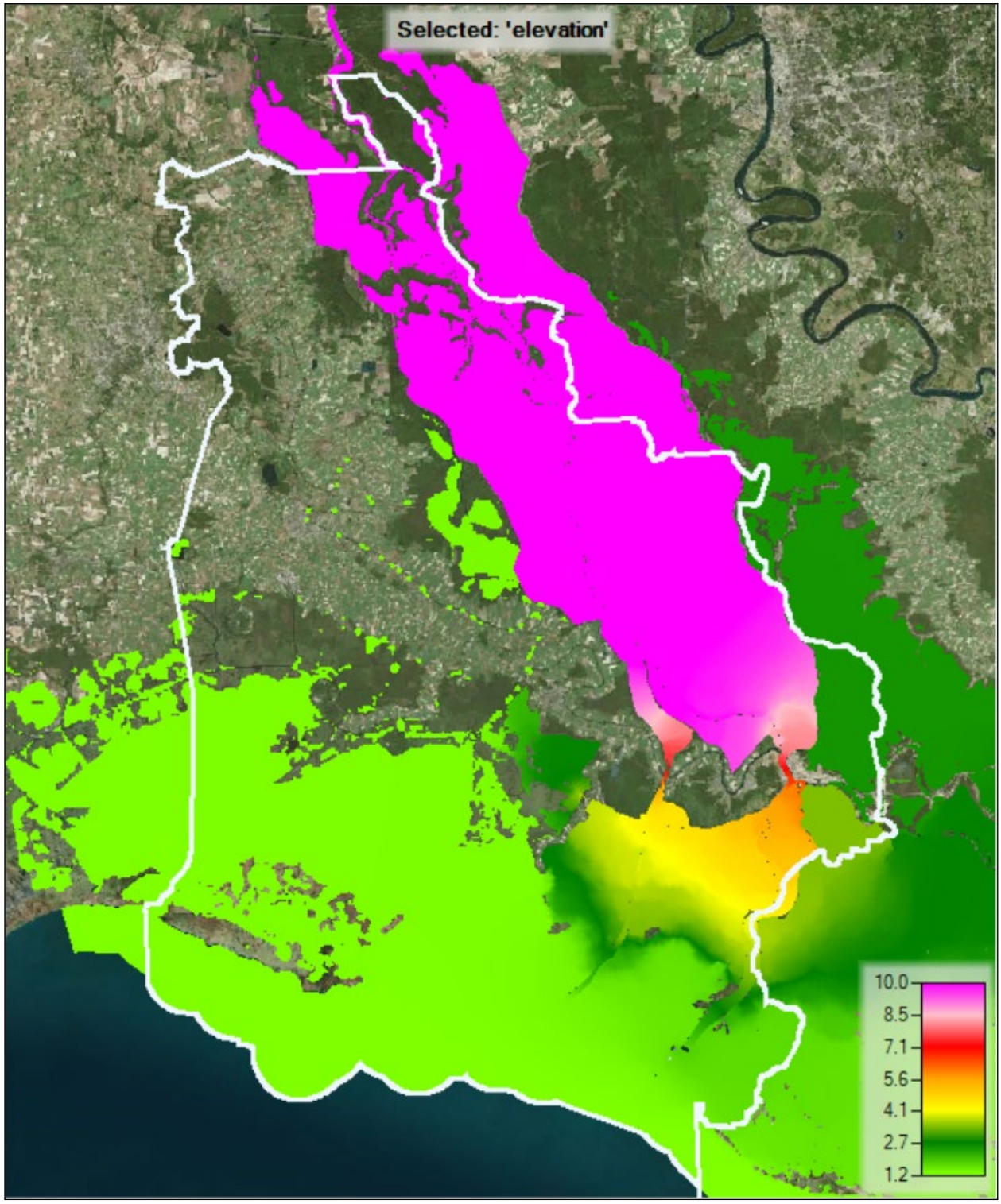

Figure 5. 20% AEP Existing Conditions Max Steady State Riverine Water Levels in ft NAVD 88

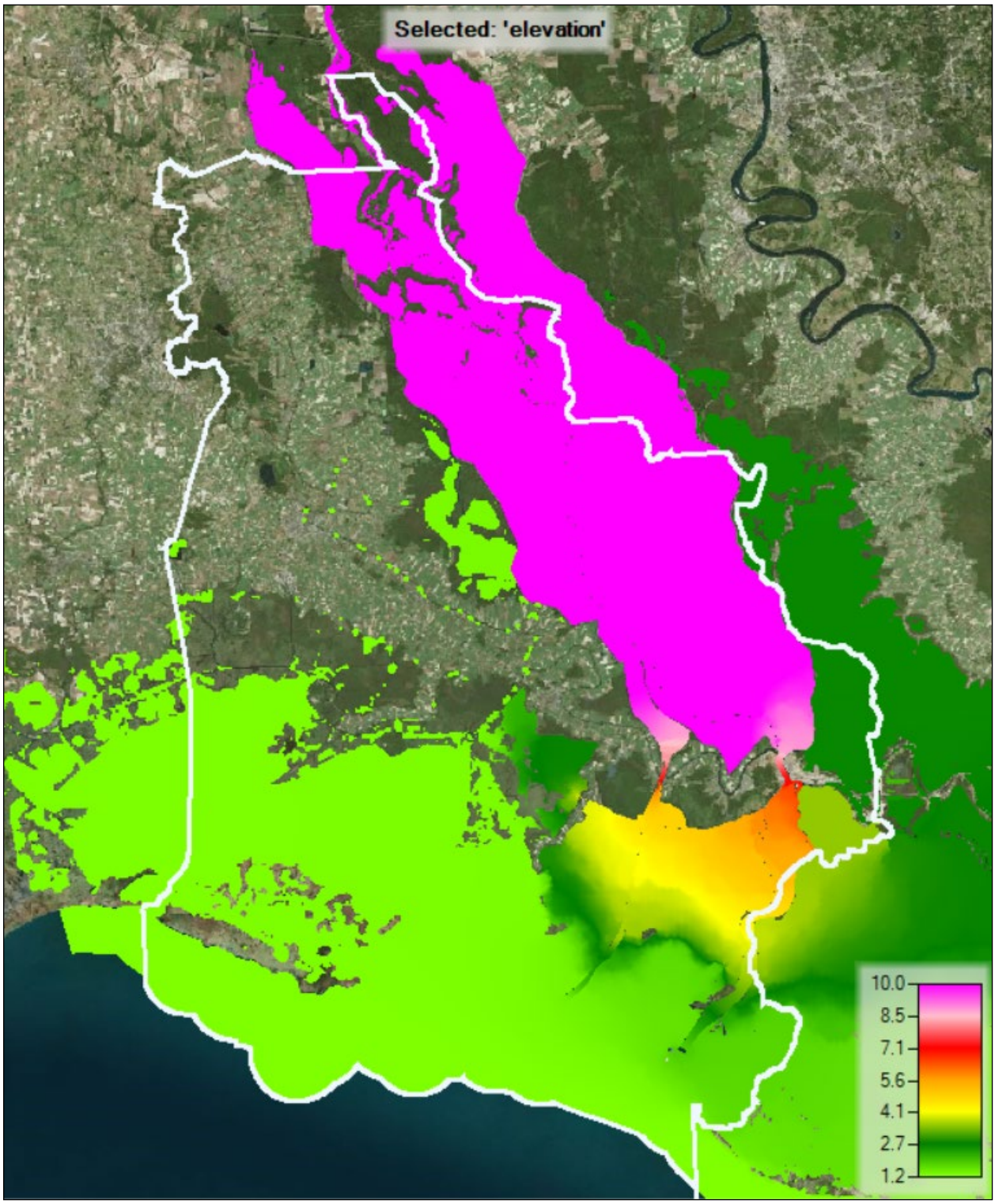

Figure C:3-7. 10% AEP Existing Conditions Max Steady State Riverine Water Levels in ft NAVD 88

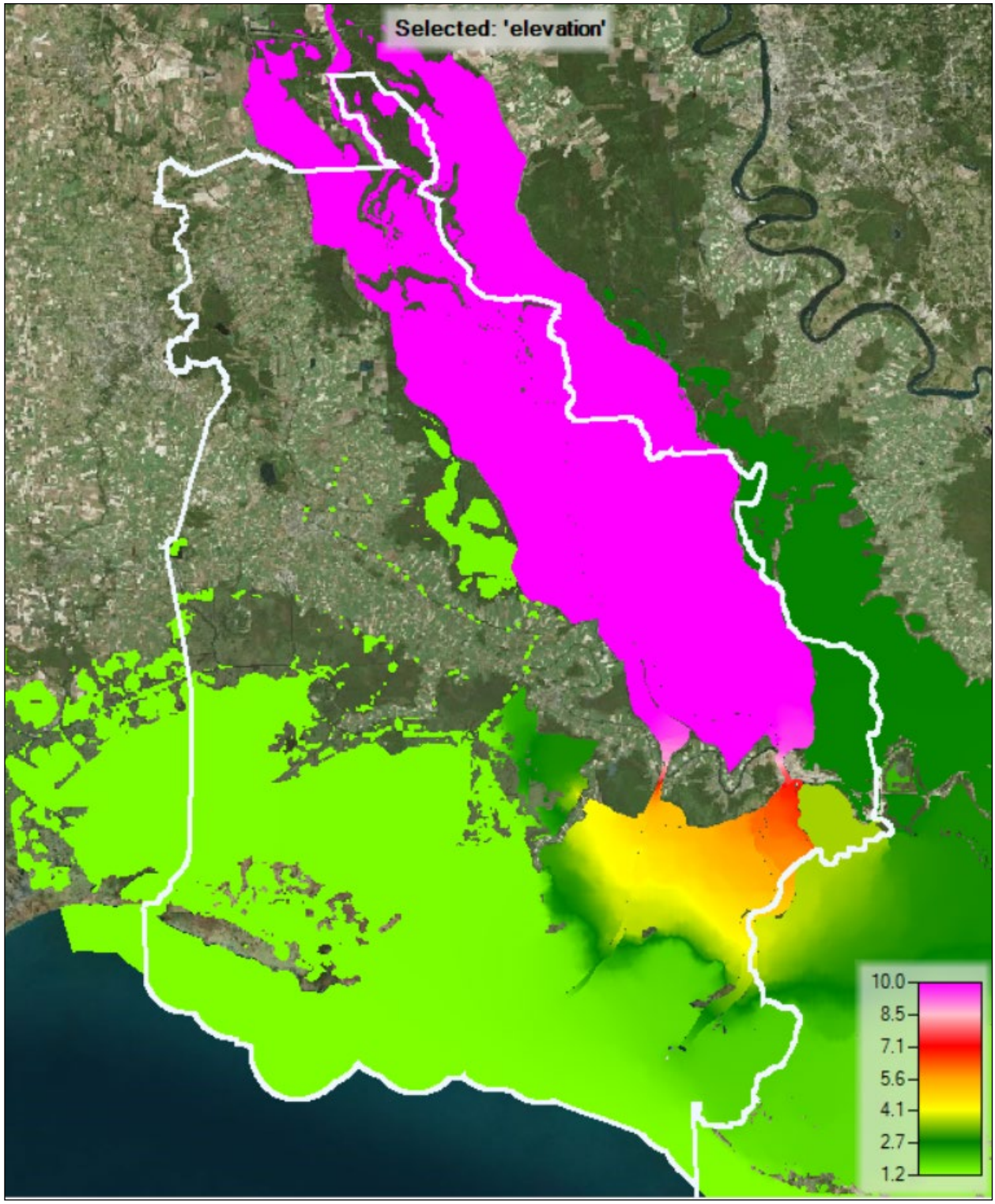

Figure C:3-8. 5% AEP Existing Conditions Max Steady State Riverine Water Levels in ft NAVD 88

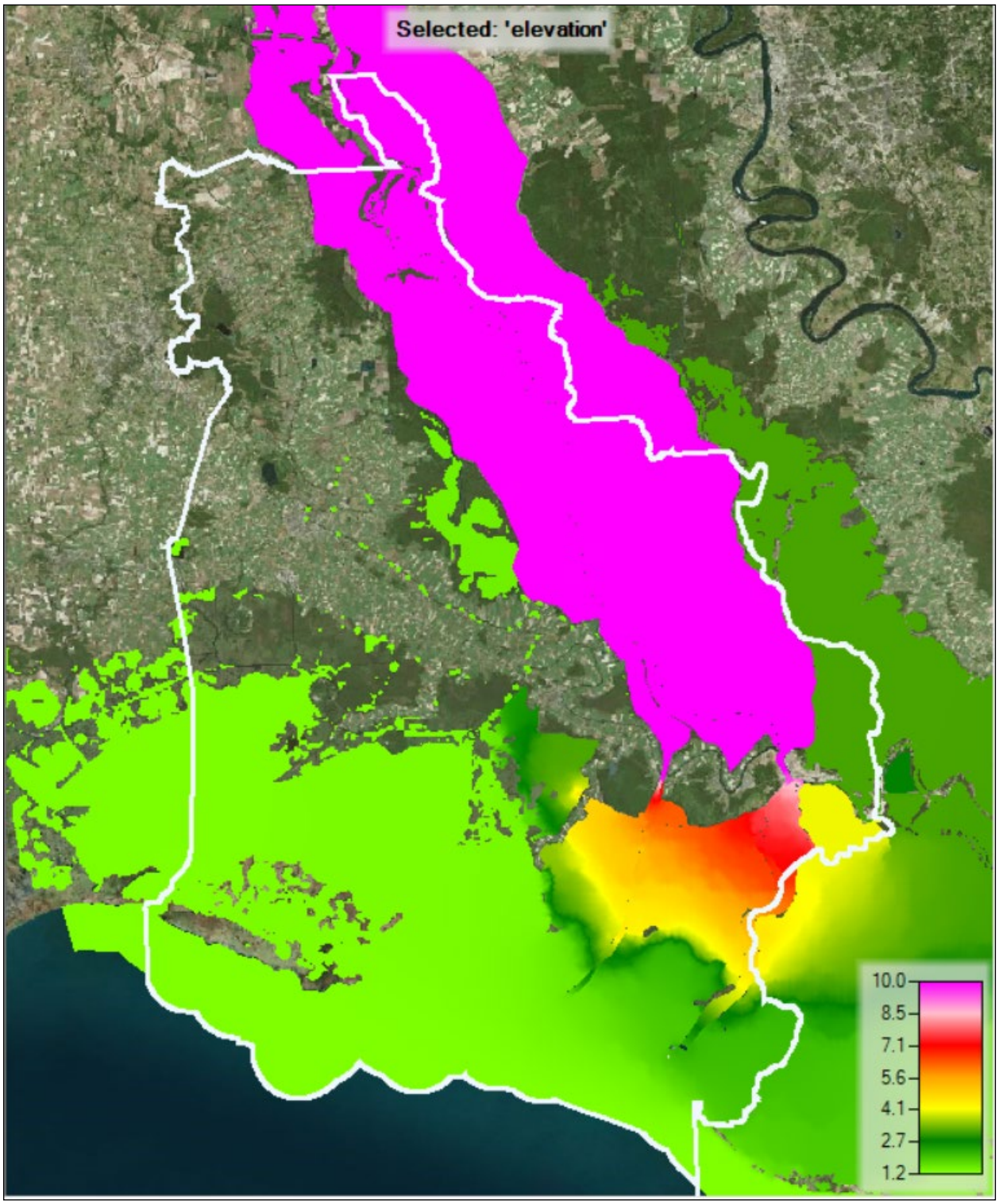

Figure C:3-9. 2% AEP Existing Conditions Max Steady State Riverine Water Levels in ft NAVD 88

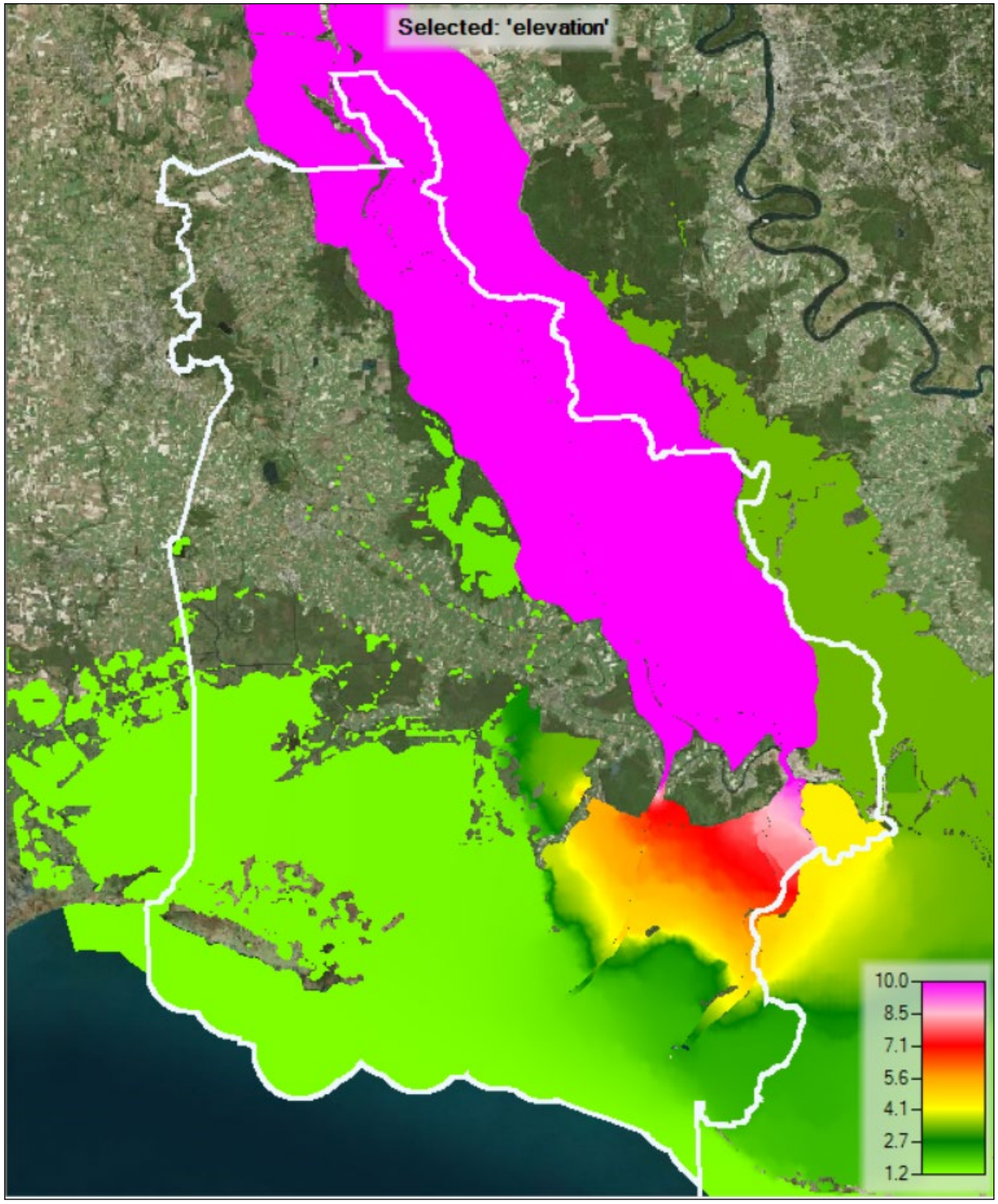

Figure C:3-10. 1% AEP Existing Conditions Max Steady State Riverine Water Levels in ft NAVD 88

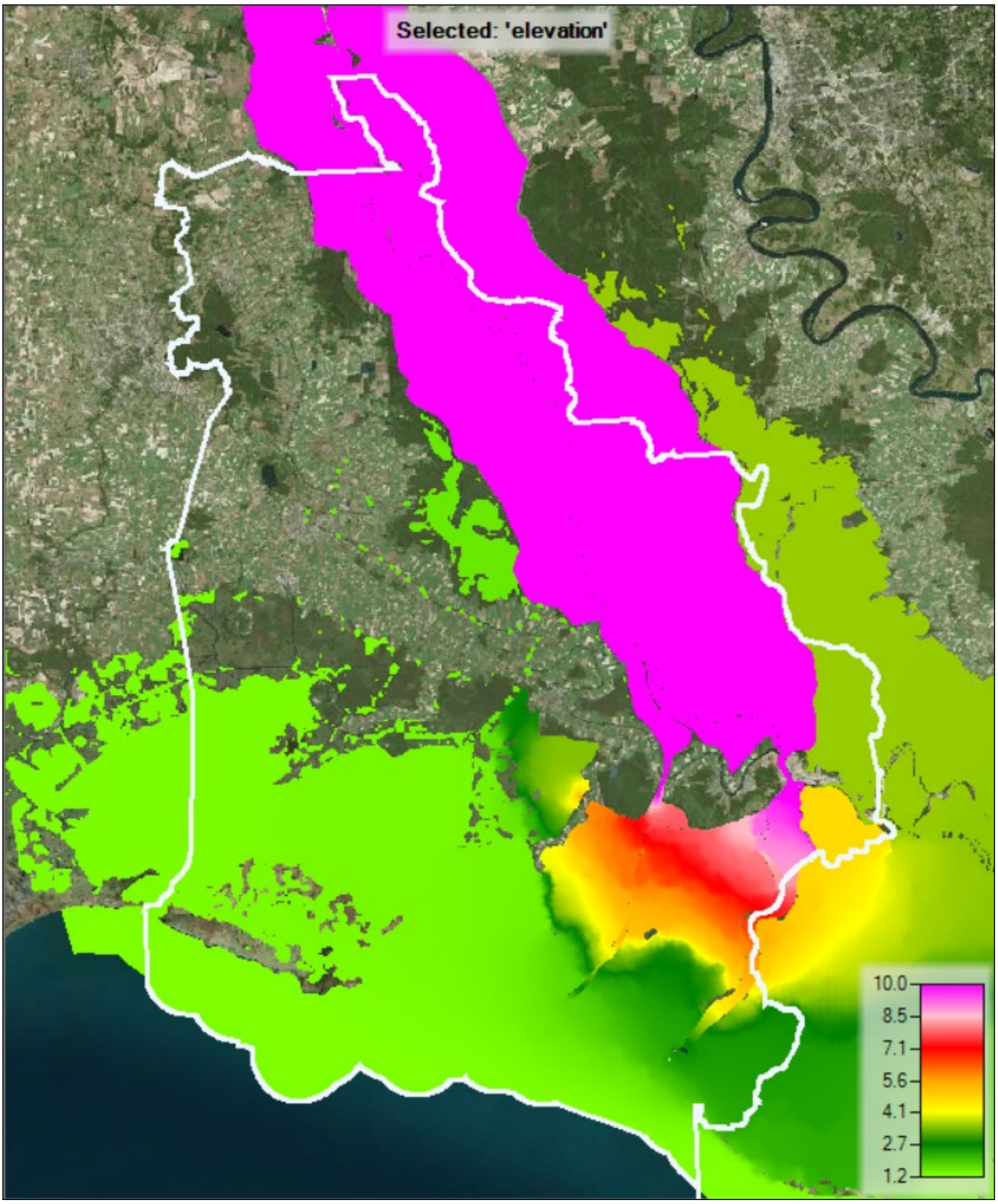

Figure C:3-11. 0.5% AEP Existing Conditions Max Steady State Riverine Water Levels in ft NAVD 88

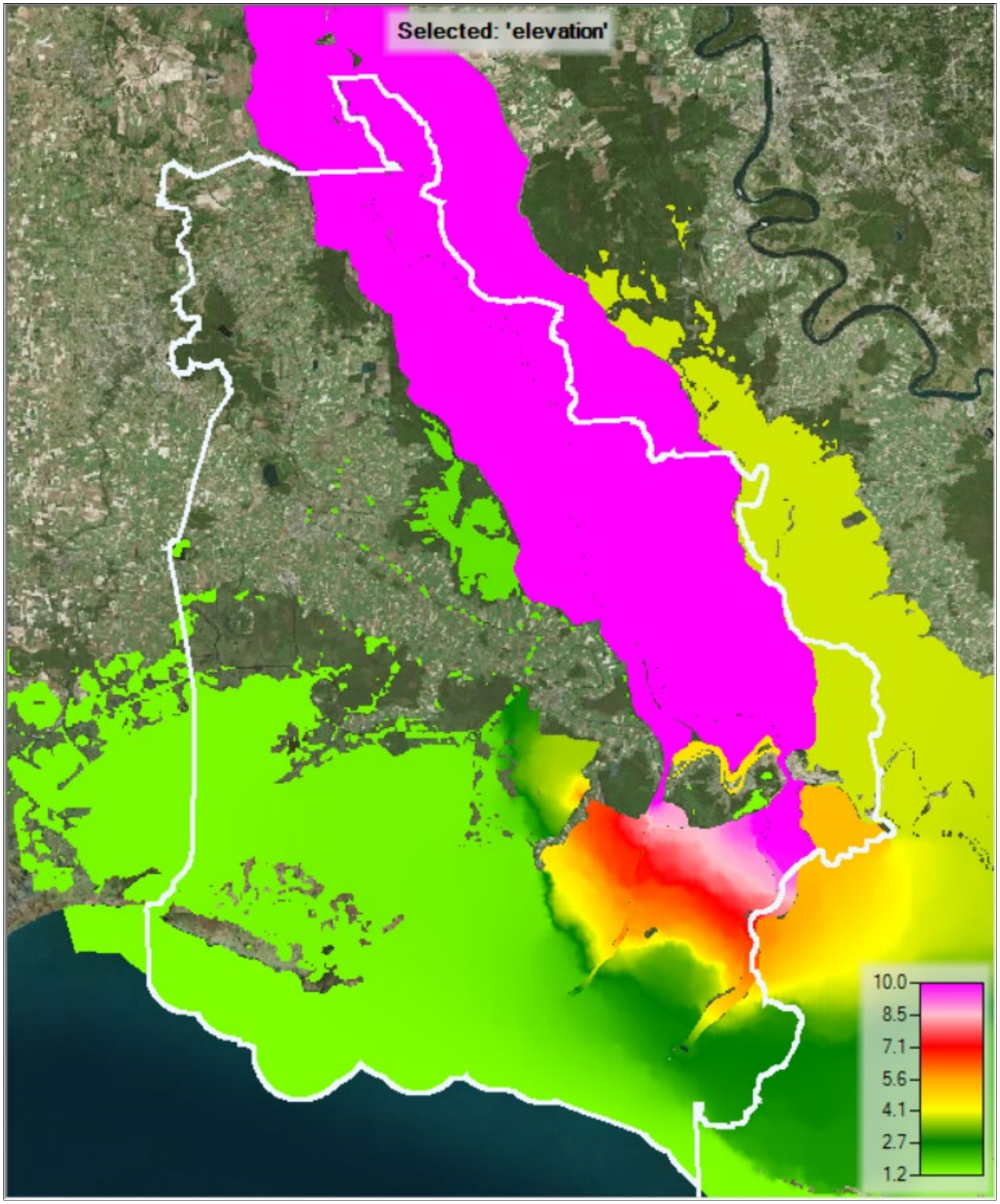

Figure C:3-12. 0.2% AEP Existing Conditions Max Steady State Riverine Water Levels in ft NAVD 88

3.3 FUTURE CONDITIONS RESULTS

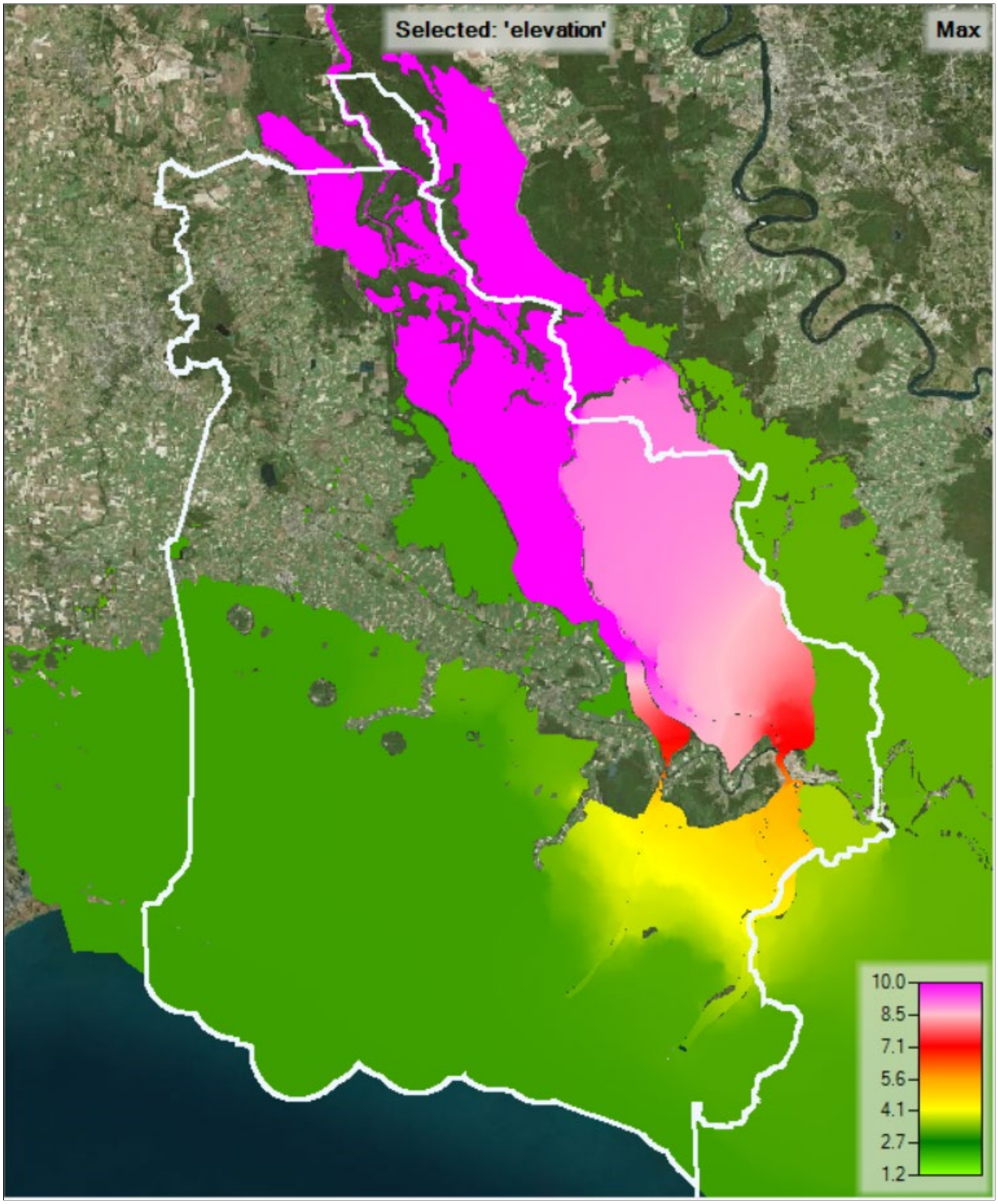

Figure C:3-13. 50% AEP Future Conditions Max Steady State Riverine Water Levels in ft NAVD 88

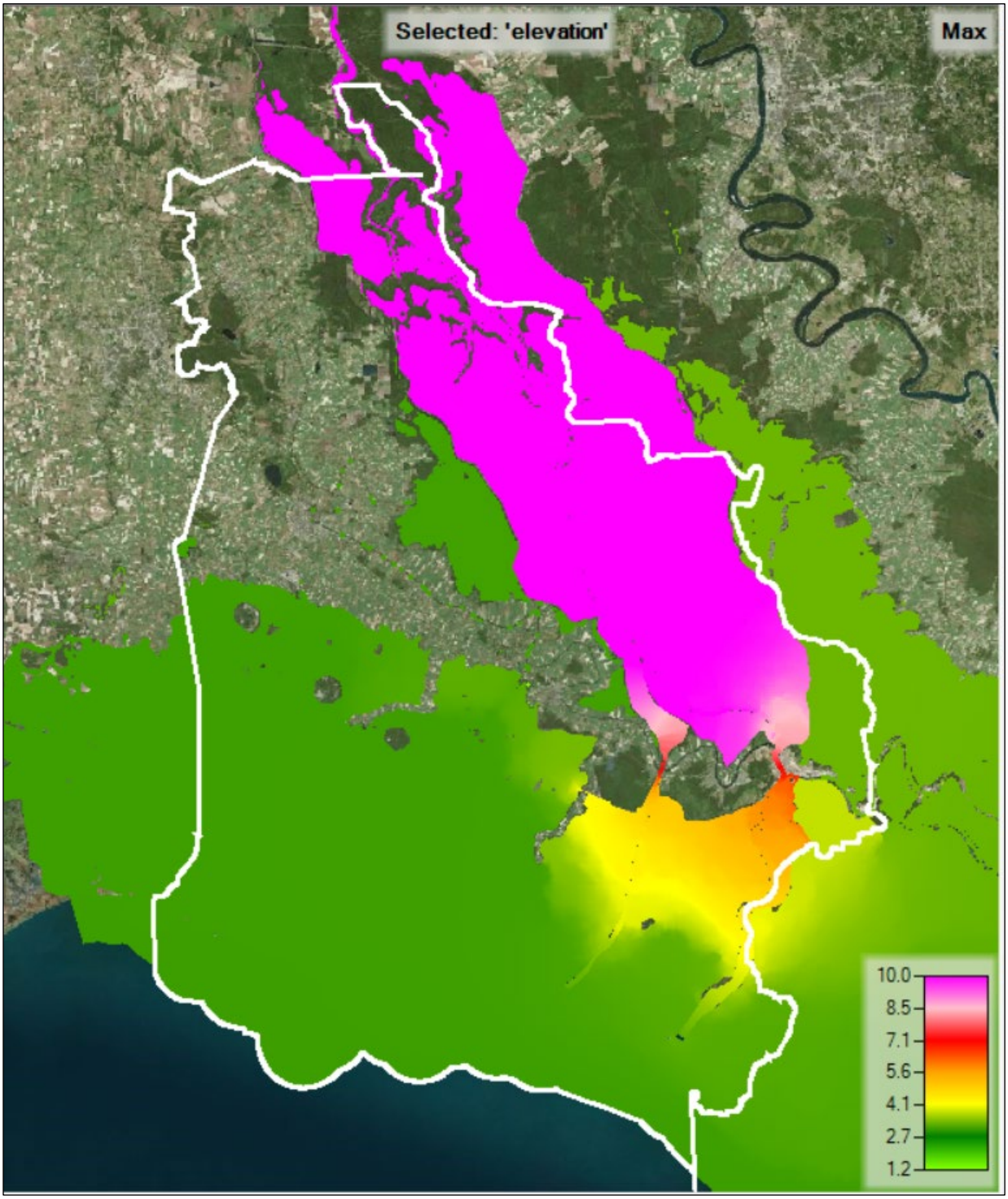

Figure C:3-14. 20% AEP Future Conditions Max Steady State Riverine Water Levels in ft NAVD88

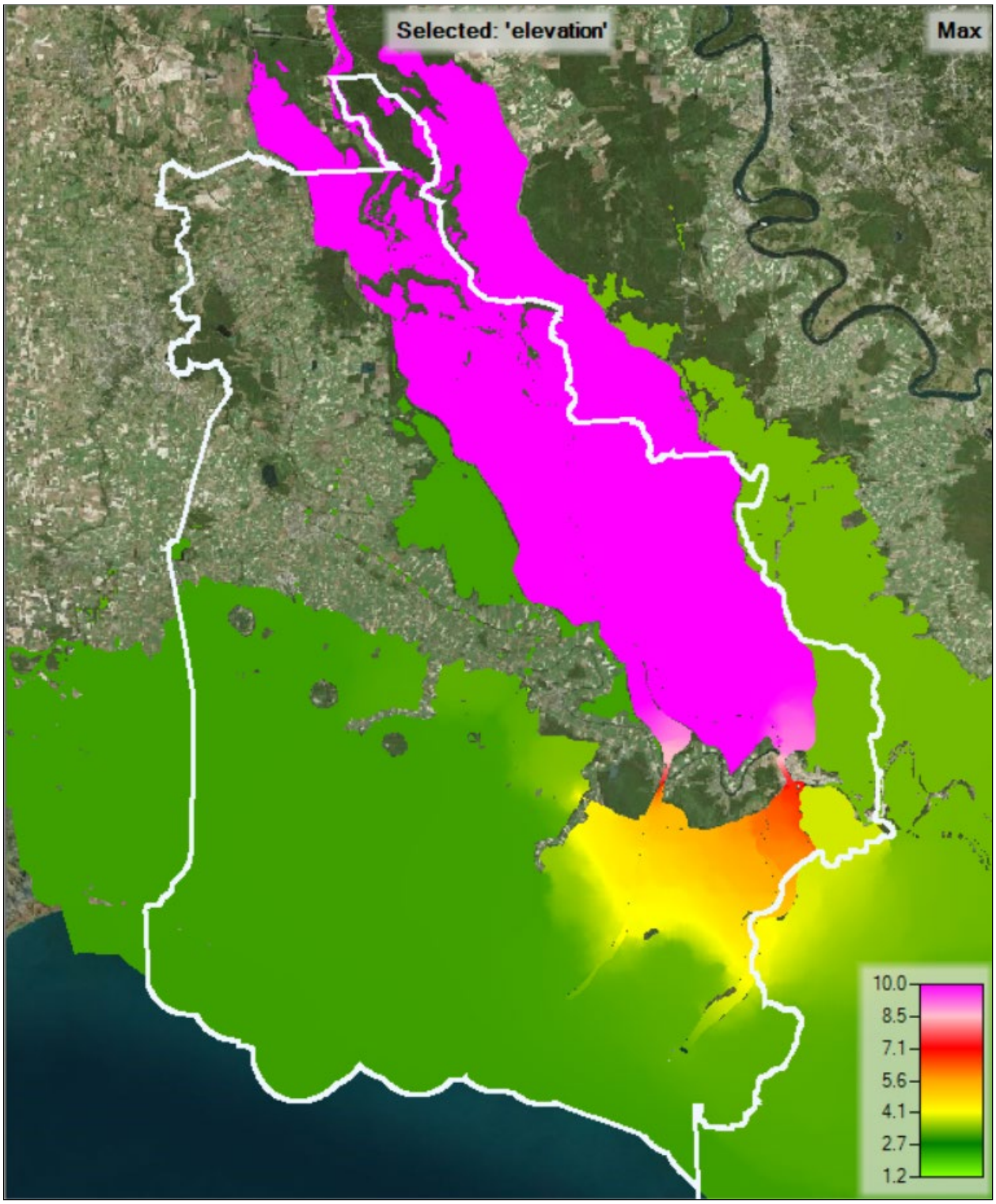

Figure C:3-15. 10% AEP Future Conditions Max Steady State Riverine Water Levels in ft NAVD 88

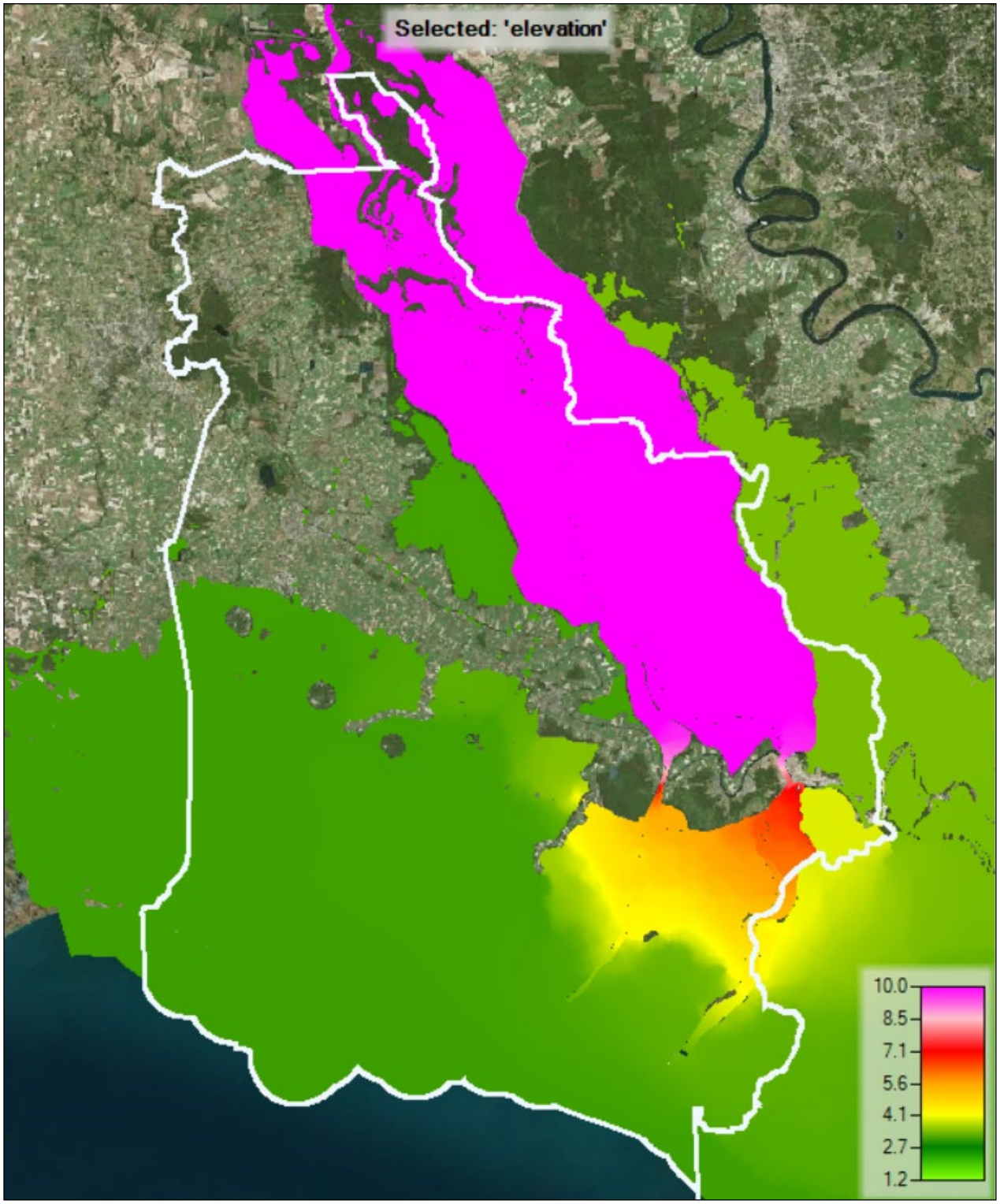

Figure C:3-16. 5% AEP Future Conditions Max Steady State Riverine Water Levels in ft NAVD 88

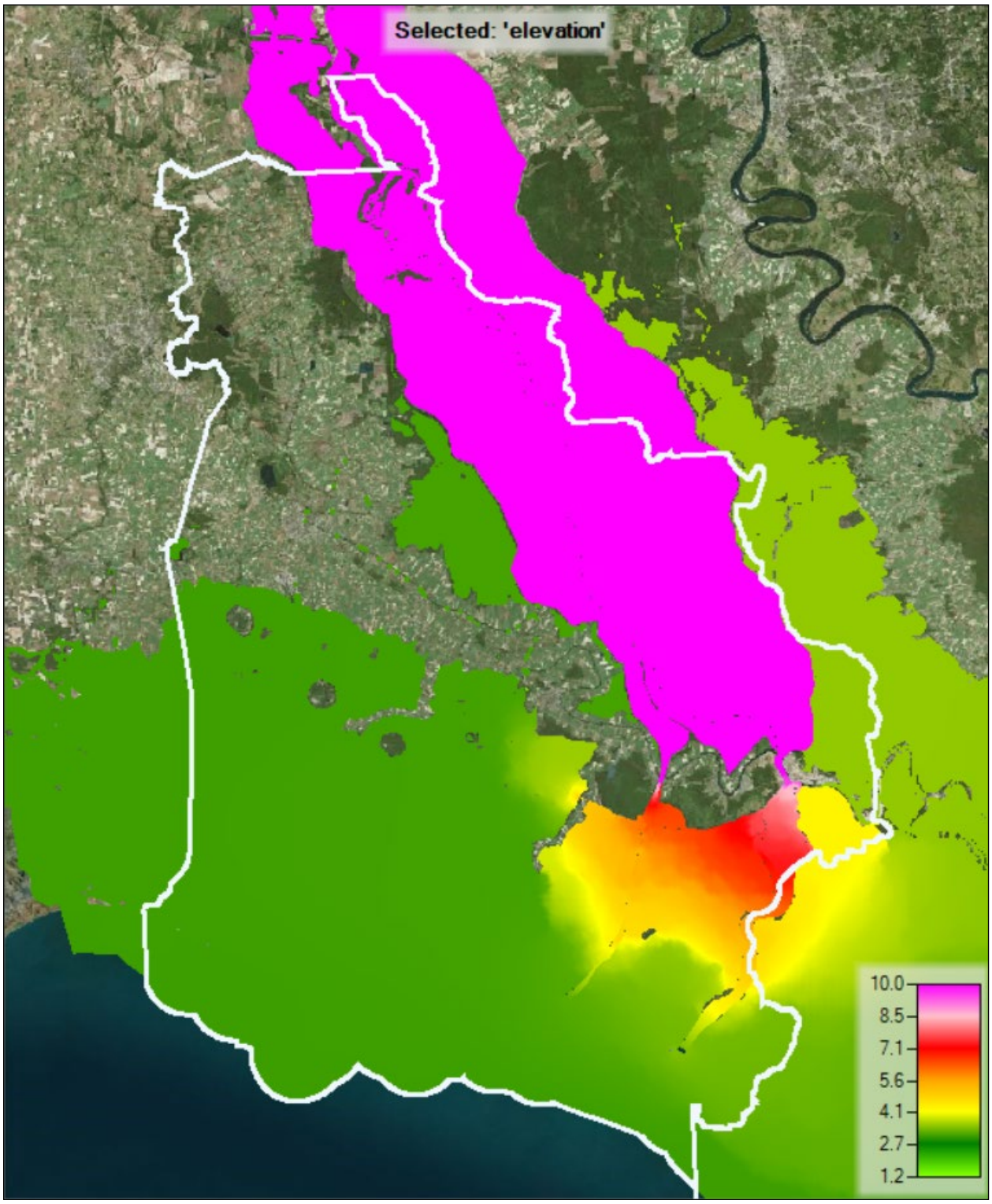

Figure C:3-17. 2% AEP Future Conditions Max Steady State Riverine Water Levels in ft NAVD 88

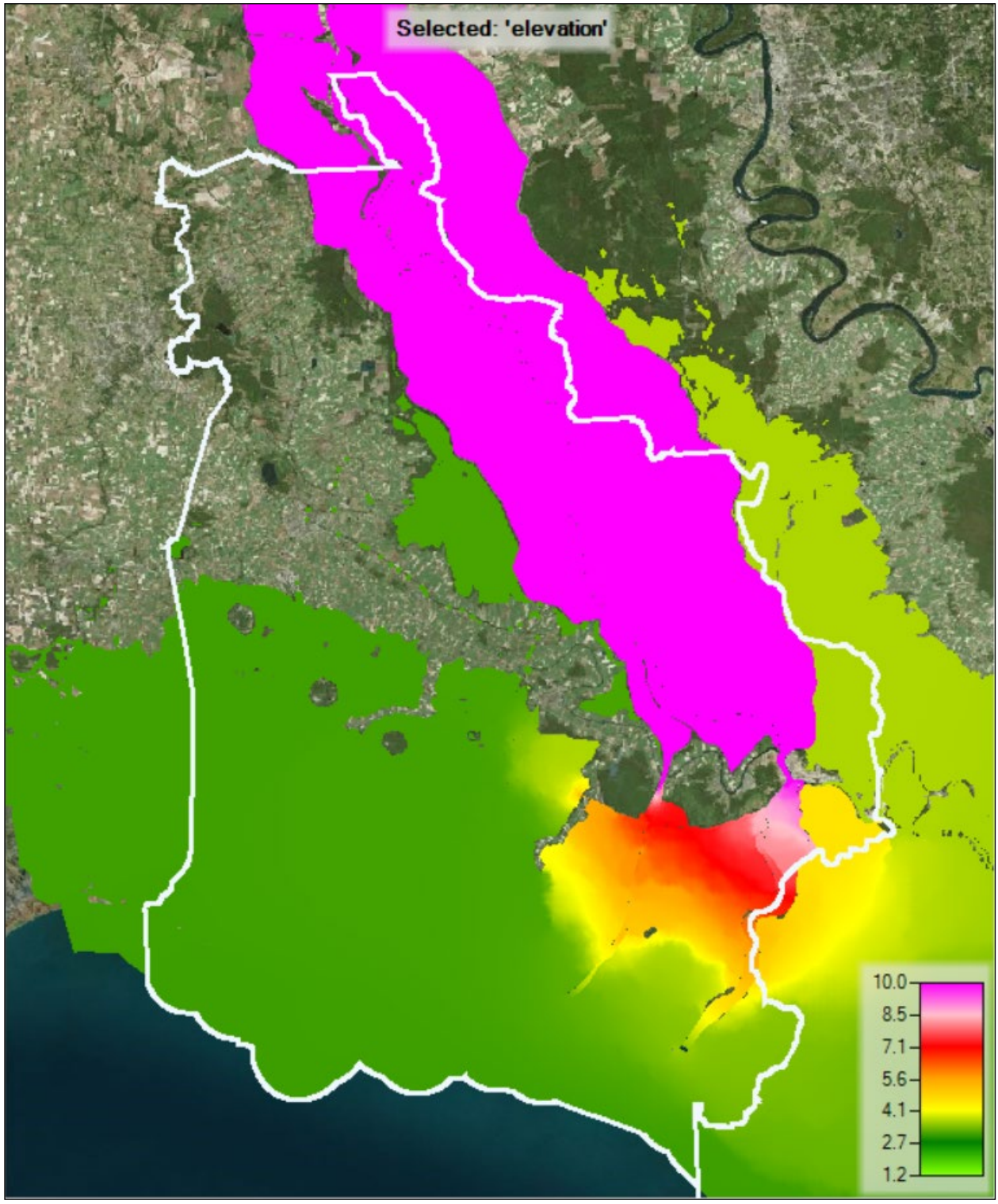

Figure C:3-18. 1% AEP Future Conditions Max Steady State Riverine Water Levels in ft NAVD 88

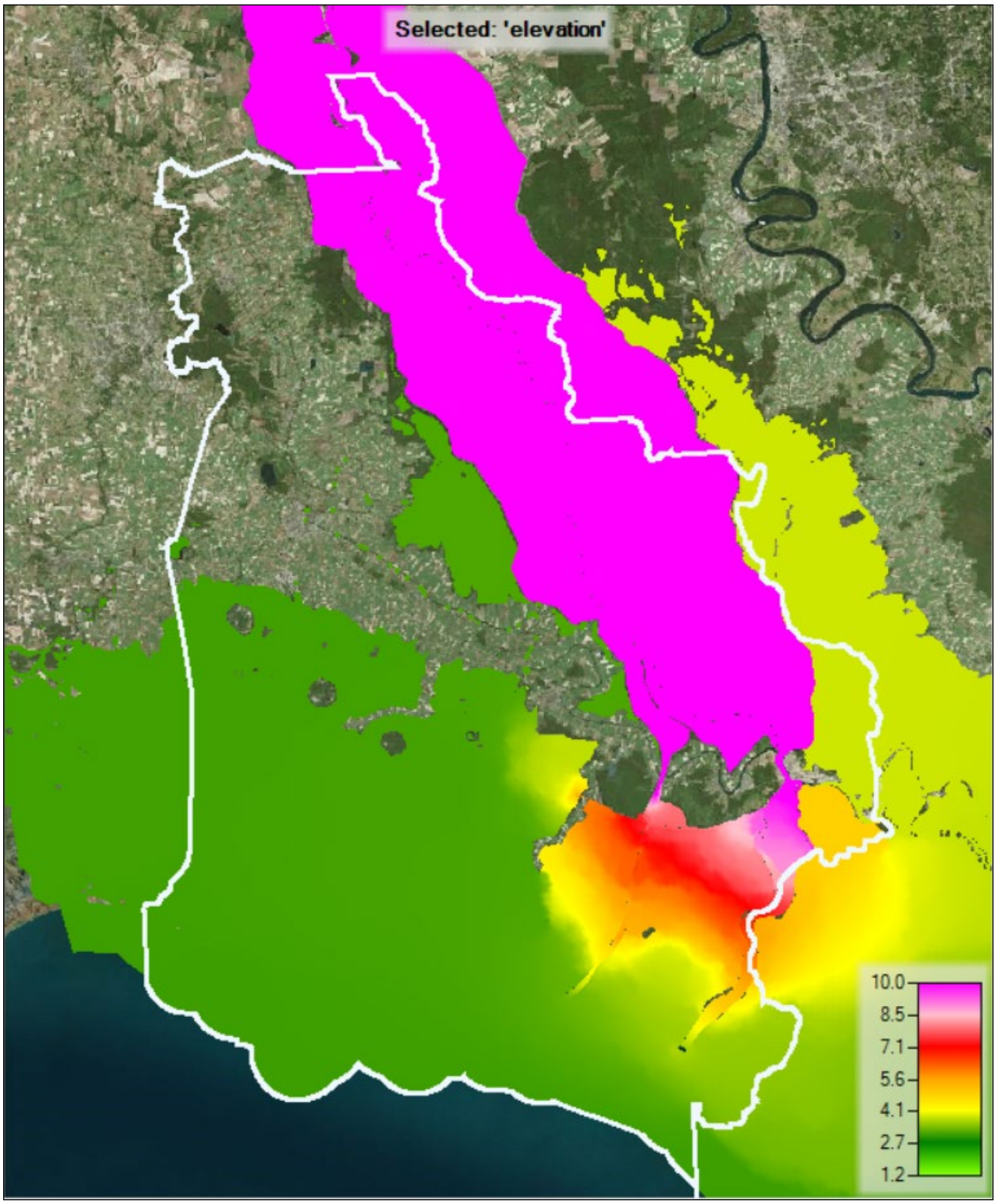

Figure C:3-19. 0.5% AEP Future Conditions Max Steady State Riverine Water Levels in ft NAVD 88

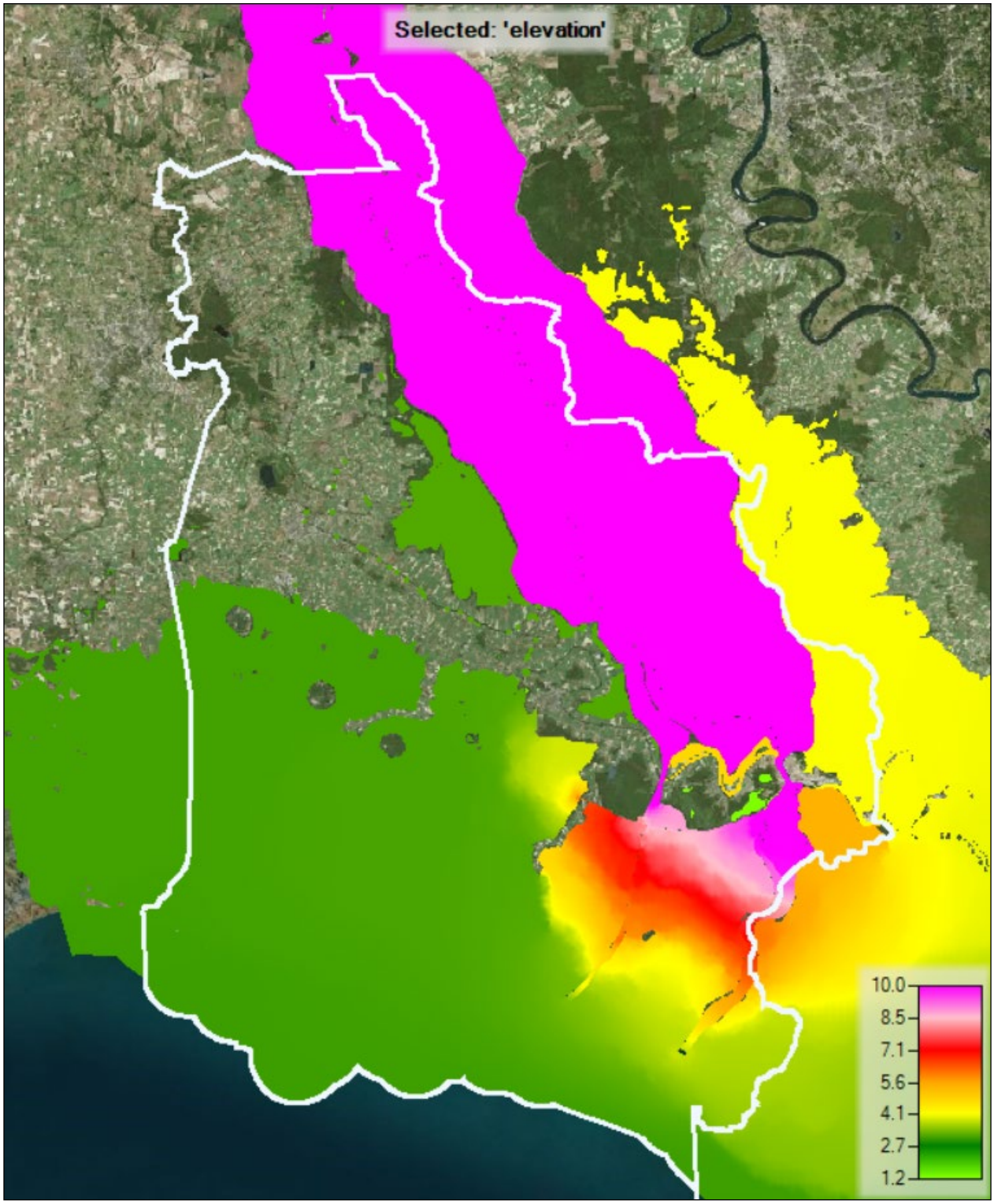

Figure C:3-20. 0.2% AEP Future Conditions Max Steady State Riverine Water Levels in ft NAVD 88

3.4 CONCLUSIONS

The impact of riverine flooding on the proposed levee measures is considered to be negligible as these levees are too far west of the hydraulic area of influence. The levees west of Berwick and the Bayou Sale levee choke the flow traveling west out of the Wax Lake delta through the GIWW. The stages reach near gulf level quickly beyond Morgan City and the Wax Lake outlet. The extent of this flooding is presented in Figure C:3-21. The proposed levee alignments are pictured in the west side of the authorization zone (black line).

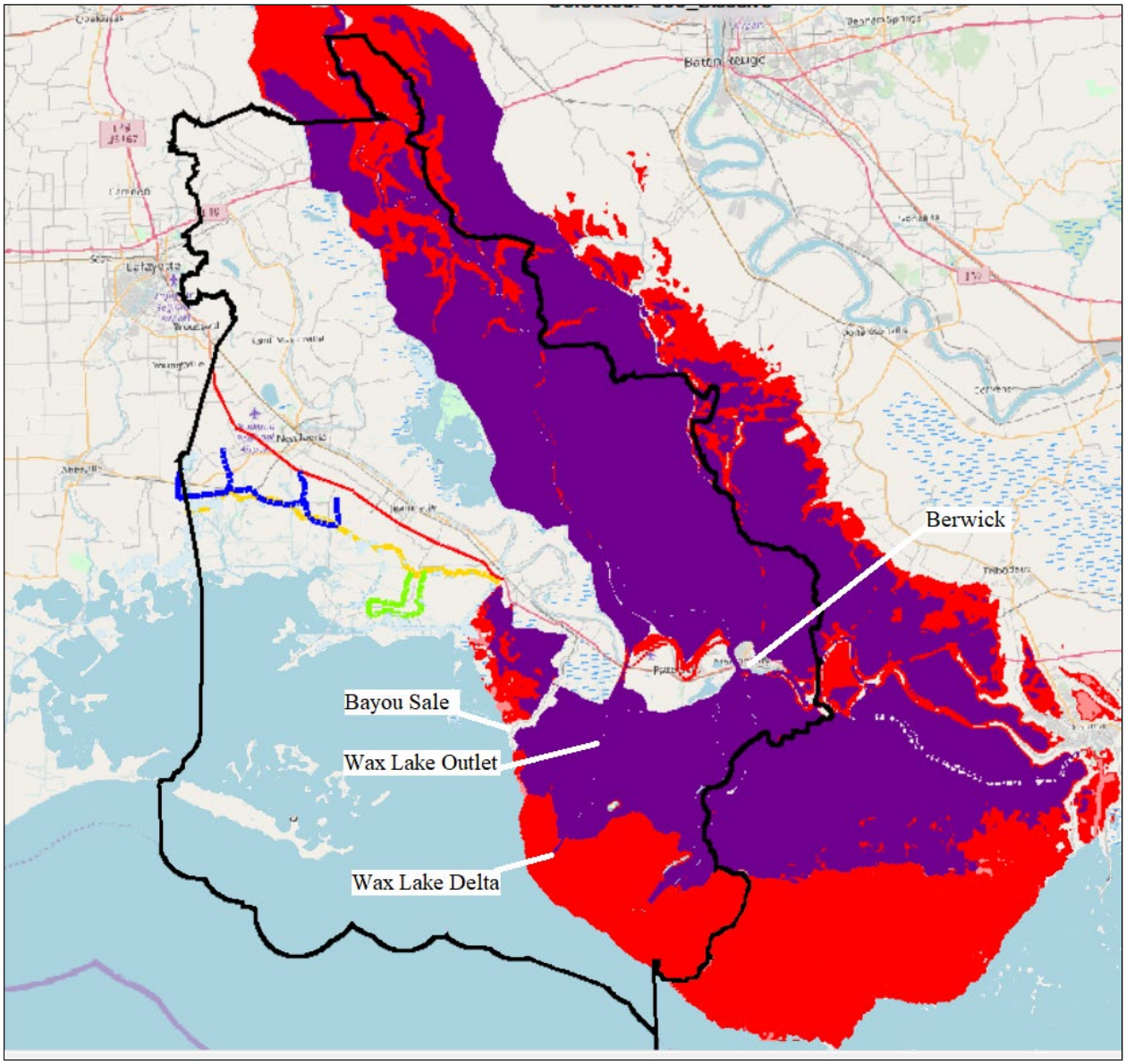

Figure C:3-21. Extent of Riverine Flooding Greater than 0.5 ft above GOM Stage for 50% (Purple) and 0.2% AEP (Red) Existing

3.5 FOLLOW UP ANALYSIS ON FLOW FREQUENCY DATA

The flow frequency statistics used for the riverine analysis was revisited and evaluated against updated results. This evaluation intended to serve as an understating of the error introduced by using the dataset ending in 2012 to inform boundary conditions instead of the updated 2019 dataset. Additionally, a comparison was conducted between the output using the expected moments analysis from bulletin 17C and the superseded method of moments analysis from bulletin 17B. The comparisons are presented in Tables C:3-5 and C:3-6. The flow frequency curves using the data range from 1962 – 2012 is not significantly different from the flow frequency curves produced with the data range extended through 2019. The maximum percent difference for any computed flow was for ACE of 20 percent at difference of 1.29 percent. The average difference for all frequencies is ~ 1 percent. This suggests that the use of the data ending in 2012 was sufficient for this analysis and reproduction of the previous modeling effort is likely unnecessary.

Table C:3-5. Comparison between Previous Riverine Statistics used (1962 -2012) and Updated Statistics (1962-2019)

	B17B 1962-2012 x1000cfs			B17B (1962-2019) x1000cfs			Δ(2012 analysis - 2019 analysis) x1000cfs			Δ(2012 analysis - 2019 analysis) % 2012		
ACE [%]	Computed	5% CI	95% CI	Computed	5% CI	95% CI	Computed	5% CI	95% CI	Computed	5% CI	95% CI
0.2	2745.2	3121.7	2495.9	2767.6	3112.4	2532.1	-22.4	9.3	-36.2	0.82	0.30	1.45
0.5	2573.1	2892.2	2358.3	2597.3	2890.6	2393.8	-24.2	1.6	-35.5	0.94	0.06	1.51
1	2439.9	2717	2250.5	2465	2720.5	2285.3	-25.1	-3.5	-34.8	1.03	0.13	1.55
2	2303	2539.2	2138.5	2328.5	2547.1	2172.1	-25.5	-7.9	-33.6	1.11	0.31	1.57
5	2113	2297.2	1980.4	2138.5	2309.7	2012.1	-25.5	-12.5	-31.7	1.21	0.54	1.60
10	1958.5	2105	1849	1983.2	2120	1878.7	-24.7	-15	-29.7	1.26	0.71	1.61
20	1787.8	1898.8	1699.3	1810.9	1915	1726.6	-23.1	-16.2	-27.3	1.29	0.85	1.61
50	1504.8	1577.8	1435	1523.6	1592.6	1457.6	-18.8	-14.8	-22.6	1.25	0.94	1.57
80	1270.2	1336.4	1195.8	1283.8	1346.5	1213.9	-13.6	-10.1	-18.1	1.07	0.76	1.51
90	1163.8	1232.5	1083.2	1174.5	1239.7	1098.9	-10.7	-7.2	-15.7	0.92	0.58	1.45
95	1083.3	1155	997.5	1091.6	1159.8	1011.2	-8.3	-4.8	-13.7	0.77	0.42	1.37
99	948.4	1026	854.2	952.3	1026.1	864.1	-3.9	-0.1	-9.9	0.41	0.01	1.16

Table C:3-6. Comparison between Previous Riverine Statistics used (1962 -2012) and Updated Statistics (1962-2019) Bulletin 17C

	B17B 1962-2012 x1000cfs			B17B (1962-2019) x1000cfs			Δ(2012 analysis - 2019 analysis) x1000cfs			Δ(2012 analysis - 2019 analysis) % 2012		
ACE [%]	Computed	5% CI	95% CI	Computed	5% CI	95% CI	Computed	5% CI	95% CI	Computed	5% CI	95% CI
0.2	2745.2	3121.7	2495.9	2769.5	3406.1	2467.8	-24.3	-284.4	28.1	0.89	9.11	1.13
0.5	2573.1	2892.2	2358.3	2601.6	3089.9	2357.7	-28.5	-197.7	0.6	1.11	6.84	0.03
1	2439.9	2717	2250.5	2470.8	2860.3	2266.4	-30.9	-143.3	-15.9	1.27	5.27	0.71
2	2303	2539.2	2138.5	2335.4	2637.7	2166.4	-32.4	-98.5	-27.9	1.41	3.88	1.30
5	2113	2297.2	1980.4	2146.4	2351.6	2016.6	-33.4	-54.4	-36.2	1.58	2.37	1.83
10	1958.5	2105	1849	1991.5	2139	1885.2	-33	-34	-36.2	1.68	1.62	1.96
20	1787.8	1898.8	1699.3	1819	1925.2	1731	-31.2	-26.4	-31.7	1.75	1.39	1.87
50	1504.8	1577.8	1435	1530	1604.6	1459	-25.2	-26.8	-24	1.67	1.70	1.67
80	1270.2	1336.4	1195.8	1287.5	1352.8	1217	-17.3	-16.4	-21.2	1.36	1.23	1.77
90	1163.8	1232.5	1083.2	1176.7	1242.6	1096.3	-12.9	-10.1	-13.1	1.11	0.82	1.21
95	1083.3	1155	997.5	1092.5	1162.3	998.2	-9.2	-7.3	-0.7	0.85	0.63	0.07
99	948.4	1026	854.2	950.6	1035.6	822.8	-2.2	-9.6	31.4	0.23	0.94	3.68

Section 4
Levee Heights

The existing (2025) and future (2075) 2 percent and 1 percent hydraulic boundary conditions were used to compute the 2 percent and 1 percent annual exceedence levee design elevations. All levees were designed using a slope of 1 on 4. The design criteria for the levees are:

For the design still water, wave height and wave period, the maximum allowable average wave overtopping of 0.1 cubic feet per second per foot (cfs/ft) at 90 percent level of assurance and 0.01 cfs/ft at 50 percent level of assurance for grass-covered levees; no minimum freeboard required.

The application of a Monte Carlo analysis was used to determine the levee design elevation. In the Monte Carlo analysis, the overtopping algorithm is repeated to compute the overtopping rate many times. Based on these outputs, a statistical distribution can be derived from the resulting overtopping rates. The parameters that are included in the Monte Carlo analysis are the surge elevation, wave height, and wave period.

To determine the overtopping rate in the Monte Carlo analysis, the probabilistic overtopping formulations from Van der Meer (TAW, 2002) are applied for levees (see Figure). Along with the geometric parameters (levee height and slope), hydraulic input parameters for determination of the overtopping rate in Equations 1 and 2 are the water elevation (ζ), the significant wave height (H_s) and the peak wave period (T_p).

Figure C:4-2 graphically shows the overtopping for a levee situation including the most relevant parameters. In the design process, we use the best estimate 2 percent and 1 percent values for these parameters from the JPM-OS method (Resio, 2007); uncertainty in these values exists. Resio (2007) has provided a method to derive the standard deviation in the 2 percent and 1 percent surge elevations. Standard deviation values of 10 percent of the average significant wave height and 20 percent of the peak period were used (Smith, 2006, pers. comm.). In the absence of data, all uncertainties are assumed to be normally distributed.

Van der Meer overtopping formulations

The overtopping formulation from Van der Meer reads (TAW, 2002):

$$\frac{q}{\sqrt{gH_{m0}^3}} = \frac{0.067}{\sqrt{\tan\alpha}}\gamma_b\xi_0\exp\left(-4.75\frac{R_c}{H_{m0}}\frac{1}{\xi_0\gamma_b\gamma_f\gamma_\beta\gamma_v}\right)$$

$$with \quad \max imum: \quad \frac{q}{\sqrt{gH_{m0}^3}} = 0.2\exp\left(-2.6\frac{R_c}{H_{m0}}\frac{1}{\gamma_f\gamma_\beta}\right) \qquad (1)$$

With:
q : average overtopping rate [cfs/ft]
g : gravitational acceleration [ft/s^2]
H_{m0} : wave height at toe of the structure [ft]
ξ_0: surf similarity parameter [-]
α : slope [-]
R_c : freeboard [ft]
γ : coefficient for presence of berm (b), friction (f), wave incidence (β), vertical wall (v)

The surf similarity parameter $\xi 0$ is defined herein as $\xi_0 = \tan\alpha / \sqrt{s_0}$ with α the angle of slope and s_0 the wave steepness. The wave steepness follows from $s0 = 2\pi H_{m0} / (g\ Tm\text{-}10^2)$. The coefficients -4.75 and -2.6 in Equation 1 are the mean values. The standard deviations of these coefficients are equal to 0.5 and 0.35, respectively and these errors are normally distributed (TAW, 2002). The reader is referred to TAW (2002) for definitions of the various coefficients for presence of berm, friction, wave incidence, vertical wall.

Equation 1 is valid for $\xi_0 < 5$ and slopes steeper than 1:8. For values of $\xi_0 > 7$ the following equation is proposed for the overtopping rate:

$$\frac{q}{\sqrt{gH_{m0}^3}} = 10^{-0.92}\exp\left(-\frac{R_c}{\gamma_f\gamma_\beta H_{m0}(0.33+0.022\xi_0)}\right) \qquad (2)$$

The overtopping rates for the range $5 < \xi_0 < 7$ are obtained by linear interpolation of Equation 1 and 2 using the logarithmic value of the overtopping rates. For slopes between 1:8 and 1:15, the solution should be found by iteration. If the slope is less than 1:15, it should be considered as a berm or a foreshore depending on the length of the section compared to the deep water wavelength. The coefficients -0.92 is the mean value. The standard deviation of this coefficient is equal to 0.24 and the error is normally distributed (TAW, 2002).

Figure C:4-1. Van der Meer Overtopping Formula

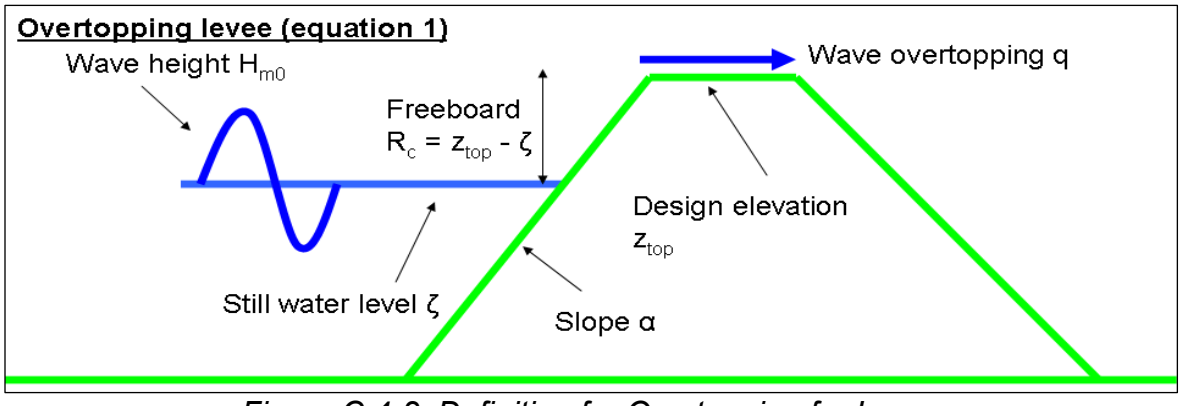

Figure C:4-2. Definition for Overtopping for Levee

The Monte Carlo Analysis is executed as:

1. Draw a random number between 0 and 1 to set the exceedence probability (p).
2. Compute the water elevation from a normal distribution using the mean 1 percent surge elevation and standard deviation as parameters and with an exceedence probability (p).
3. Draw a random number between 0 and 1 to set the exceedence probability (p).
4. Compute the wave height and wave period from a normal distribution using the mean 1 percent wave height/wave period and the associated standard deviation and with an exceedence probability (p).
5. Repeat step 3 and 4 for the three overtopping coefficients independently.
6. Compute the overtopping rate for these hydraulic parameters and overtopping coefficients determined in step 2, 4 and 5 using the Van der Meer overtopping formulations for levees or the Franco & Franco equation for floodwalls (see Equations 1 and 2 in the textbox).
7. Repeat the Step 1 through 5 a large number of times. (N)
8. Compute the 50 percent and 90 percent confidence limit of the overtopping rate. (i.e. q_{50} and q_{90})

The procedure is implemented in the numerical software package MATLAB because it is a computationally intensive procedure. MATLAB is a high-level technical computing language and interactive environment for algorithm development, data visualization, data analysis, and numeric computation.

The results were compiled for the 2 percent and 1 percent elevations for existing and future conditions. The segments for each levee alignment are presented in Figures C:4-3 through C:4-6 and the data is tabulated in Tables C:4-1 through C:4-16.

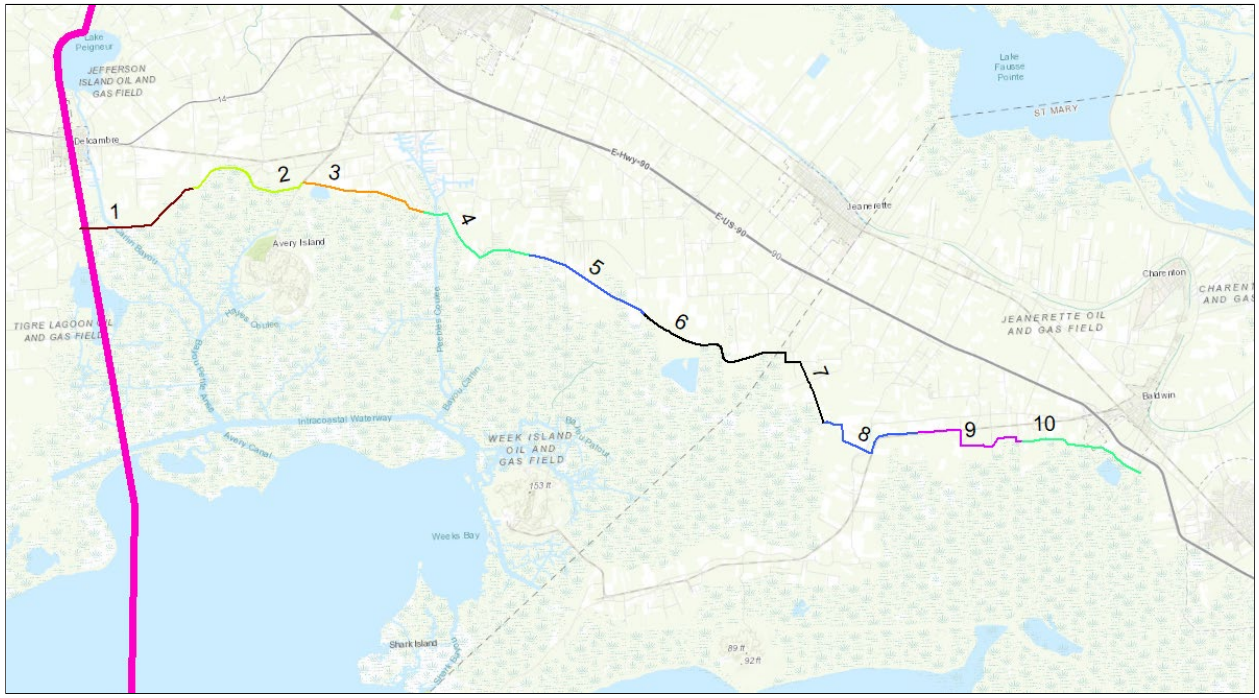

Figure C:4-3. Segments of the CLA

Table C:4-1. Existing Conditions 2% Surge, Wave Parameters & Levee Elevations for the Comprehensive Levee Alignment

Hydraulic Reach	SWE (ft)	Std. Dev.	Hs (ft)	Tp (s)	Levee Elevation (ft) NAVD 88(2004.65)
1	8.7	1.2	3.0	7.0	15.0
2	8.4	1.2	2.0	7.0	12.5
3	7.7	1.2	3.0	7.0	14.0
4	7.4	1.2	2.0	7.0	11.5
5	6.5	1.2	2.0	7.0	10.5
6	6.0	1.2	1.5	5.0	8.5
7	5.9	1.2	1.5	5.0	8.5
8	6.1	1.2	3.0	5.0	10.5
9	6.5	1.2	1.5	8.0	9.0
10	6.3	1.2	3.0	7.0	11.5

Table C:4-2. Existing Conditions 1% Surge and Wave Parameters with Levee Elevations for the Comprehensive Levee Alignment

Hydraulic Reach	SWE (ft)	Std. Dev.	Hs (ft)	Tp (s)	Levee Elevation (ft) NAVD88(2004.65)
1	10.3	1.2	4.0	8.0	19.5
2	9.9	1.2	3.0	8.0	16.5
3	9.3	1.2	4.0	8.0	17.5
4	9.0	1.2	3.0	8.0	15.5
5	8.3	1.2	3.0	8.0	15.0
6	8.0	1.2	2.0	7.0	12.0
7	7.8	1.2	2.0	8.0	11.5
8	7.8	1.2	4.0	7.0	14.5
9	8.0	1.2	4.0	8.0	15.0
10	7.8	1.2	4.0	8.0	15.0

Table C:4-3 Future Conditions 2% Surge and Wave Parameters with Levee Elevations for the Comprehensive Levee Alignment

Hydraulic Reach	SWE (ft)	Std. Dev.	Hs (ft)	Tp (s)	Levee Elevation (ft) NAVD 88(2004.65)
1	11.1	1.2	4.0	7.0	20.0
2	10.8	1.2	3.5	7.0	18.5
3	10.2	1.2	3.5	7.0	18.0
4	9.9	1.2	3.0	7.0	16.5
5	9.1	1.2	3.0	7.0	15.5
6	8.8	1.2	1.5	7.0	11.5
7	8.6	1.2	1.5	7.0	11.5
8	8.6	1.2	3.5	7.0	16.0
9	9.0	1.2	4.0	7.0	17.0
10	8.6	1.2	3.0	8.0	15.0

Table C:4-4. Future Condition 1% Surge and Wave Parameters with Levee Elevations for the Comprehensive Levee Alignment

Hydraulic Reach	SWE (ft)	Std. Dev.	Hs (ft)	Tp (s)	Levee Elevation (ft) NAVD88(2004.65)
1	12.7	1.2	5.5	8.0	24.5
2	12.5	1.2	4.5	8.0	23.0
3	12.0	1.2	4.5	8.0	22.5
4	11.7	1.2	4.0	8.0	21.0
5	11.1	1.2	4.0	8.0	20.5
6	10.9	1.2	2.5	7.0	16.0
7	10.7	1.2	2.5	8.0	16.0
8	10.4	1.2	4.5	7.0	19.5
9	10.6	1.2	5.0	8.0	20.5
10	10.2	1.2	4.0	8.0	19.5

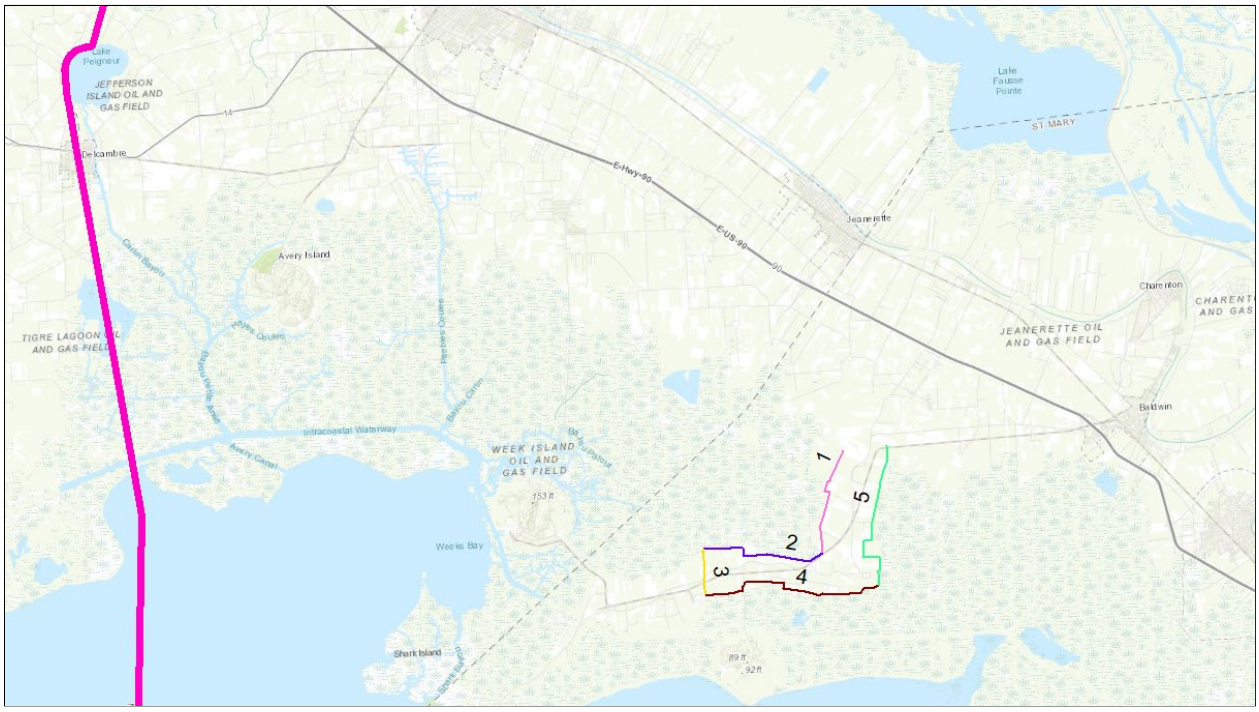

Figure C:4-4. Segments of the Proposed State Alignment HWY 83 EXT

Table C:4-5. Existing Conditions 2% Surge and Wave Parameters with Levee Elevations for the HWY 83 EXT Alignment

Hydraulic Reach	SWE (ft)	Std. Dev.	Hs (ft)	Tp (s)	Levee Elevation (ft) NAVD 88 (2004.65)
1	6.3	1.2	1.5	5.0	9.0
2	7.1	1.2	1.5	7.0	10.0
3	7.8	1.2	3.0	7.0	14.0
4	8.7	1.2	3.0	7.0	15.0
5	7.5	1.2	3.0	5.0	12.5

Table C:4-6. Existing Conditions 1% Surge and Wave Parameters with Levee Elevations for the HWY 83 EXT Alignment

Hydraulic Reach	SWE (ft)	Std. Dev.	Hs (ft)	Tp (s)	Levee Elevation (ft) NAVD 88 (2004.65)
1	8.2	1.2	2.0	7.0	12.0
2	9.2	1.2	2.0	7.0	13.0
3	9.6	1.2	5.0	8.0	19.0
4	10.3	1.2	5.0	7.0	20.0
5	9.0	1.2	5.0	9.0	18.0

Table C:4-7. Future Conditions 2% Surge and Wave Parameters with Levee Elevations for the HWY 83 EXT Alignment

Hydraulic Reach	SWE (ft)	Std. Dev.	Hs (ft)	Tp (s)	Levee Elevation (ft) NAVD88(2004.65)
1	8.6	1.2	1.5	5.0	11.5
2	9.4	1.2	1.5	7.0	12.0
3	9.8	1.2	3.5	7.0	17.5
4	10.4	1.2	5.5	8.0	20.5
5	9.4	1.2	5.0	8.0	18.0

Table C:4-8. Future Conditions 1% Surge and Wave Parameters with Levee Elevations for the HWY 83 EXT Alignment

Hydraulic Reach	SWE (ft)	Std. Dev.	Hs (ft)	Tp (s)	Levee Elevation (ft) NAVD88(2004.65)
1	10.6	1.2	2.5	7.0	16.0
2	11.4	1.2	2.5	7.0	16.5
3	11.6	1.2	5.0	8.0	22.5
4	12.0	1.2	6.5	7.0	22.0
5	11.1	1.2	6.0	9.0	22.0

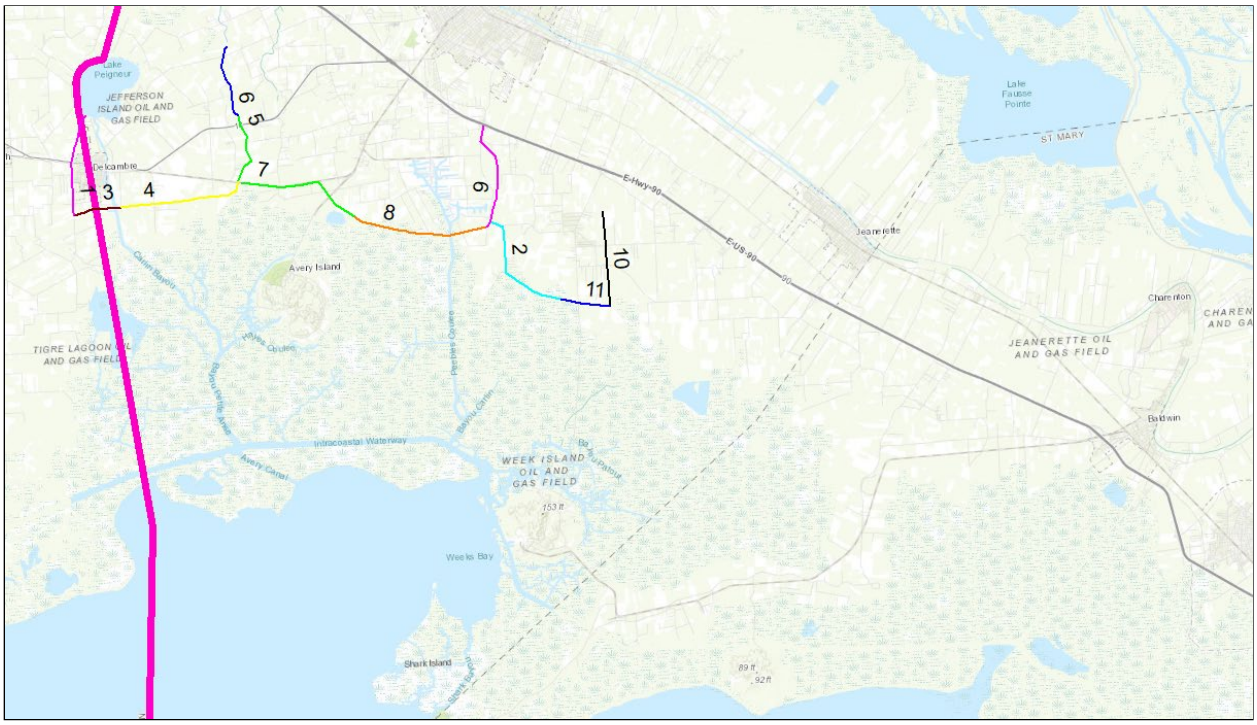

Figure C:4-5. Segments of the Proposed West Ring Levees

Table C:4-9. 2025 2% Surge and Wave Parameters with Levee Elevations for the West Ring Levees

Hydraulic Reach	SWE (ft)	Std. Dev.	Hs (ft)	Tp (s)	Levee Elevation (ft) NAVD 88 (2004.65)
1	7.0	1.2	3.0	3.0	9.5
2	7.2	1.2	2.0	7.0	11.0
3	9.0	1.2	3.0	6.0	15.0
4	8.7	1.2	2.0	7.0	12.5
5	8.3	1.2	2.0	7.0	12.0
6	6.7	1.2	2.0	7.0	10.5
7	8.2	1.2	2.0	7.0	12.0
8	7.5	1.2	3.0	7.0	13.5
9	7.0	1.2	1.5	7.0	9.5
10	6.3	1.2	1.5	4.0	8.5
11	6.6	1.2	2.0	7.0	10.5

Table C:4-10. Existing Conditions 1% Surge and Wave Parameters with Levee Elevations for the West Ring Levees

Hydraulic Reach	SWE (ft)	Std. Dev.	Hs (ft)	Tp (s)	Levee Elevation (ft) NAVD 88 (2004.65)
1	9.3	1.2	4.0	7.0	17.5
2	8.7	1.2	3.0	8.0	15.0
3	10.7	1.2	4.0	7.0	19.5
4	10.3	1.2	4.0	7.0	19.0
5	10.0	1.2	3.0	8.0	16.5
6	9.0	1.2	3.0	8.0	15.5
7	9.8	1.2	3.0	8.0	16.5
8	9.2	1.2	4.0	8.0	17.5
9	8.3	1.2	2.0	8.0	12.0
10	8.0	1.2	3.0	8.0	14.5
11	8.4	1.2	3.0	8.0	15.0

Table C:4-11. Future Conditions 2% Surge and Wave Parameters with Levee Elevations for the West Ring Levees

Hydraulic Reach	SWE (ft)	Std. Dev.	Hs (ft)	Tp (s)	Levee Elevation (ft) NAVD88(2004.65)
1	9.6	1.2	3.0	6.0	15.5
2	9.7	1.2	3.0	7.0	16.0
3	11.3	1.2	3.5	7.0	19.0
4	11.1	1.2	4.0	7.0	20.0
5	10.4	1.2	3.0	7.0	17.0
6	9.0	1.2	3.0	7.0	15.5
7	10.6	1.2	3.5	7.0	18.5
8	10.0	1.2	3.5	7.0	17.5
9	9.2	1.2	2.5	7.0	14.5
10	8.6	1.2	2.5	7.0	14.0
11	9.2	1.2	3.0	7.0	15.5

Table C:4-12. 2075 1% Surge and Wave Parameters with Levee Elevations for the West Ring Levees

Hydraulic Reach	SWE (ft)	Std. Dev.	Hs (ft)	Tp (s)	Levee Elevation (ft) NAVD88(2004.65)
1	12.0	1.2	4.0	8.0	21.5
2	11.4	1.2	4.0	8.0	20.5
3	13.1	1.2	5.0	8.0	25.0
4	12.8	1.2	5.0	8.0	24.5
5	12.4	1.2	4.0	8.0	21.5
6	11.6	1.2	4.0	8.0	21.0
7	12.4	1.2	4.5	8.0	23.0
8	11.9	1.2	5.0	8.0	23.0
9	10.8	1.2	4.0	8.0	20.0
10	10.6	1.2	3.0	8.0	17.0
11	11.2	1.2	4.0	8.0	20.5

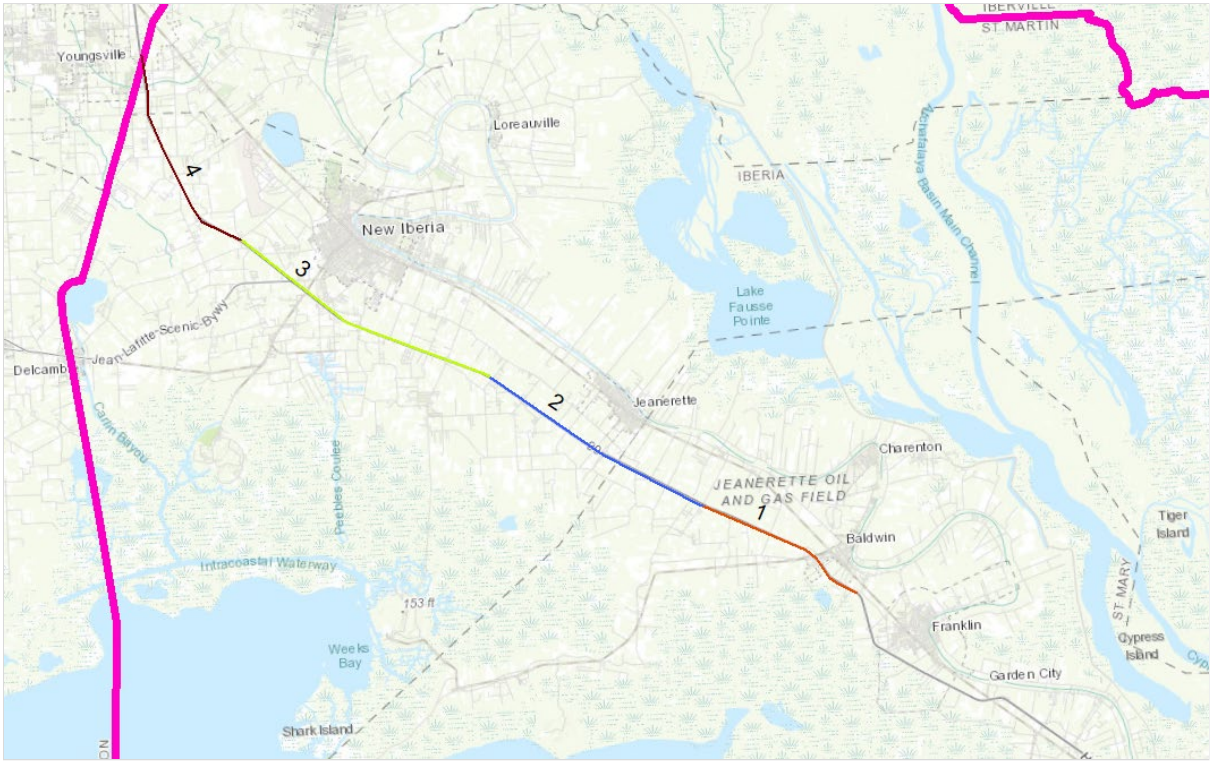

Figure C:4-6. Segments of Proposed HWY90 Alignment

Table C:4-13. Existing Conditions 2% Surge and Wave Parameters with Levee Elevations for HWY90 Alignment

Hydraulic Reach	SWE (ft)	Std. Dev.	Hs (ft)	Tp (s)	Levee Elevation (ft) NAVD 88 (2004.65)
1	6.0	1.2	3.0	6.0	11.0
2	5.9	1.2	1.5	5.0	8.5
3	7.1	1.2	2.0	7.0	11.0
4	6.3	1.2	1.5	3.0	8.0

Table C:4-14. Existing Conditions 1% Surge and Wave Parameters with Levee Elevations for HWY90 Alignment

Hydraulic Reach	SWE (ft)	Std. Dev.	Hs (ft)	Tp (s)	Levee Elevation (ft) NAVD 88 (2004.65)
1	7.4	1.2	3.0	7.0	13.5
2	7.8	1.2	2.0	7.0	11.5
3	8.8	1.2	3.0	8.0	15.5
4	8.7	1.2	2.0	4.0	11.5

Table C:4-15. Future Conditions 2% Surge and Wave Parameters with Levee Elevations for HWY90 Alignment

Hydraulic Reach	SWE (ft)	Std. Dev.	Hs (ft)	Tp (s)	Levee Elevation (ft) NAVD 88 (2004.65)
1	8.7	1.2	4.0	8.0	17.0
2	8.4	1.2	3.0	7.0	15.0
3	9.8	1.2	3.0	7.0	16.5
4	8.0	1.2	2.0	6.0	12.0

Table C:4-16. Future Conditions 1% Surge and Wave Parameters with Levee Elevations for HWY90 Alignments

Hydraulic Reach	SWE (ft)	Std. Dev.	Hs (ft)	Tp (s)	Levee Elevation (ft) NAVD 88 (2004.65)
1	9.6	1.2	5.0	8.0	19.0
2	9.7	1.2	4.0	8.0	18.5
3	10.6	1.2	3.5	7.0	18.5
4	10.7	1.2	2.5	7.0	16.0

Section 5
Subunits

The study area was subdivided into regions called subunits to aid the economic analysis. The previous hydraulic subunits near this study area were developed from census blocks and the land-water boundary. For this analysis, the PDT requested subunits that were more hydraulics dependent in delineation. The methodology by used is:

1. The project study boundary identified the outer boundary for the subunits shown in Figure C:5-1.

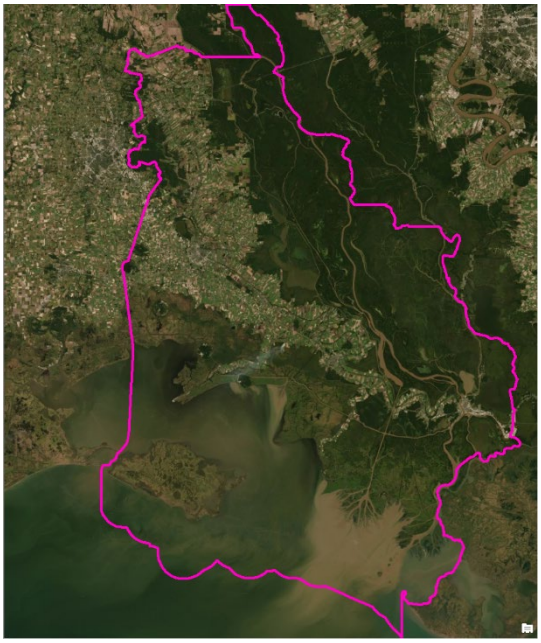

Figure C:5-1. Segments of Proposed HWY90 Alignment

2. Next, a land water boundary layer was used to determine the extent of the Gulf of Mexico into the project area shown in Figure C:5-2.

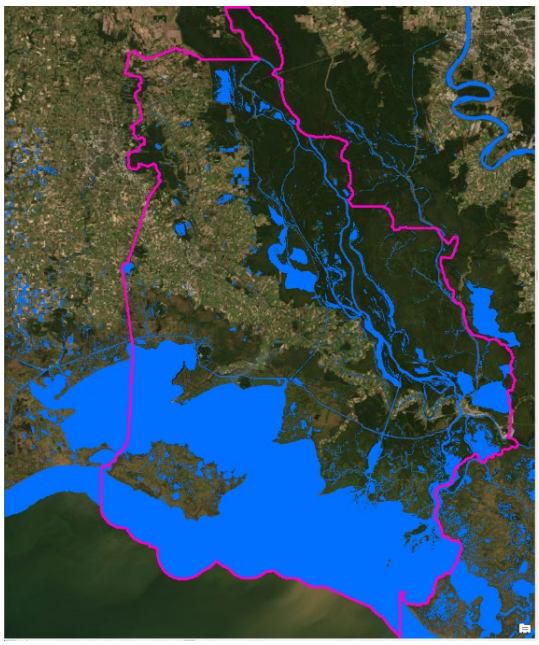

Figure C:5-2. Segments of Proposed HWY90 Alignment

3. The zone was split along this coastal boundary, preserving the inland riverine regions shown in Figure C:5-3.

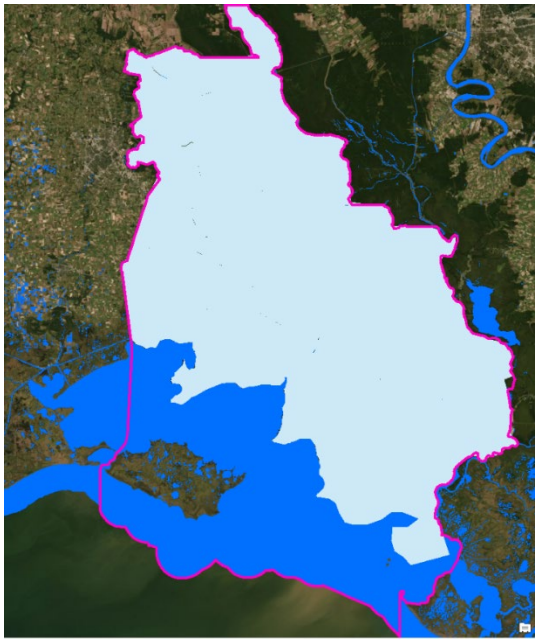

Figure C:5-3. Segments of Proposed HWY90 Alignment

4. 1 percent AEP LACPR surge elevation heights were converted into polygons grouped together by stage elevations in increments of 0.5 foot (i.e. any continuous set of points with elevations between 1 foot and 1.5 feet were grouped and the boundary was delineated into a polygon) shown in Figure C:5-4.

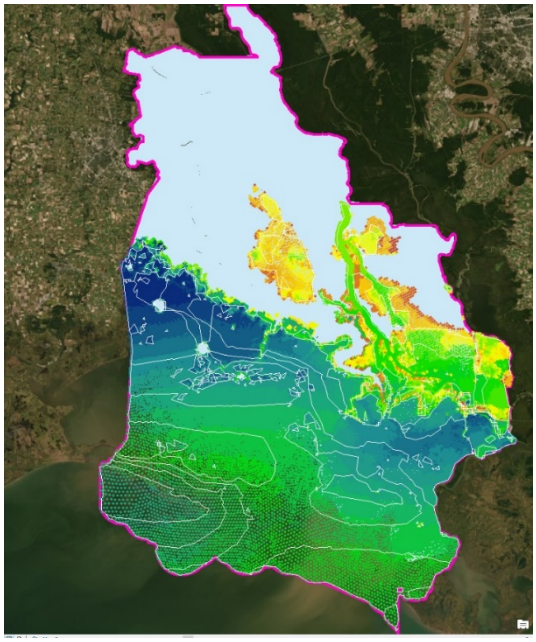

Figure C:5-4. Segments of Proposed HWY90 Alignment

5. After a union was performed on the shape, those polygons were split with existing levees shown in Figure C:5-5

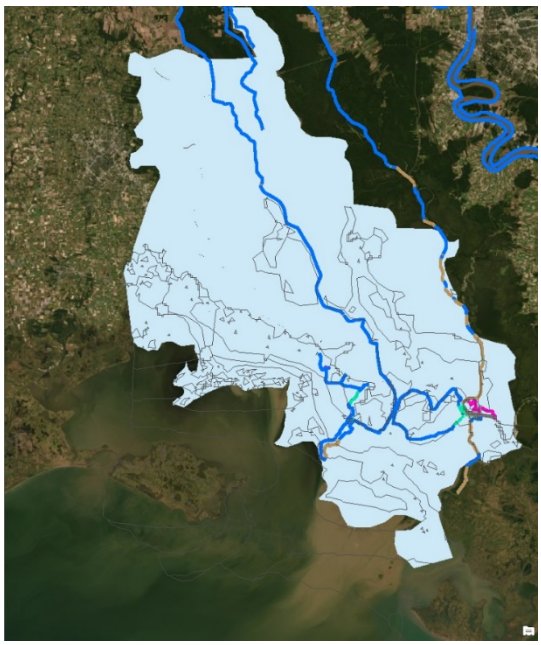

Figure C:5-5. Segments of Proposed HWY90 Alignment

6. Next, the subunits shape was split with proposed SCCL levee measures shown Figure C:5-6.

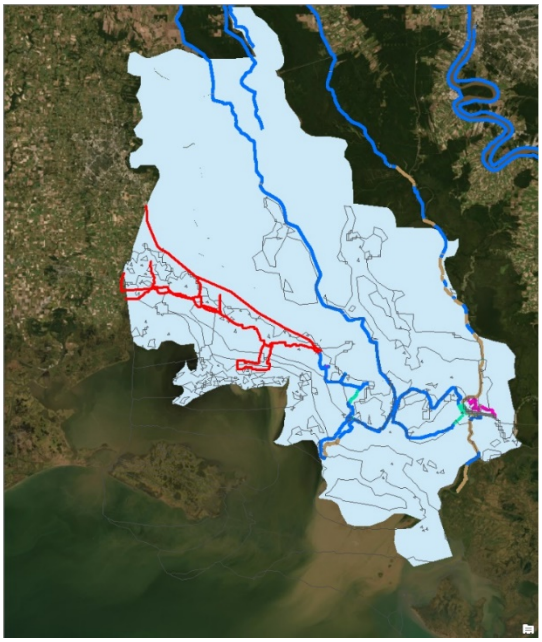

Figure C:5-6. Segments of Proposed HWY90 Alignment

7. Then, the units were split with additional features like Bayou Teche, major roads, and high ground Figure C:5-7.

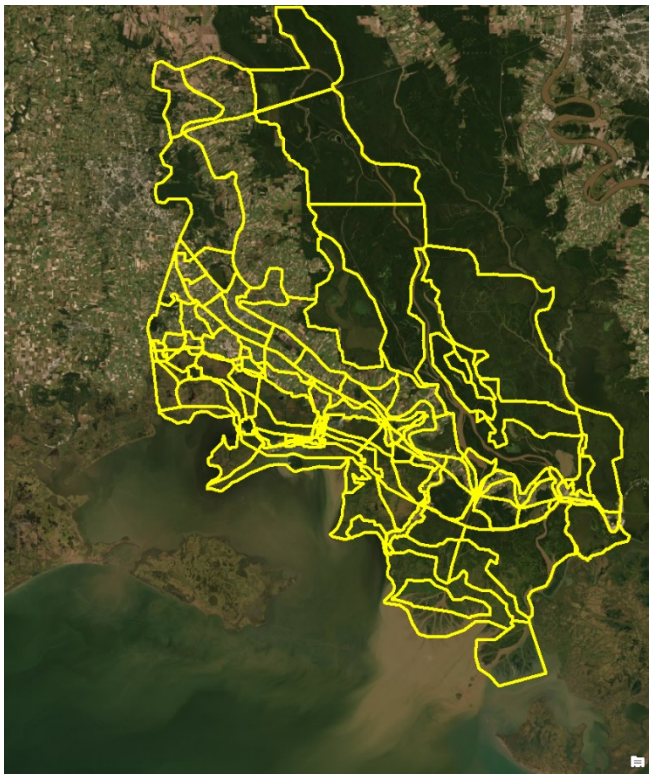

Figure C:5-7. Segments of Proposed HWY90 Alignment

Section 6
Climate Change

6.1 RELATIVE SEA LEVEL CHANGE (RSLC)

In coastal Louisiana, relative sea level rise (RSLR) is the term applied to the difference between the change in eustatic (global) sea level and the change in land elevation. According to Intergovernmental Panel on Climate Change (IPCC 2007), the global mean sea level rose at an average rate of about 1.7 mm/yr during the 20th Century. Recent climate research has documented global warming during the 20th Century, and has predicted either continued or accelerated global warming for the 21st Century and possibly beyond (IPCC 2007).

Land elevation change can be positive (accreting) or negative (subsiding). Land elevations decrease due to natural causes, such as compaction and consolidation of Holocene deposits and faulting, and human influences such as sub-surface fluid extraction and drainage for agriculture, flood protection, and development. Forced drainage of wetlands results in lowering of the water table resulting in accelerated compaction and oxidation of organic material. Areas under forced drainage can be found throughout coastal Louisiana and the study area. Land elevations increase as a result of sediment accretion (riverine and littoral sources) and organic deposition from vegetation. Vertical accretion in most of the area; however, is insufficient to offset subsidence, causing an overall decrease in land elevations. The combination of subsidence and eustatic sea level rise is likely to cause the landward movement of marine conditions into estuaries, coastal wetlands, and fringing uplands (Day and Templet, 1989; Reid and Trexler 1992).

The locations of the RSLC gages are presented in Figure C:6-1 near the southwestern border of the project area. The results in the calculation table were determined with equation 2 from the EC 1165-2-212. The eustatic sea level rise rate of 0.0017 myr^{-1} is combined with 50-year subsidence values of 1.9, 0.06, and 0.9 feet for G88800, G03820, and G76360 respectively. Figure C:6-2 depicts the intermediate RSLC graphically for the three gages in addition to the averaged intermediate rate. The values are tabulated in Table C:6-1.

The projections in Figure C:6-2 are based on the parameters defined in EC 1165-2-212, where the rate of eustatic sea level rise is determined with:

Equation Used by this Calculator

EC 1165-2-212, Equation 2 is as follows:

$$E(t) = (0.0017+M)t + bt^2$$

The acceleration constant “b” is adjusted to achieve the medium and high curves, while the low curve is the extrapolated historical rate from gauge data.

The baseline gulf water level is considered to be 1.2 feet NAVD 88. The three gages chosen for estimating future conditions are G88800, G03820, and G76360. These are located near the south end of the lower Atchafalaya guide levee (G03820 & G88800) and south of Morgan City (G76360). The 50-year intermediate rates were averaged resulting in a future sea level condition of 3.0 feet A sensitivity analysis on the RSLR was performed in conjunction with economics to determine impacts on the TSP selection. (see appendix E.)

Included in figures C:6-3 through C:6-9 are the projected high sea level rise scenarios for 2075. As mentioned in section 2.4, the high sea level rise rate assumes +3.4 ft eustatic sea level rise above 2025 conditions. Under these high scenarios, large sections of HWY 190 begins to be significantly impacted by surge above the 1% AEP.

Figure C:6-1. Locations of the Three RSLC Gages

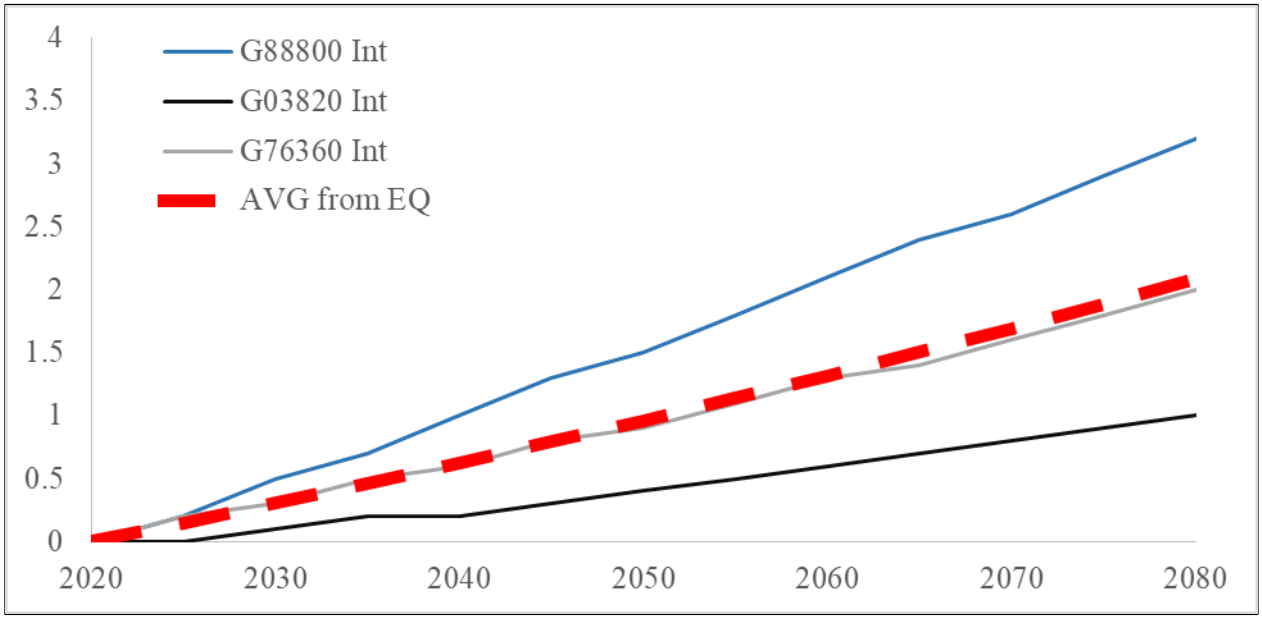

Figure C:6-2. The Relative Intermediate RSLC Average Rate

Table C:6-1. RSLC Rates for the Three Gauges in the Project Area

Average				
All values are in feet				
Year	**G88800 Int**	**G03820 Int**	**G76360 Int**	**Average RSLR**
2020	0	0	0	0.0
2025	0.2	0	0.2	0.1
2030	0.5	0.1	0.3	0.3
2035	0.7	0.2	0.5	0.5
2040	1	0.2	0.6	0.6
2045	1.3	0.3	0.8	0.8
2050	1.5	0.4	0.9	0.9
2055	1.8	0.5	1.1	1.1
2060	2.1	0.6	1.3	1.3
2065	2.4	0.7	1.4	1.5
2070	2.6	0.8	1.6	1.7
2075	2.9	0.9	1.8	1.9
2080	3.2	1	2	2.1
2085	3.5	1.1	2.2	2.3
2090	3.8	1.2	2.4	2.5
2095	4.1	1.3	2.6	2.7
2100	4.4	1.5	2.8	2.9

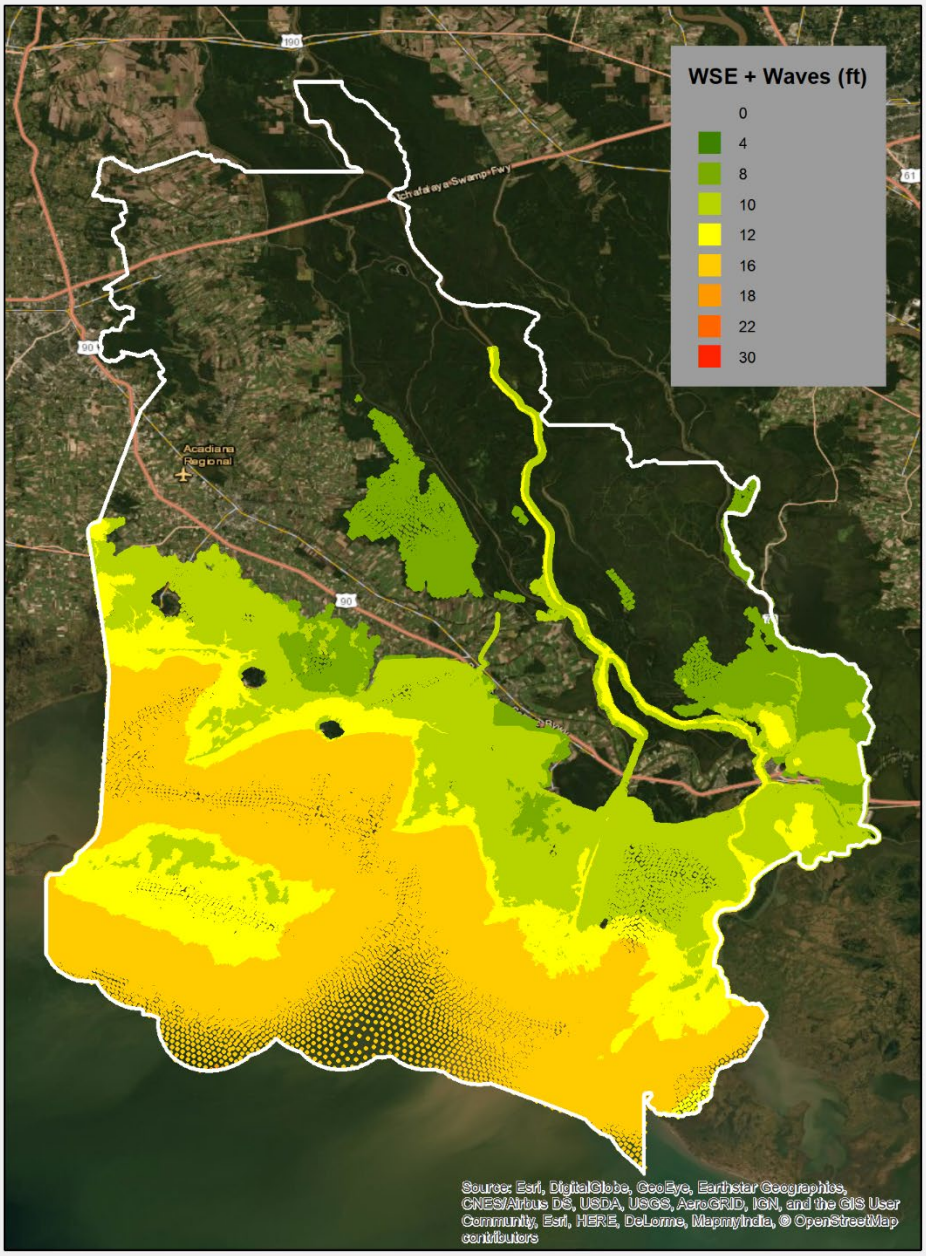

Figure C:6-3. 10% AEP; 2075 Future Conditions High; Surge plus Wave Elevations (ft NAVD88) for the SCCL

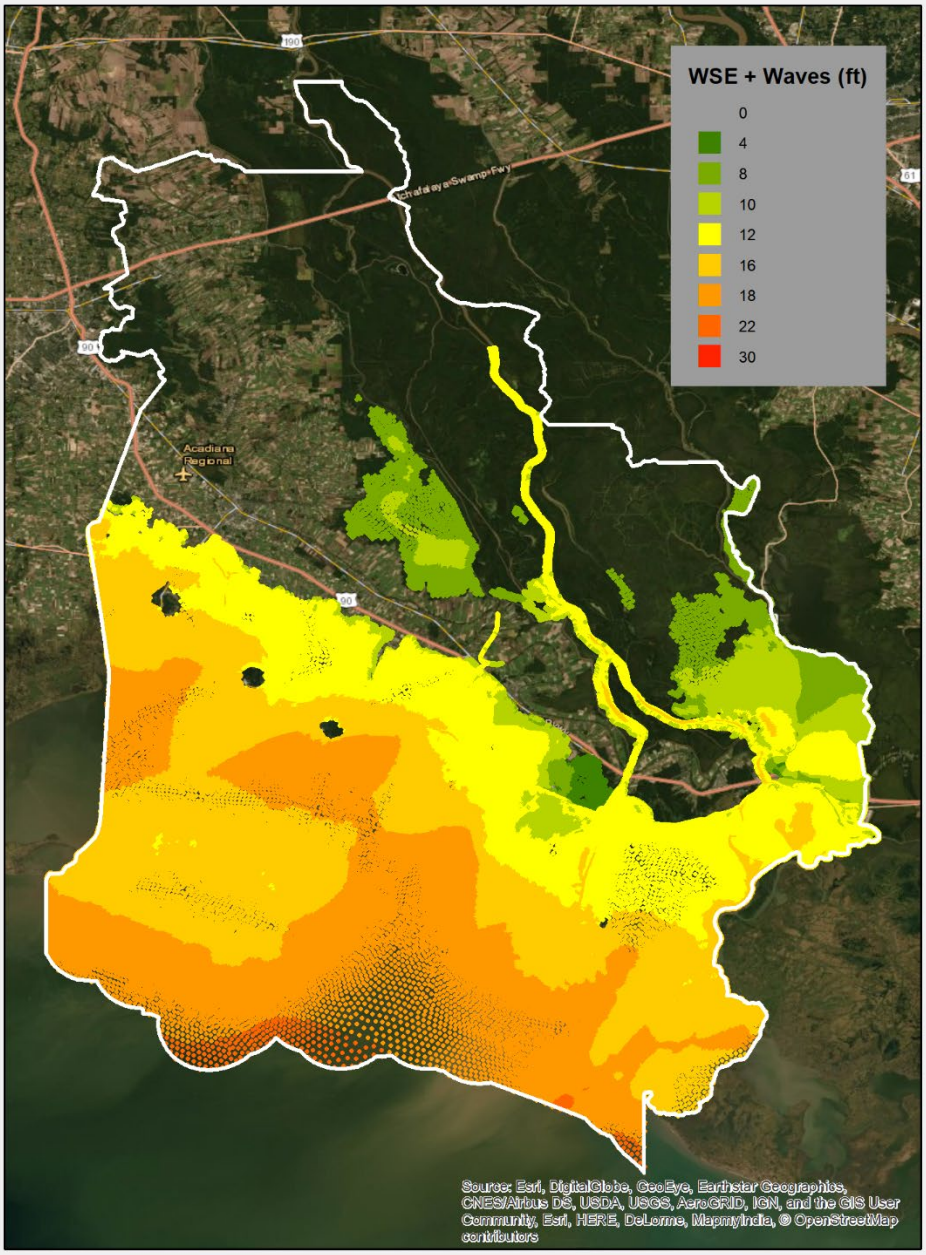

Figure C:6-4. 5% AEP; 2075 Future Conditions High; Surge plus Wave Elevations (ft NAVD88) for the SCCL

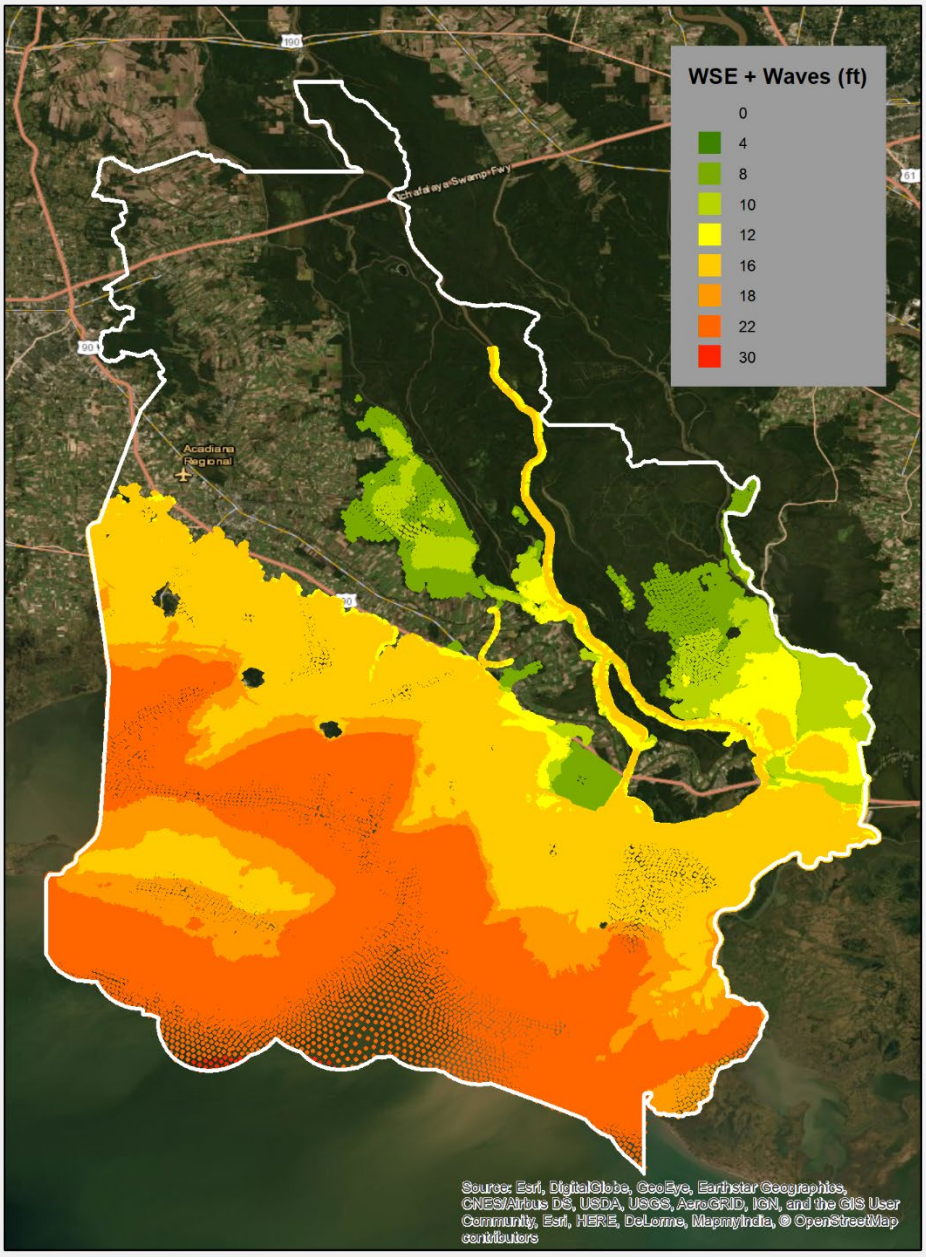

Figure C:6-5. 2% AEP; 2075 Future Conditions High; Surge plus Wave Elevations (ft NAVD88) for the SCCL

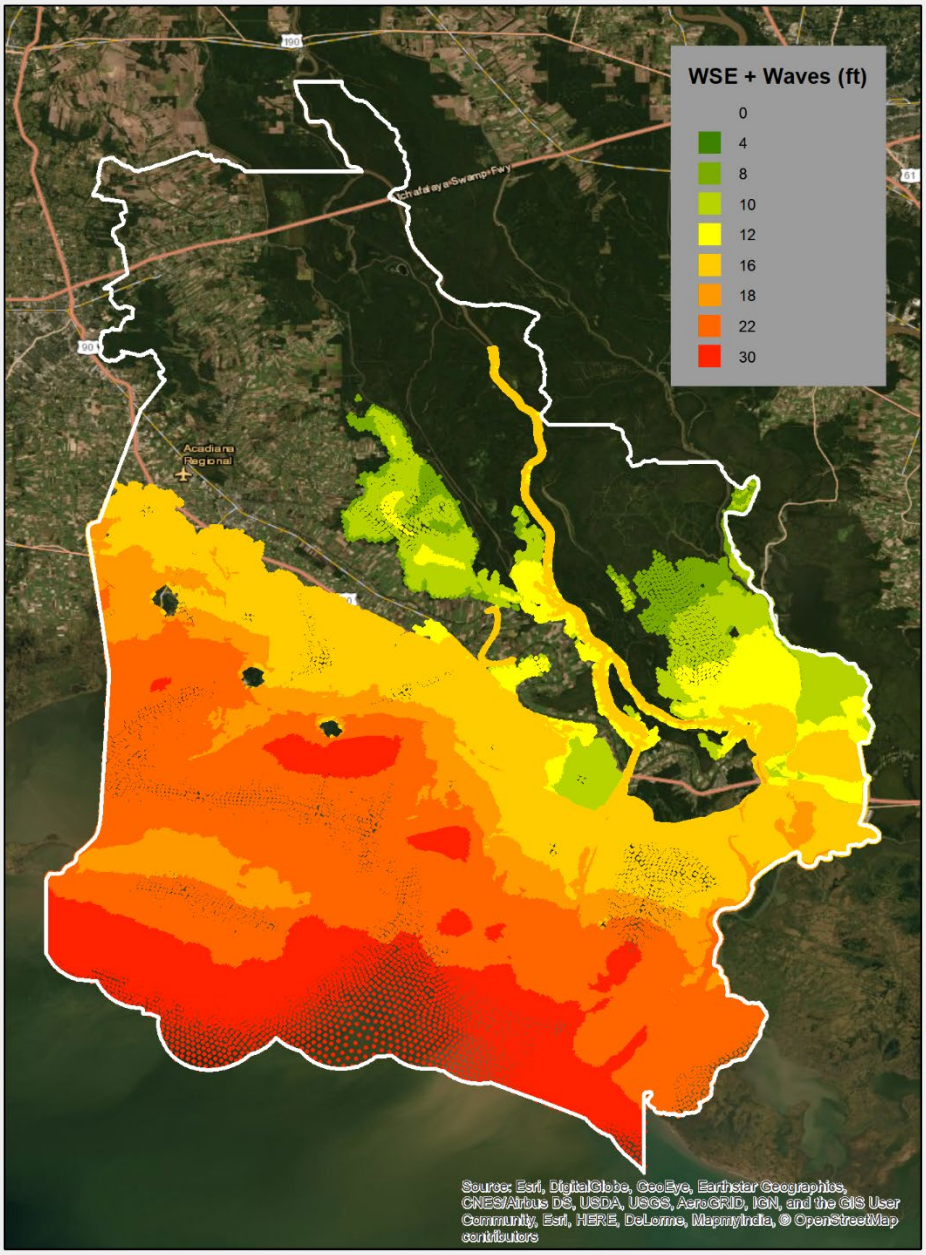

Figure C:6-6. 1% AEP; 2075 Future Conditions High; Surge plus Wave Elevations (ft NAVD88) for the SCCL

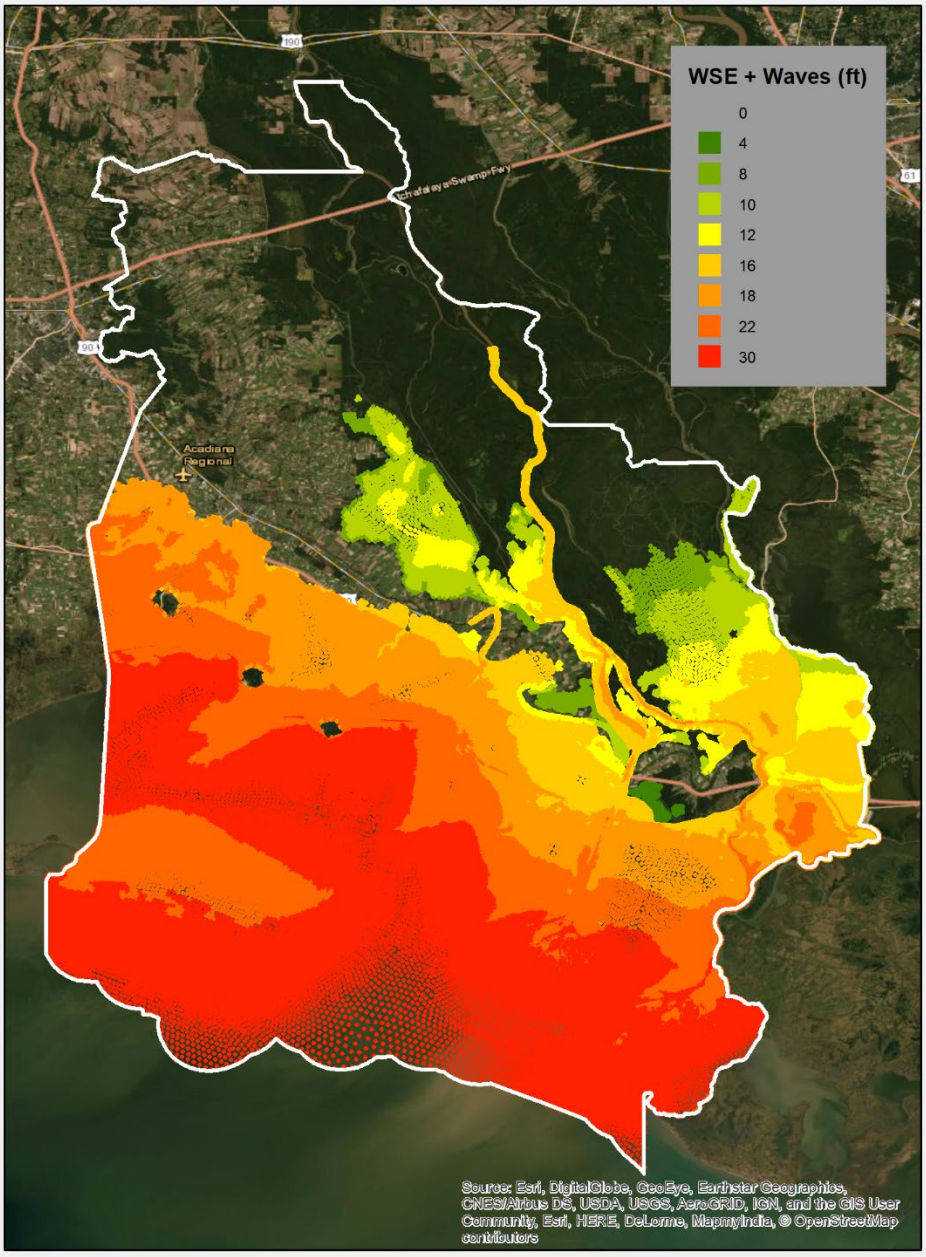

Figure C:6-7. 0.5% AEP; 2075 Future Conditions High; Surge plus Wave Elevations (ft NAVD88) for the SCCL

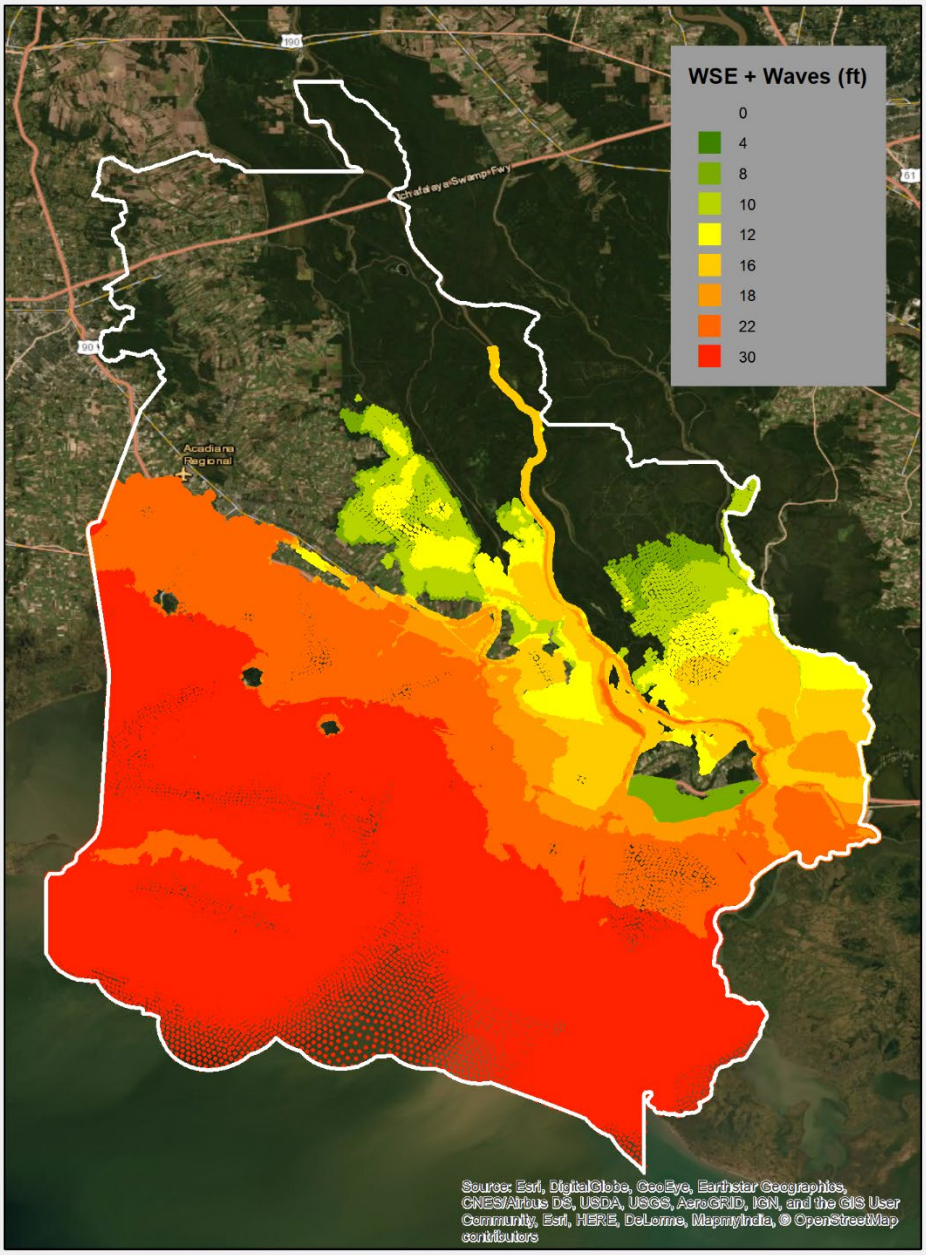

Figure C:6-8. 0.2% AEP; 2025 Future Conditions High; Surge plus Wave Elevations (ft NAVD88) for the SCCL

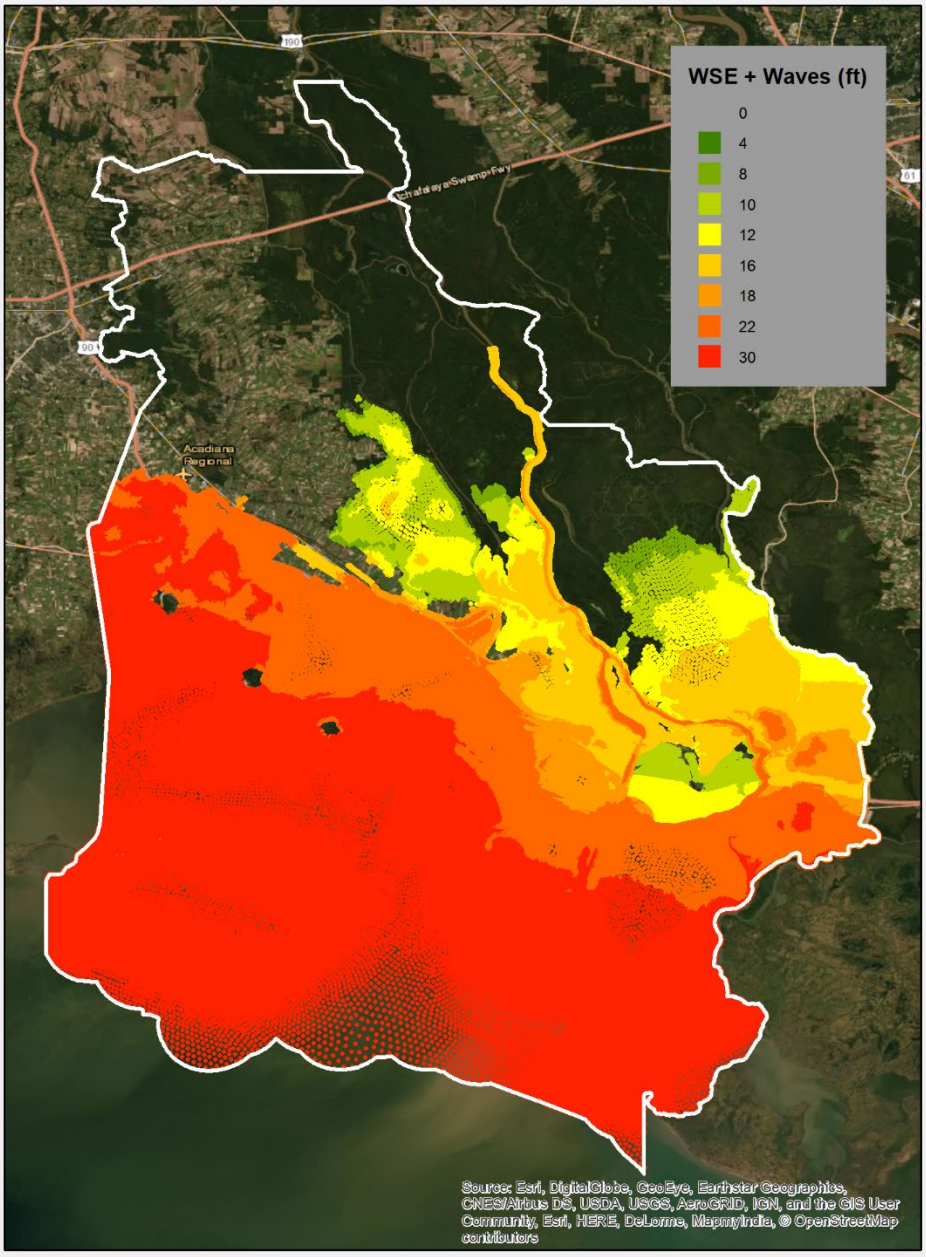

Figure C:6-9. 0.1% AEP; 2075 Future Conditions High; Surge plus Wave Elevations (ft NAVD88) for the SCCL

6.2 2125 ESTIMATED PROTECTION

In order to estimate the level of protection of the system beyond the year 2075, the statistical data was used to produce equivalent ACE's (or return periods) from estimated future surge values. All values between 2025 and 2075 were interpolated from the statistical surge elevations and wave output. For stage estimates beyond 2075, the annual RSLR rate was applied to each year linearly until 2125. The locations of the sample points are presented in Figure C:6-10.

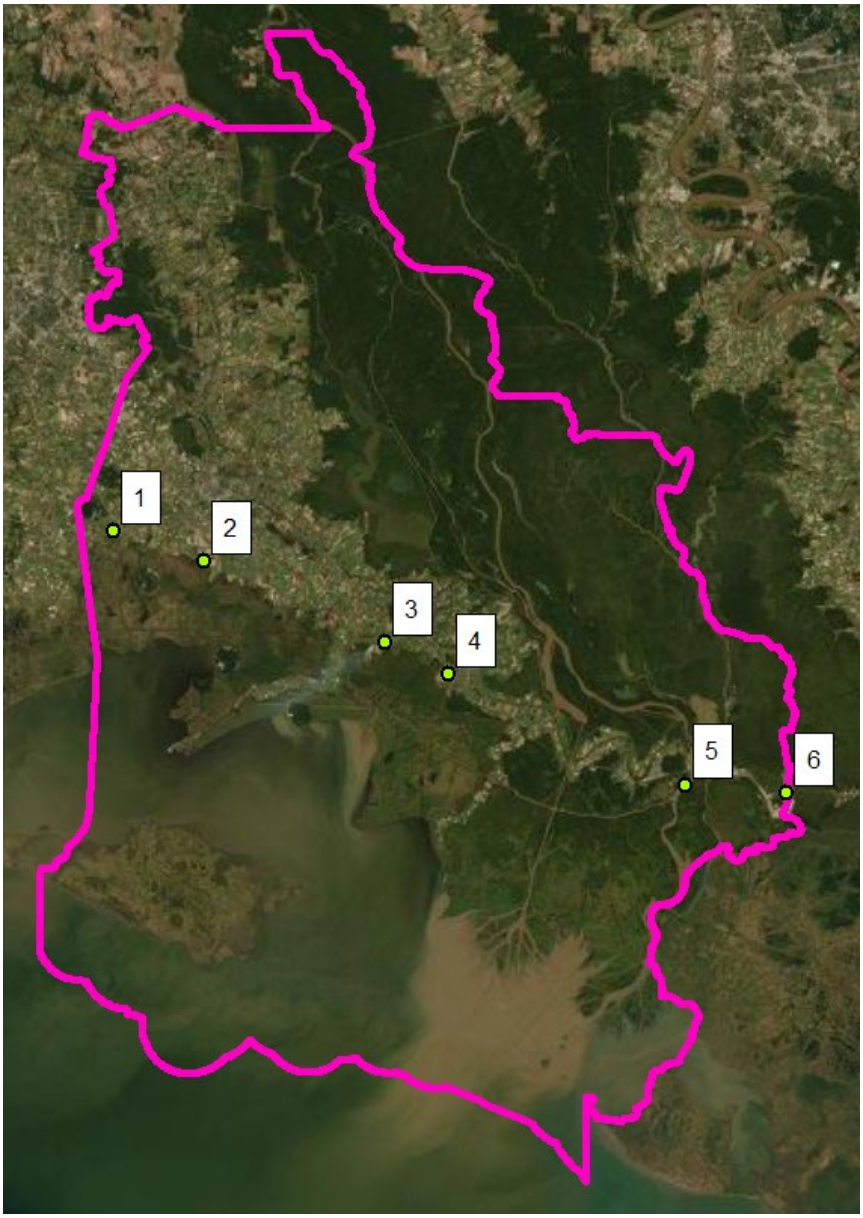

Figure C:6-10. Sampling Locations for 2125 Future Protection Evaluation

The six sampling locations were selected to sparsely represent the remainder of the entire system due to their proximity to a high number of structures and areas susceptible to coastal flooding. Locations 1 and 2 are in the west side of the domain, near the community of Delcambre and the Port of Iberia. Locations 3 and 4 straddle the Charenton canal, located to the west of Baldwin and in the low-lying area of Franklin. Locations 5 and 6 are located south of Morgan City, on the west and east side of the Bayou Beouf Lock.

Figures C:6-11 through C:6-16 depict the performance of the 2075 0.04 percent design elevation assuming intermediate SLR. All locations generally show the same trend for the intermediate SLR scenario in that the system-wide protection diminishes from a 0.04 percent ACE level of protection in 2075 to a 0.8 percent ACE level of protection in 2125. The high SLR scenario, the system-wide protection diminishes drastically, generally becoming deficient around 2050 and dropping to 2-4 percent ACE protection in 2125.

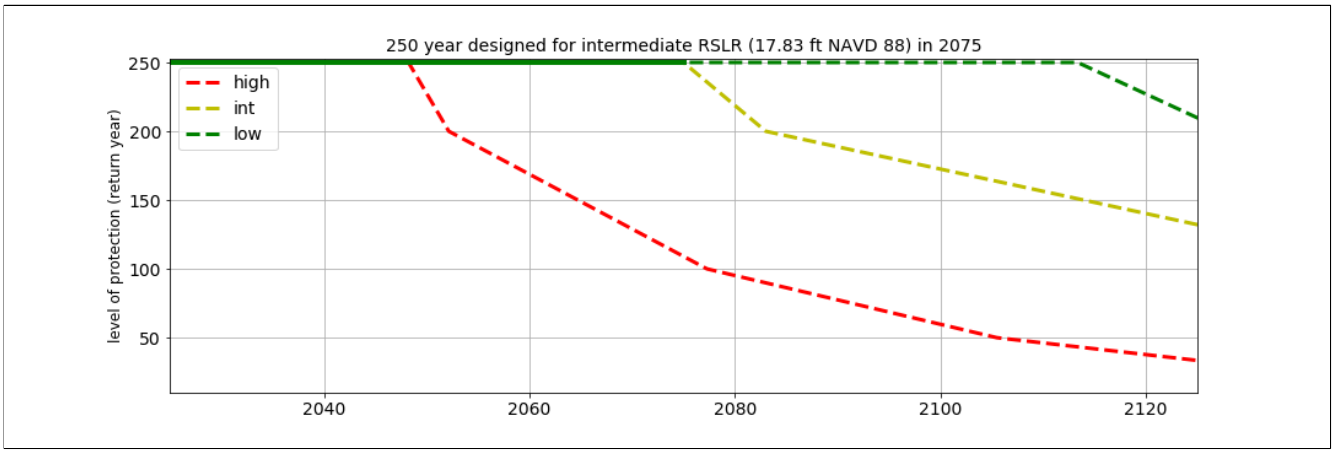

Figure C:6-11. Estimated Level of Protection over 100 Years for Location 1

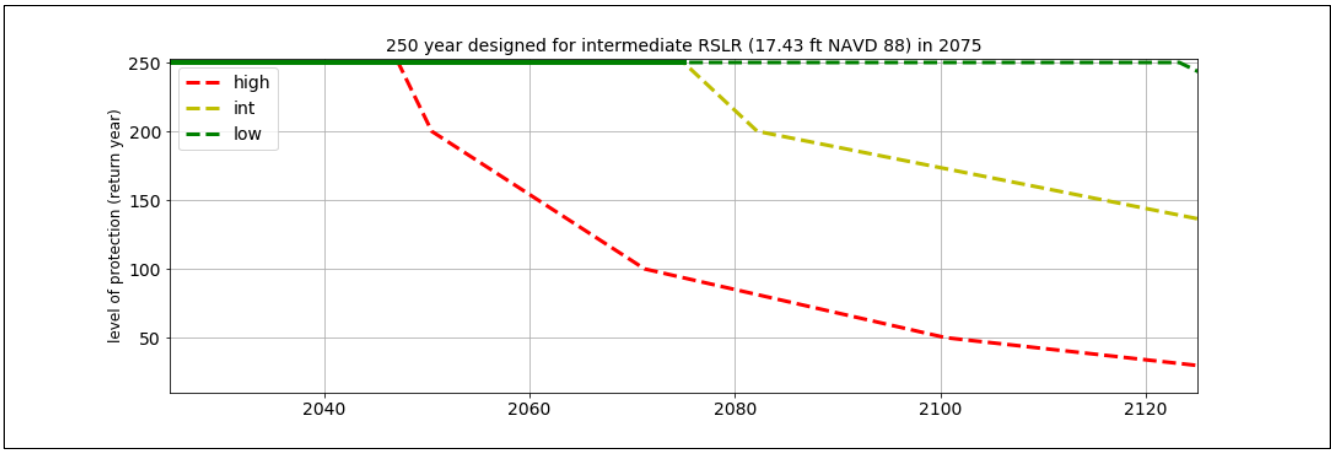

Figure C:6-12. Estimated Level of Protection over 100 Years for Location 2

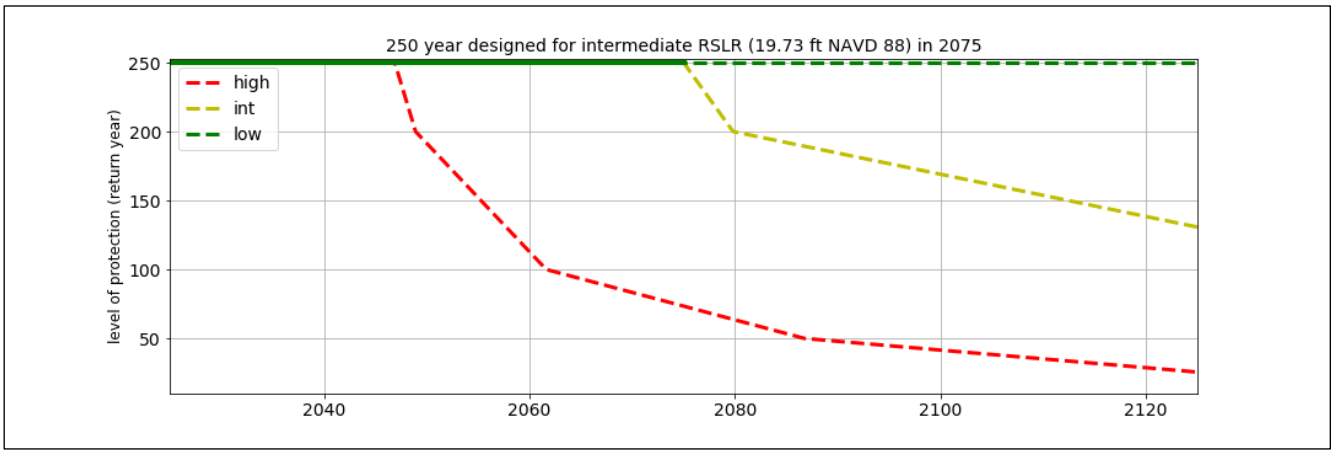

Figure C:6-13. Estimated Level of Protection over 100 Years for Location 3

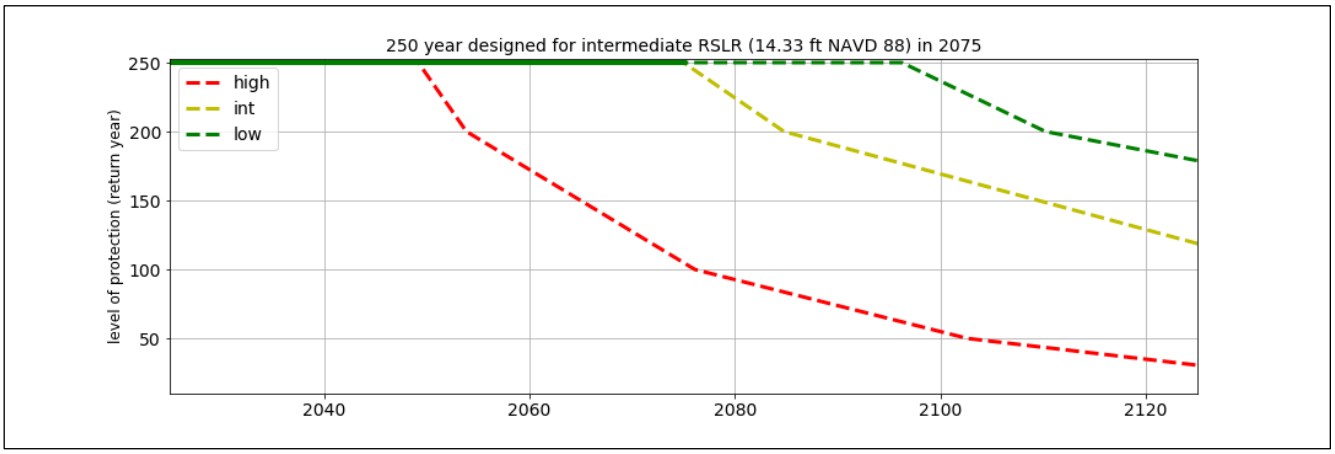

Figure C:6-14. Estimated Level of Protection over 100 Years for Location 4

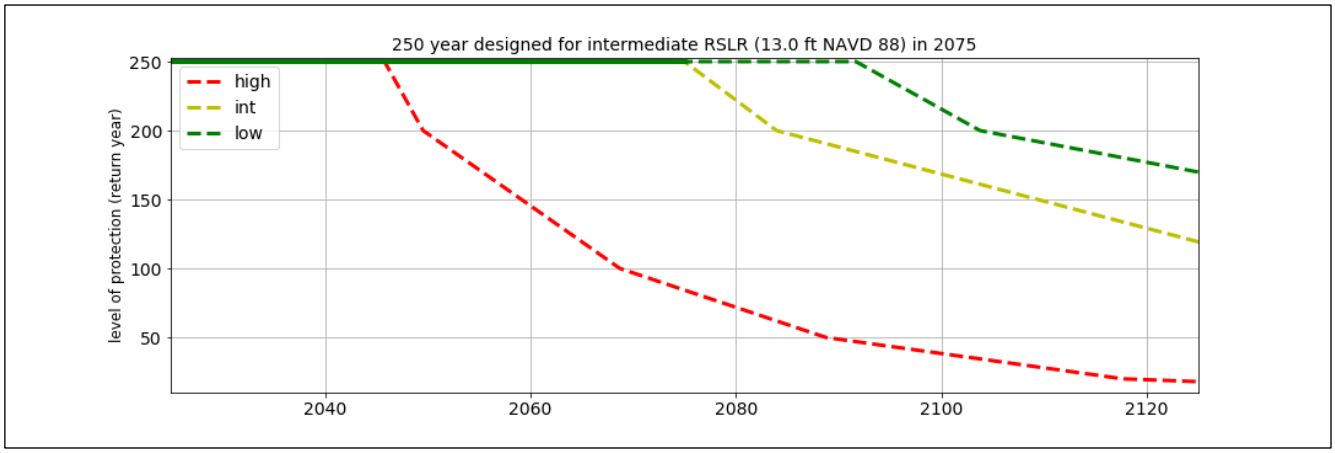

Figure C:6-15. Estimated Level of Protection over 100 Years for Location 5

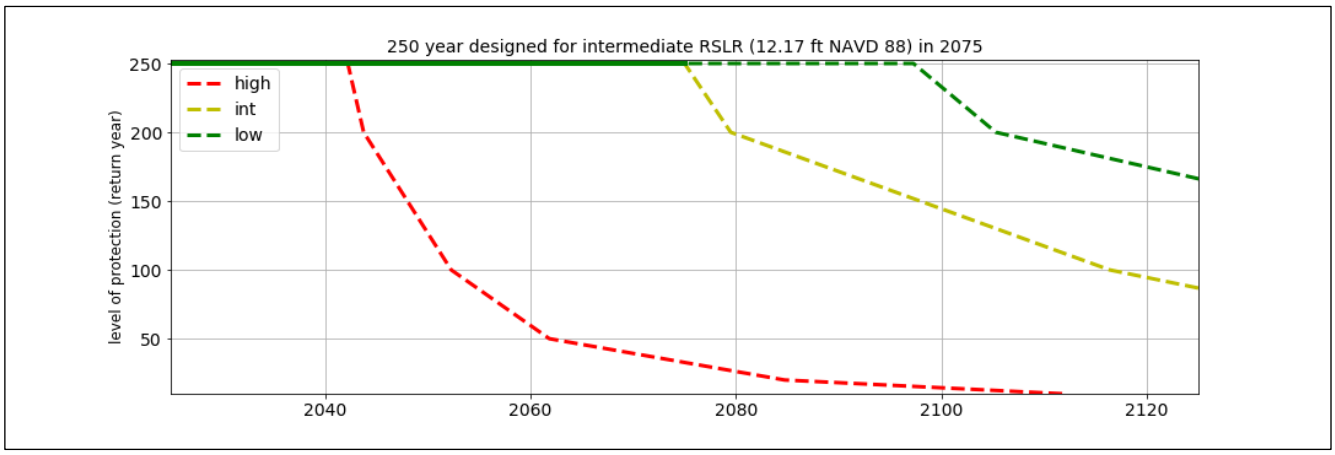

Figure C:6-16. Estimated Level of Protection over 100 Years for Location 6

6.3 HYDROLOGY AND NON-STATIONARITY

USACE guidance for analyzing the impacts of climate change on inland hydrology is included in Engineering and Construction Bulletin (ECB) 2018-14, entitled *Guidance for Incorporating Climate Change Impacts to Inland Hydrology in Civil Works Studies, Designs, and Projects* (USACE 2018). The bulletin provides a framework for evaluating the effects of climate change on inland hydrology and related climate variables (including but not limited to temperature, precipitation, and evaporation), as well as the effects of climate change on non-climate variables affecting inland hydrology (for example, sedimentation). The analysis is intended to aid in reducing climate change-related vulnerabilities and enhancing the resilience of USACE projects, and it can be used to inform decisions pertaining to project planning, engineering, operations, and maintenance. The focus of the analysis is the evaluation of observed and projected

trends for project area air temperature, precipitation, and streamflow, based on literature review and USACE climate tools, which are described later in this section.

ECB 2018-14 specifies that the assessment of climate change impacts on inland hydrology includes a literature review summarizing observed and projected climate trends applicable to the project area, with an emphasis on the climate variables of air temperature, precipitation, and streamflow. Literature reviewed for the SCCL study includes *Recent Climate Change and Hydrology Literature Applicable to U.S. Army Corps of Engineers Missions – Lower Mississippi River Region* (USACE 2015), the *Louisiana State Climate Summary* (NOAA 2019), *Climate Change Indicators in the United States* (USEPA 2016), and volumes I and II of the *National Climate Assessment* (USGCRP 2017/2018). The following sections summarize literature review findings for observed and projected air temperature, precipitation, and streamflow trends.

6.3.1 Air Temperature

Observed Trends

Climate Change and Hydrology Literature Applicable to U.S. Army Corps of Engineers Missions – Lower Mississippi River Region: Although there are no studies evaluating historical temperature trends specifically within the Lower Mississippi River Region, several studies are available evaluating historical temperature trends on a national scale, from which trends within the Lower Mississippi River Region can be ascertained. Findings from Wang et al. (2009) and Westby et al. (2013) suggest a slight cooling trend occurred in the region during the second half of the 20th century, while Liu et al. (2012) suggests a cooling trend occurred during the third quarter of the 20th century and was followed by a warming trend during the final quarter of the century. The third National Climate Assessment (Carter et al. 2014) also suggests the region experienced a cooling period near mid-century and has been warming since the latter 20th century. Wang et al. (2009) and Carter et al. (2014) found no significant seasonal trends in the region.

Louisiana State Climate Summary: Temperatures in the state were historically warm in the early 20th century, and were cooler from the 1950s to 1970s. Since the 1970s, temperatures have warmed by about 2°F.

Climate Change Indicators in the United States: Since the beginning of the 20th century, temperatures in the project area have risen slightly (0-0.5°F/century). Nationwide, daily highs and lows have been increasing since the 1970s.

National Climate Assessment: Recent (1986-2016) temperatures in southeast Louisiana were slightly cooler compared to the first half of the 20th century.

Projected Trends

Climate Change and Hydrology Literature Applicable to U.S. Army Corps of Engineers Missions – Lower Mississippi River Region: Several global climate models predict a future increase in air temperatures in the Lower Mississippi River region. Liu et al. (2013), Zhang et al. (2010), and Jayakody et al. (2013) predict increases ranging from 0.9-7.2°F by mid-21st century. Elguindi and Grundstein (2013) predict a shift to warmer climate types by mid-21st century. Liu et al. (2012), Scherer and Diffenbaugh (2014), and Carter et al. (2014) predict increases typically between 3.6-9°F by the end of the 21st century. Tebaldi (2006), Kunkel et al. (2010) , and Gao et al. (2012) predict an increase in the number of heat wave days by the end of the 21st century. Jayakody et al. (2013) also predicts an extended summer weather period that will change from July-August to June-September.

Louisiana State Climate Summary: By the end of the 21st century, temperatures in Louisiana are expected to warm by approximately 1.5-12°F. Warming is predicted to increase heat wave intensities and decrease cold front intensities.

National Climate Assessment: Annual average air temperatures in the southeastern U.S. are predicted to increase by 3.4-4.3°F by the mid-21st century, and by 4.4-7.7°F by the late 21st century. By the mid-21st century, the coldest day of the year is predicted to be 5°F warmer than the recent (1976-2005) average, and the warmest day of the year is predicted to be 5.8°F warmer. The southeastern U.S. will experience about 40-50 more days per year with maximum temperatures above 90°F by the mid-21st century.

6.3.2 Precipitation

Observed Trends

Climate Change and Hydrology Literature Applicable to U.S. Army Corps of Engineers Missions – Lower Mississippi River Region: Findings from Grundstein (2009), Wang et al. (2009), McRoberts and Nielsen-Gammon (2011), Pryor et al. (2009), and Small et al. (2006) suggest an increasing trend in annual precipitation in the region occurred during the 20th century and the second half of the century. Wang and Zhang (2008) found that the frequency of extreme (20-year) rainfall events in the region increased by 25-50 percent during the last quarter of the 20th century compared to the third quarter, while Pryor et al. (2009) did not find an increase in extreme (annual 90th percentile) precipitation intensity during the 20th century. Li et al. (2011) and Villarini et al. (2013) found an increase in the frequency and magnitude of anomalous summer precipitation in the southeastern U.S. during the second half of the 20th century.

Louisiana State Climate Summary: The state has experienced variable precipitation since the early 20th century, with wetter periods in the 1940s, from the 1970s to the early 2000s, with the wettest period on record in the 2010s.

Climate Change Indicators in the United States: Since about the 1970s, the continental U.S. has experienced an increasing frequency of extreme precipitation events. Precipitation in the project area has increased slightly (2-10 percent) since the beginning of the 20th century.

National Climate Assessment: Recent (1986-2016) precipitation in southeast Louisiana was slightly (0-5 percent) greater compared to the first half of the 20th century. Seasonal precipitation was substantially higher (>15 percent) during the fall, slightly higher (0-5 percent) during the winter and summer, and lower (-5-0 percent) during the spring. The southeastern U.S. has experienced a large increase in extreme precipitation events.

Projected Trends

Climate Change and Hydrology Literature Applicable to U.S. Army Corps of Engineers Missions – Lower Mississippi River Region: Projections of future precipitation in the region are generally lacking in consensus. Zhang et al. (2010) and Gao et al. (2012) predict an increase in precipitation in the coastal portion of the Lower Mississippi River region by the mid-21st century. Liu et al. (2012) predicts a slight (additional 10-50 mm/year) increase in annual precipitation by the end of the 21st century. Gao et al. (2012), Tebaldi et al. (2006), and Wang and Zhang (2008) predict an increase in frequency and intensity of extreme precipitation events by the end of the 21st century. Modeling by Joetzjer et al. (2013) suggests an increase in frequency and aerial extent of droughts in the region during the second half of the 21st century.

Louisiana State Climate Summary: Summer precipitation is predicted to decrease by between 5-10 percent in Louisiana by the mid-21st century. However, the predicted decrease is much smaller than the natural variability in rainfall in the state.

National Climate Assessment: Small changes in seasonal precipitation are predicted for southeast Louisiana by the end of the 21st century, including slight (0-10 percent) increases in the fall and winter and slight (-10-0 percent) decreases in the spring and summer. Recent increases in the frequency and intensity of extreme rainfall events, which are the result of increased atmospheric water vapor associated with higher air temperatures, are expected to continue. In the southeastern U.S., extreme precipitation events are predicted to increase in frequency by approximately 20-40 percent by the mid-21st century and 40-100 percent by the end of the 21st century. The intensity of extreme events is predicted to increase by 9-12 percent by the mid-21st century and by 13-21 percent by the end of the 21st century in the southeastern U.S.

6.3.3 Streamflow

Observed Trends

Climate Change and Hydrology Literature Applicable to U.S. Army Corps of Engineers Missions – Lower Mississippi River Region: Studies of trends and nonstationarity in

streamflows within the region over the past century generally suggest increasing streamflows. Xu et al. (2013) and Small et al. (2006) found increases in annual streamflow and baseflow for several streams within the region during the second half of the 20th century, while Kalra et al. (2008) found no trends in annual or seasonal flows for several streams within the region over a similar time period.

Louisiana State Climate Summary: In the southeastern U.S., the frequency and magnitude of flooding has generally decreased since the mid-1960s, although decreases were not statistically significant. Since the beginning of the 20th century, the continental U.S. has experienced several major drought periods including in the 1930s, 1950s, early 1960s, late 1980s, and 2000s, with wetter periods in the 1900s, 1940s, 1970s until the late 1980s, and the 1990s.

Projected Trends

Climate Change and Hydrology Literature Applicable to U.S. Army Corps of Engineers Missions – Lower Mississippi River Region: Projected changes in streamflow are based on global climate modeling and macro-scale hydrologic models. Döll and Zhang (2010) predict a small (10-20%) decrease in low flows and average annual flows in the region by mid-21st century, while Carter et al. (2014) also predicts a decrease in water availability by the end of the 21st century. Hagemann et al. (2013) predicts a 200 mm/year reduction in runoff by the late 21st century.

6.3.4 Summary

Since the 1970s, air temperatures in the southeastern U.S. and in Louisiana have warmed slightly. Air temperatures are projected to increase by 0.9-7.2°F by the mid-21st century and by 1.5-12°F by the end of the 21st century. Annual low and high temperatures are predicted to increase by approximately 5-6°F, and increases in the annual number of extremely hot days and the duration of summer weather are predicted. A slight increase in precipitation has occurred concurrent with increasing temperatures, which is associated with an increasing frequency and intensity of extreme rainfall events and greater seasonal rainfall during the fall. Although annual precipitation amount is not expected to change significantly in the future, the recent trends of increasing frequency and intensity of extreme rainfall events and greater seasonal rainfall are expected to continue, and droughts may become more common and widespread. There is a lack of consensus concerning historical streamflow trends, while streamflow modeling suggests slightly decreasing streamflow by both the middle and end of the 21st century.

6.4 CLIMATE TOOLS

Vulnerability assessment also includes the use of USACE climate tools to provide information on observed and projected climate trends relevant to the project area. The Climate Hydrology Assessment Tool (CHAT), Nonstationarity Detection Tool (NSD), and

Time Series Toolbox can be used to determine historical trends, while the CHAT and Vulnerability Assessment (VA) tools can be used to project future trends. Tools are available on the USACE Climate Preparedness and Resilience CoP Applications Portal (https://maps.crrel.usace.army.mil/projects/rcc/portal.html).

Because no long-term streamflow data is available within the project area, the NSD tool could not be used. Instead, long-term daily discharge data was evaluated using Time Series Toolbox. The Time Series Toolbox can be used to determine nonstationarity similar to the NSD tool. Figure C:6-17 and Table C:6-2 depict study area and fourth level watershed boundaries (level 4 HUCs), and discharge measurement sites evaluated using USACE climate tools. HUC 0808 was evaluated using the climate tools because it includes most of the study area.

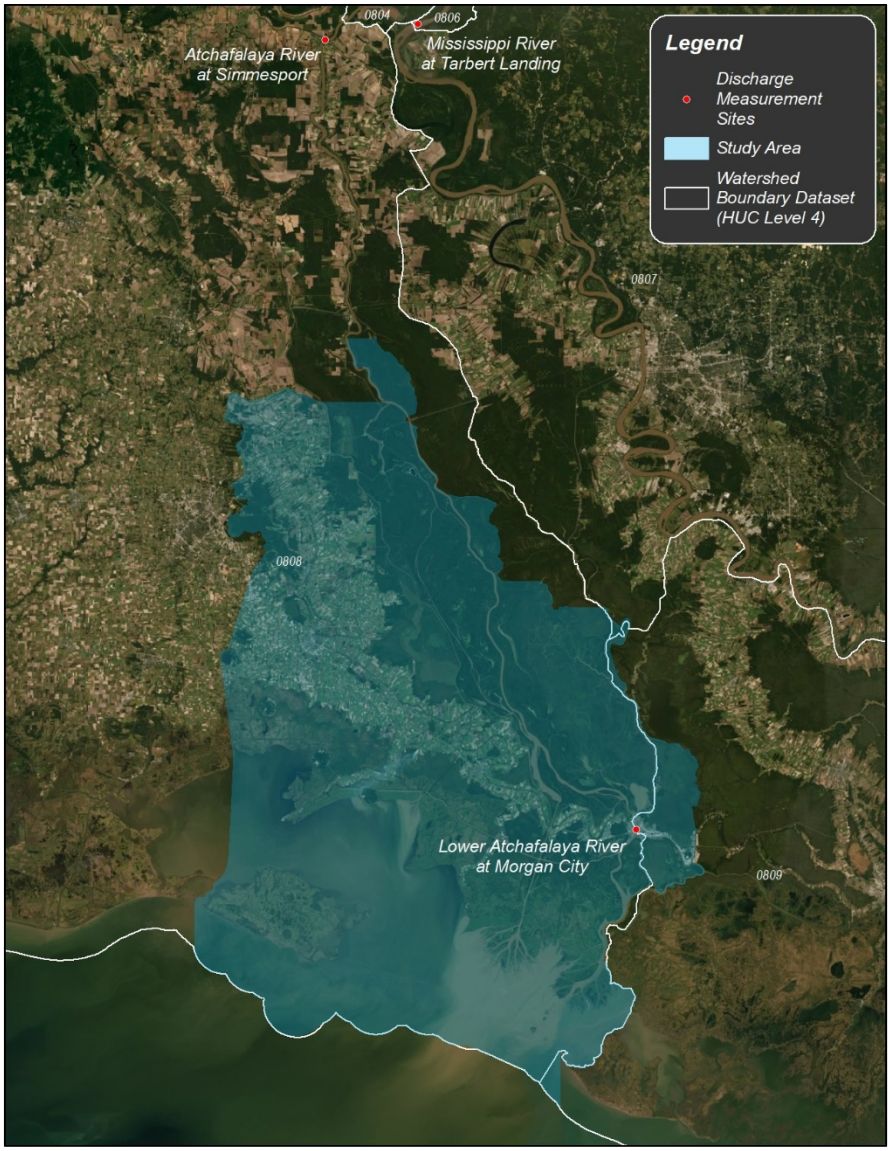

Figure C:6-17. Study Area, Watershed Boundaries, and Discharge Measurement Sites

Table C:6-2. Discharge Measurement Site Information

Tool/Toolbox:	CHAT	Time Series	
Name	Lower Atchafalaya River at Morgan City	Mississippi River at Tarbert Landing	Atchafalaya River at Simmesport
Site ID	03780	01100	03045
Latitude	29.696389	31.008083	30.982500
Longitude	-91.210833	-91.623611	-91.798333
River Mile	117.7	306.3	4.9
Start	1995	1930	
End	2014	2019	

6.4.1 CHAT Tool

The CHAT can be used to evaluate historical annual peak streamflows and projections of watershed mean annual maximum monthly streamflows. Trends in annual peak streamflow are evaluated using linear regression. Projections of watershed mean annual maximum monthly streamflows are based on results from a suite of 93 climate change hydrology models.

For the SCCL study, 1995-2014 annual peak flows for the the Lower Atchafalaya River at Morgan City were chosen for evaluation. Peak flows in this period were all between 175,000-375,000 cfs with the exception of 2011 (512,000 cfs), when the Morganza Floodway was operated. No significant trend in annual peak flows was observed using linear regression (p=0.98) (Figure C:6-18).

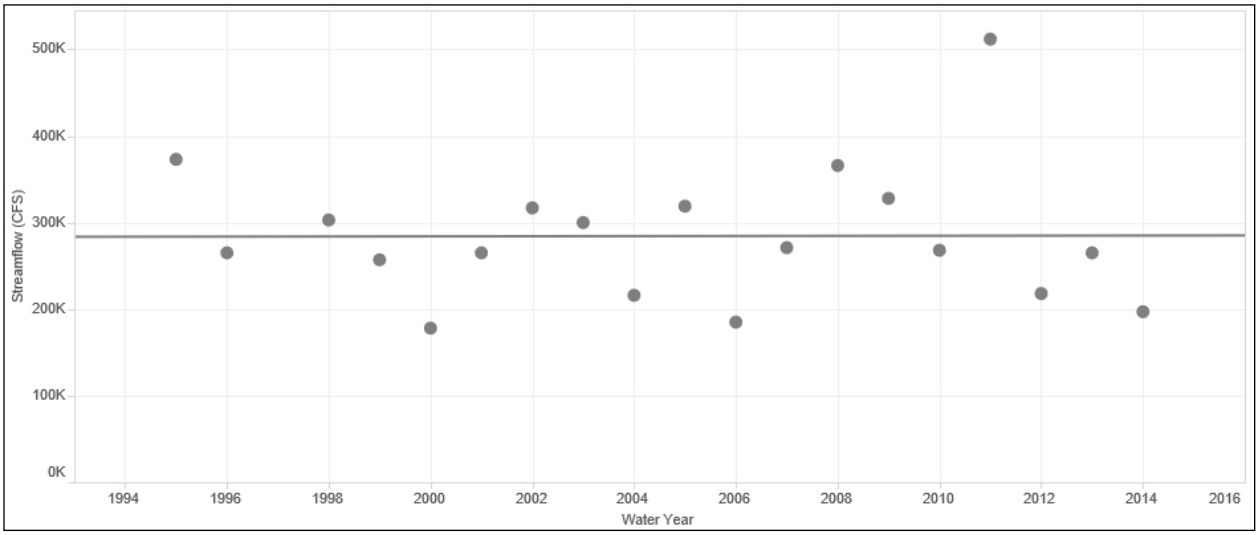

Figure C:6-18. Lower Atchafalaya River at Morgan City Annual Peak Discharge, 1995-2014

Climate change hydrology modeling of HUC 0808 predicts that the mean of annual maximum monthly streamflows within the study area should continue to remain near 60,000 cfs over the remainder of the 21st century (Figures C:6-19, C:6-20, C:6-21). Beginning around 2000, the 'wettest' models predict a 40,000-60,000 cfs increase in annual maximum monthly streamflows (an increase of 67-100 percent), and throughout the period evaluated the 'driest' models predict a slight and gradual decrease in annual maximum monthly streamflows.

Trend evaluation for the mean of projected annual maximum monthly streamflows for the entire period (1952-2100) reveals slight increasing trend (+15 cfs/year) with a p-value of 0.086 (almost significant at α=0.05). When 1952-1999 and 2000-2099 are evaluated separately, a slight decreasing trend occurs for both periods (-18 cfs/year for 1952-1999 and -31 cfs/year for 2000-2099), but only the 2000-2099 trend has a p-value considered significant (0.017). The mean of projected annual maximum monthly streamflows appears to undergo a step increase starting in 2000, which may be related to extreme drought conditions associated with a La Niña event that affected the watershed from 1998-2000 (Lindstedt and Swenson 2006).

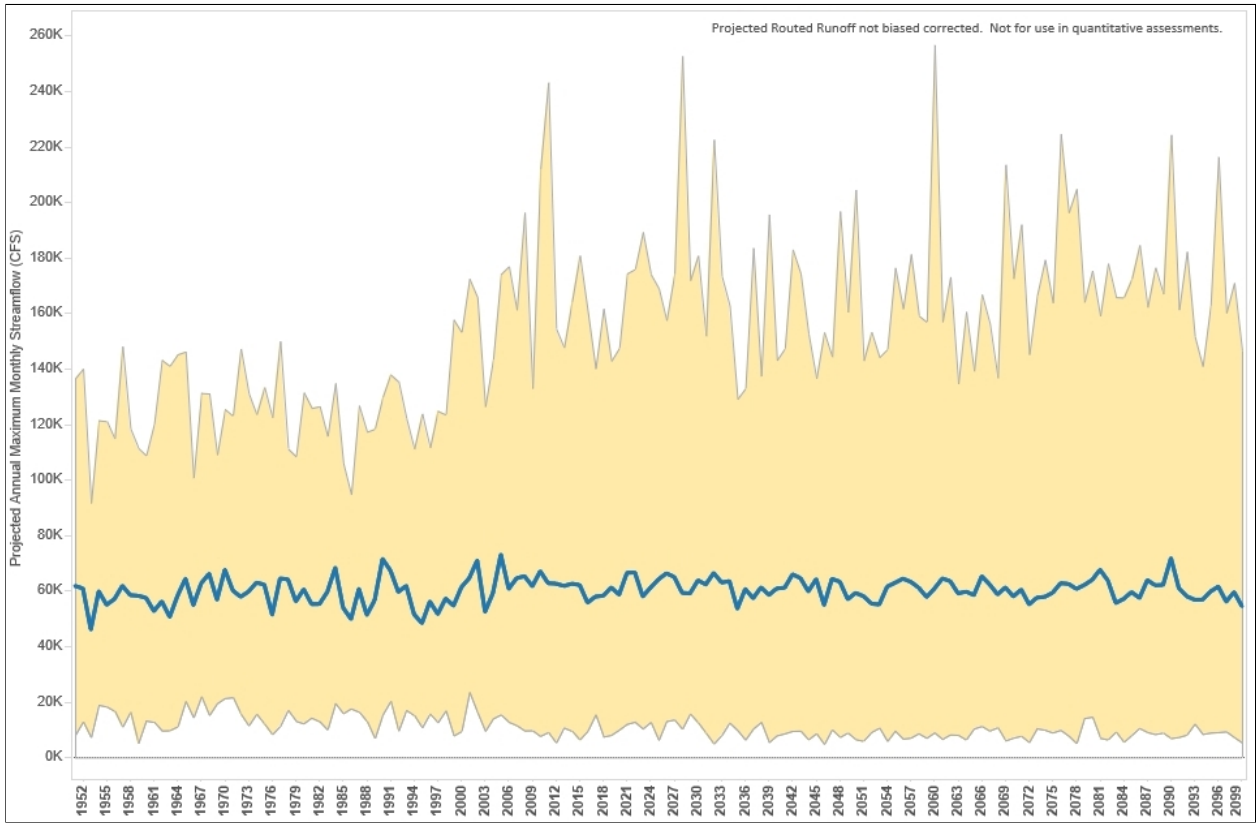

Figure C:6-19. Annual Average and Range of Projected Annual Maximum Monthly Streamflow for Streams within HUC 0808 based on Climate Change Hydrology Models

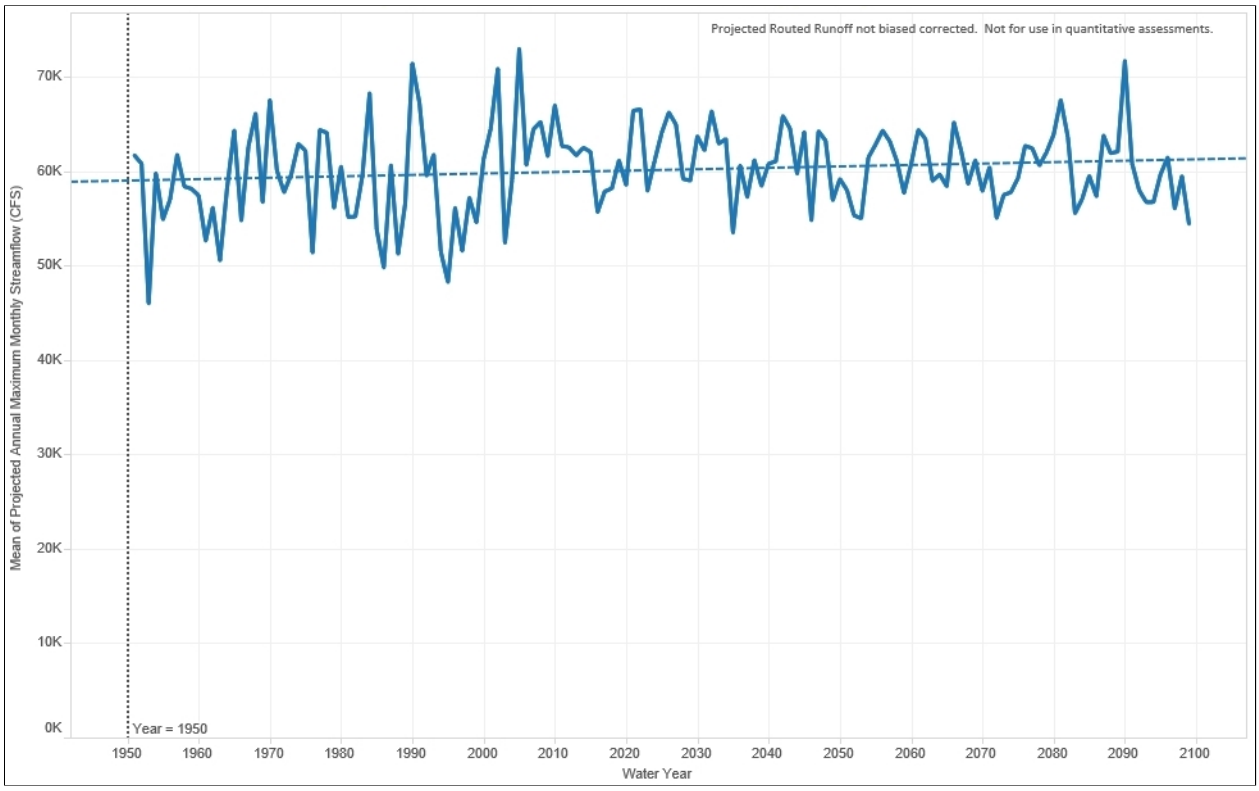

Figure C:6-20. Annual Average of Projected Annual Maximum Monthly Streamflow for Streams within HUC 0808 based on Climate Change Hydrology Models, with Trendline

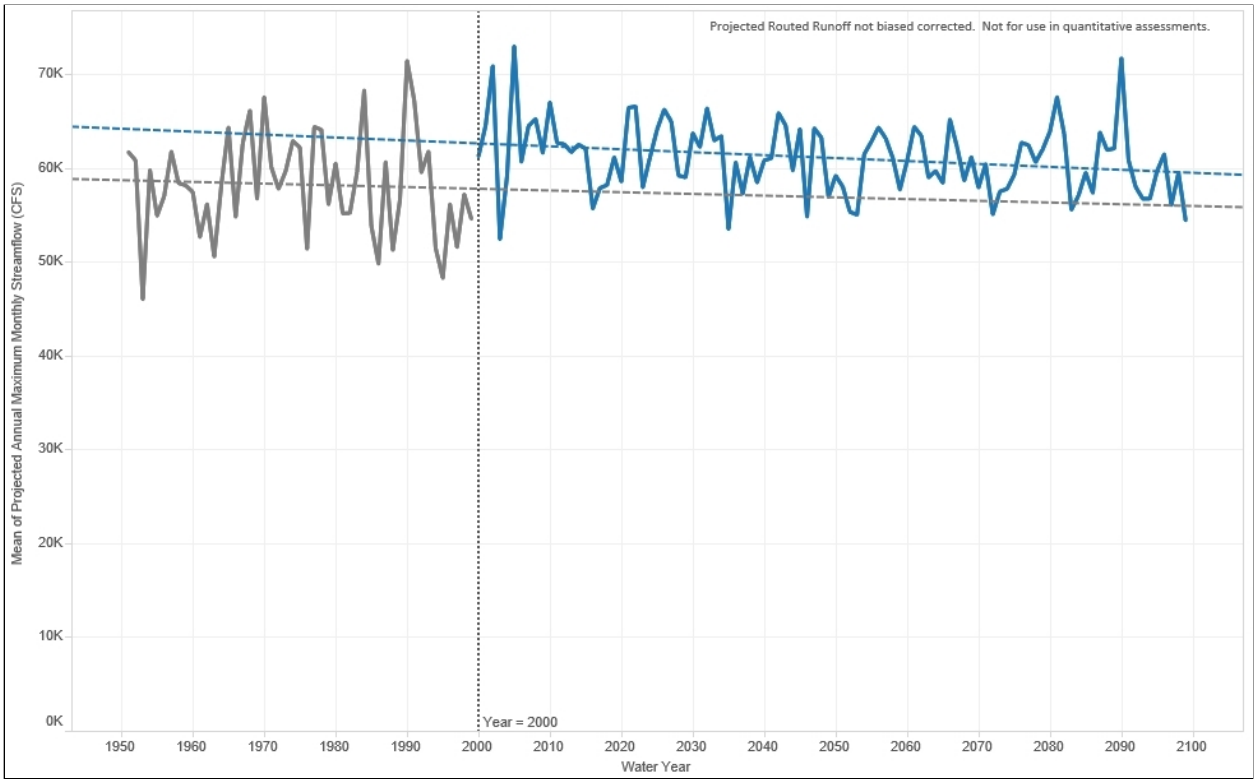

Figure C:6-21. Annual Average of Projected Annual Maximum Monthly Streamflow for Streams within HUC 0808 based on Climate Change Hydrology Models, with Separate Trendlines for 1952-1999 (Grey) and 2000-2099 (Blue)

6.4.2 Time Series Toolbox

The Time Series Toolbox was developed by the USACE to address the need for multiple types of analytical methods for time series data analysis. Climate-related data can come from a variety of sources (e.g., streamflow, water levels, tide gauge data, or precipitation data) where some datasets can be very large. The Time-Series Toolbox provides automated data pre-processing, and works to standardize and streamline common approaches to time series analysis by performing trend analysis and nonstationarity detection for user-supplied datasets. A common use for the toolbox is to use it in place of the NSD when a climate assessment is needed for a climate variable other than flow (e.g. precipitation), or if the NSD does not have a gauge in close proximity to the project area. The toolbox includes tools for model-based analysis of trend, seasonality, nonstationarity detection, and time series.

The toolbox was used to evaluate 1930-2019 estimated Atchafalaya River discharge, which was calculated as 30 percent of the combined latitude flows of the Mississippi

River at Tarbert Landing and the Atchafalaya River at Simmesport (see Table C:6-2 for site information).

6.4.3 Model-Based Analysis

Trend Analysis

The Trend Analysis Tool is used to measure trends in hydrologic data by fitting regression curves to the data and determining regression slopes. The tool uses both parametric (t-Test) and non-parametric (Spearman Rank-Order and Mann-Kendall) regression techniques to test the significance of the trend line slopes. It also computes a fitted trendline using Sen's slope, an approach that is more robust to outliers than a traditional least-squares regression. Sen's slope is the median of the slopes between every pair of data points.

Figure C:6-22 provides trend analysis data and trendlines. Both the traditional and Sens slope trendlines are positive (+883 and +868 ft^3/s per year), suggesting an increase in discharge over the period of record. Table C:6-3 provides p-values for t-test, Spearman rank-order, and Mann Kendall tests for the significance of the trendline slope, which were all less than or equal to $2.2x10^{-16}$ and therefore significant at $\alpha=0.05$.

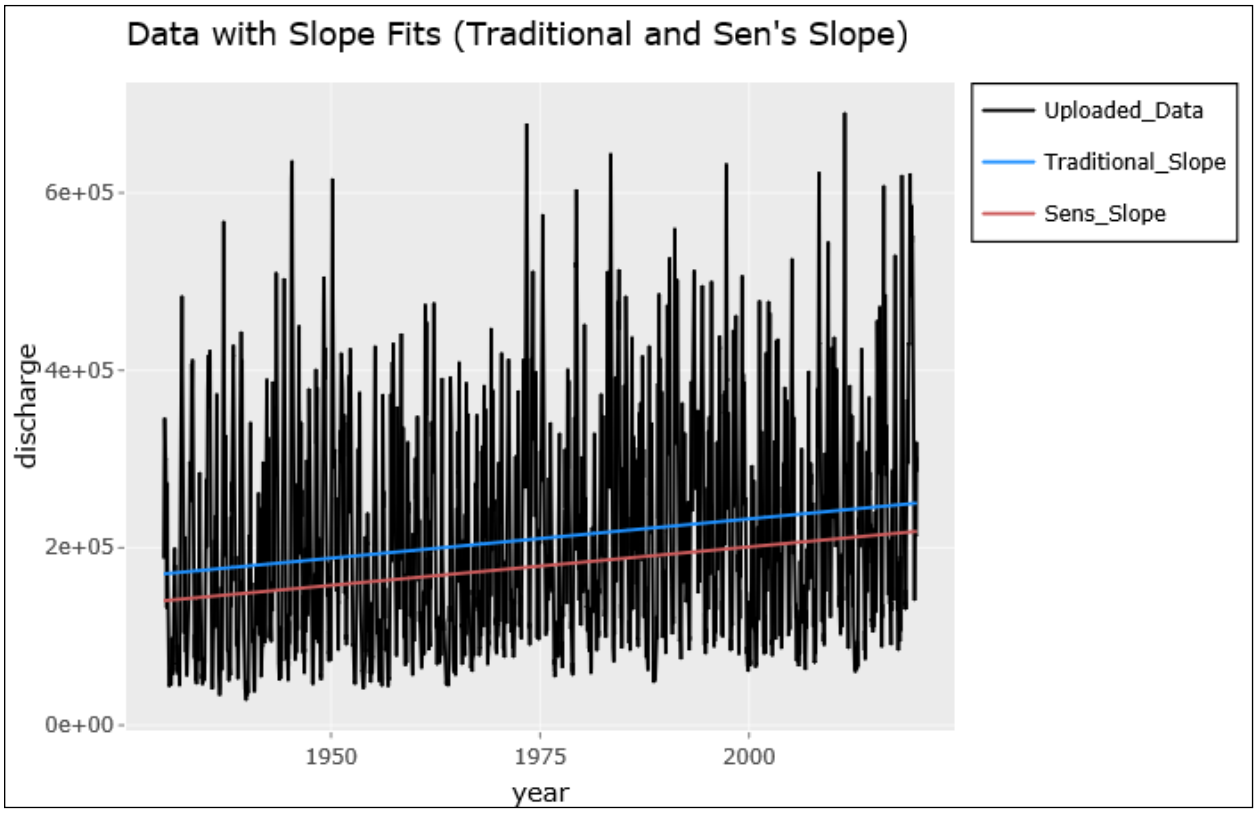

Figure C:6-22. Estimated Atchafalaya River Daily Discharge Data and Trendlines

Table C:6-3. Trend Test p-values

Test	p-value
t-Test	6.3453E-252
Mann-Kendall	2.20E-16
Spearman Rank-Order	2.20E-16

Seasonality

The Seasonality Tool uses a series of statistical methods to identify and define seasonal patterns in data, taking into account underlying trends in data as well as noise and natural volatility. The tool uses two different methods of decomposing the original data to better capture seasonality, trends, and random effects. The first, Moving Average Decomposition, uses moving averages to identify trends and seasonality, while the second, Seasonal-Trend Decomposition by LOESS (local polynomial regression), uses LOESS curves for the same purpose.

Figure C:6-23 provides an example seasonality data plot series, which is for the LOESS method with an individual Y-scale visualization format. All seasonality plot series show similar patterns for trend, seasonality, and random effects. Periodic increasing and decreasing trends appear to occur within the period of record, and over the entire period of record there appears to be an overall increasing trend.

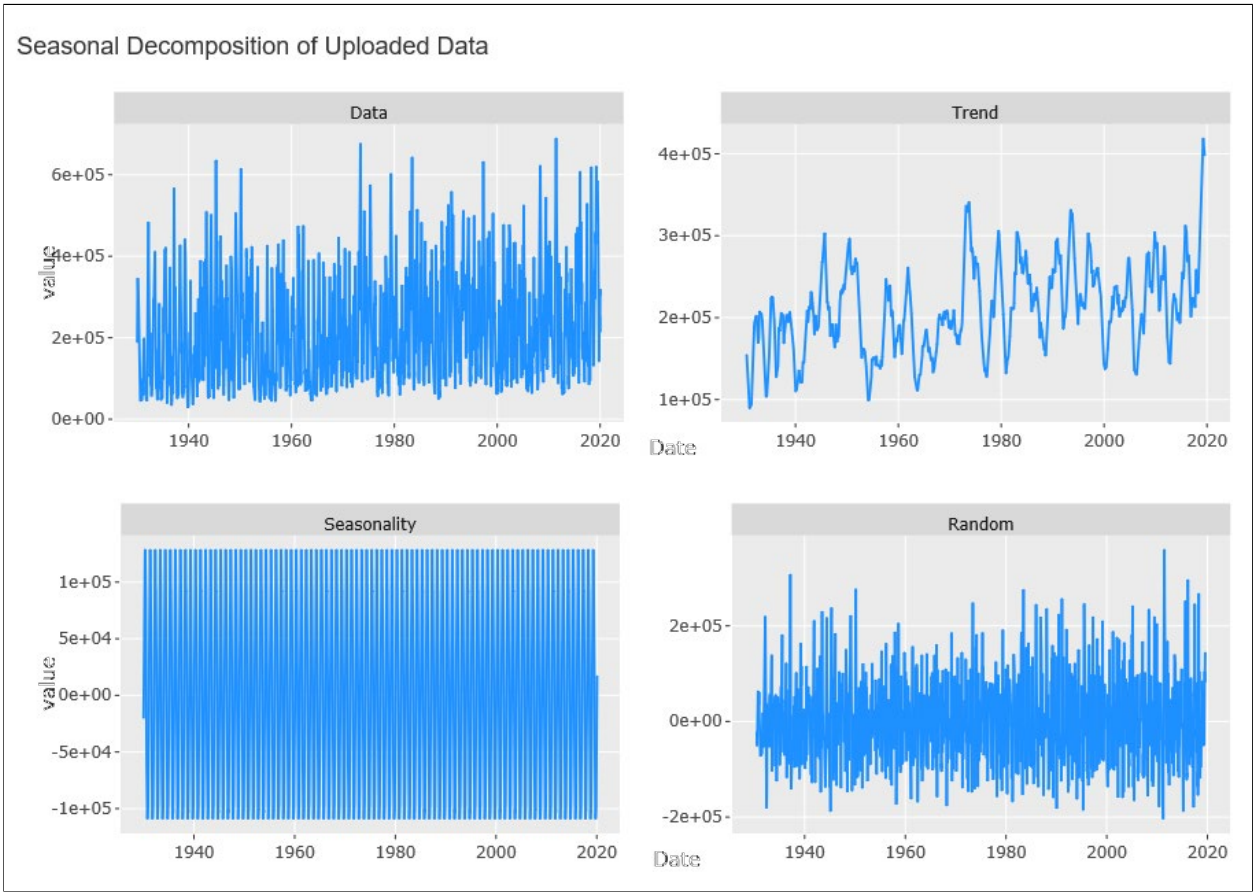

Figure C:6-23 Example Seasonality Data Plot Series

6.4.4 Nonstationarity Detection and Breakpoint Analysis

USACE projects, programs, missions, and operations have generally proven robust enough to accommodate the range of natural climate variability over their operational life. However, in some places and for some impacts relevant to USACE operations, climate change and modifications to watersheds are undermining the fundamental design assumption of stationarity (the statistical characteristics of hydrologic data are consistent with respect to time), an assumption has enabled the use of well-accepted statistical methods in water resources planning and design that rely primarily on the observed hydrologic data records. Nonstationarities are identified when the statistical characteristics of a hydrologic data series are not constant through time. USACE Engineering Technical Letter (ETL) 1100-2-3, entitled *Guidance for Detection of Nonstationarities in Annual Maximum Discharges* (USACE 2017), provides technical guidance on detecting nonstationarities in the hydrologic record, which may continue to impact hydrology into the future and should be considered under future project conditions.

The Nonstationarity Detection Tab includes both the NSD Tool and Breakpoint Analysis. The NSD tool, which is based on ETL 1100-2-3, uses an array of statistical tests to detect the presence of nonstationarities in the data mean (Lombard Wilcoxon, Pettitt, Mann-Whitney, and Bayesian CPD), variance (Mood and Lombard Mood), or distribution (Cramer-Von-Mises, Kolmogorov-Smirnov, LePage, and Energy Divisive). The confirmation of nonstationarities by multiple tests provides robust evidence for nonstationarity. In combination with the NSD Tool, Breakpoint Analysis uses linear regression and the analysis of model errors with hypothesis testing to also identify points in the data that reflect sharp changes in behavior, suggesting the need for segmented analysis. In short, the Nonstationarity Analysis identifies when the statistical characteristics of the data have changed to the point that they may be considered two distinct datasets, while the Breakpoint Analysis identifies when the initial statistical model no longer fits the data and should be replaced with a new model.

Figures C:6-24 through C:6-26 depict NSD results for annual daily maximum discharge, annual discharge volume, and annual daily minimum discharge. For annual minimum discharge (Figure C:6-24), the CVM test suggests changes in the distribution of annual minimum discharge in 1940 and 1968, and the LP and END tests also suggest a change in distribution in the mid- to late-1960s. The LW and MW tests suggest a change in the mean of annual minimum discharge during the mid-1960s, and the MW test also suggests a change in 1940. The Mood (MD) test indicates a change in variance in 1940, while the Smooth Lombard Wilcoxon (SLW) test indicated a change from 1930-1983. Overall, it appears that the distribution and mean of annual minimum discharge underwent a step increase beginning in the mid-1960s.

For annual maximum discharge (Figure C:6-25), the Cramer-Von-Mises (CVM) and energy divisive (END) tests suggest a change in the distribution of annual maximum discharge in the early 1970s, and the Lombard-Wilcoxon (LW) and Mann-Whitney (MW) tests suggest a change in the mean of annual maximum discharge in the early 1970s. Overall, it appears that the distribution and mean of annual minimum discharge underwent a step increase beginning in the early 1970s.

For annual discharge volume (Figure C:6-26), the CVM, LePage (LP), and END tests suggest a change in the distribution of annual volume in the early 1970s. The LW and MW tests suggest a change in the mean of annual volume in the early 1970s, and the Bayesian CPD (BAY) test suggests a change in the mean of annual volume beginning in 2018. Also, the Smooth Lombard Mood (SLM) test suggests a change in the variance of annual volume beginning in 2016. Overall, it appears that the distribution and mean of annual volume underwent a step increase beginning in the early 1970s.

Overall, breakpoint analyses strongly suggest increases in the distribution and mean of flows occurring around the mid-1960s/early 1970s.

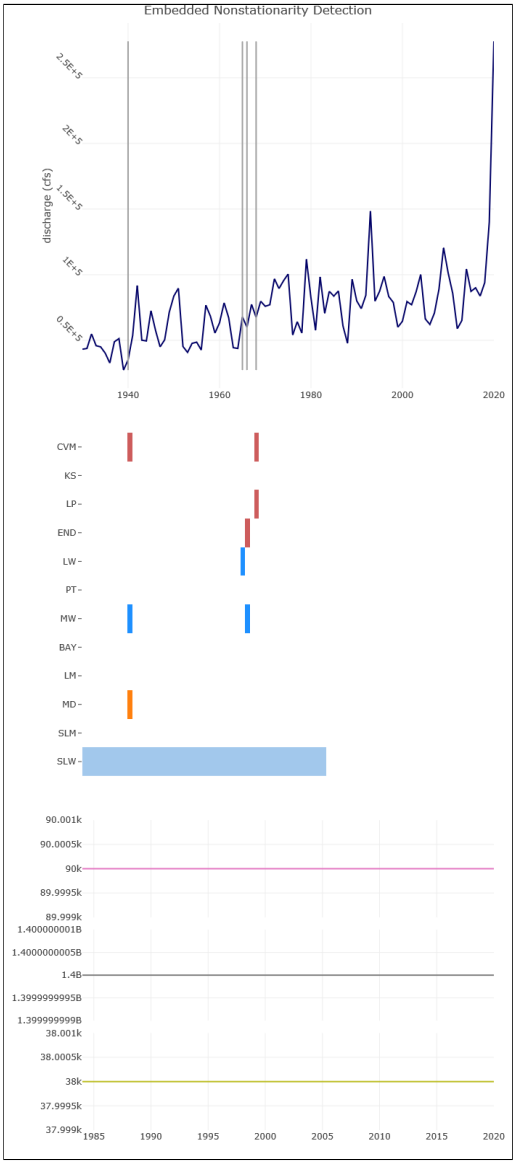

Figure C:6-24. Nonstationarity Detection Results for Annual Minimum Discharge

(Distribution-based tests: CVM=Cramer-Von-Mises, S=Kolmogorov-Smirnov, LP=LePage, END=Energy Divisive; Mean-based tests: LW=Lombard Wilcoxon, PT=Pettitt, MW=Mann-Whitney, BAY=Bayesian CPD; Variance-based tests: LM=Lombard Mood, MD=Mood SLM=Smooth Lombard Mood, SLW=Smooth Lombard-Wilcoxon)

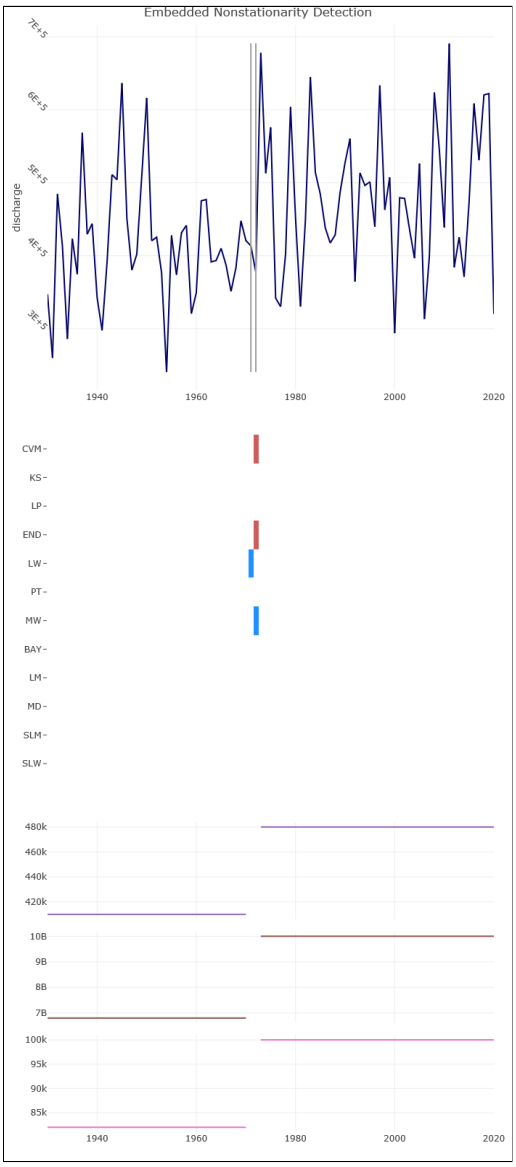

Figure C:6-25. Nonstationarity Detection Results for Annual Maximum Discharge

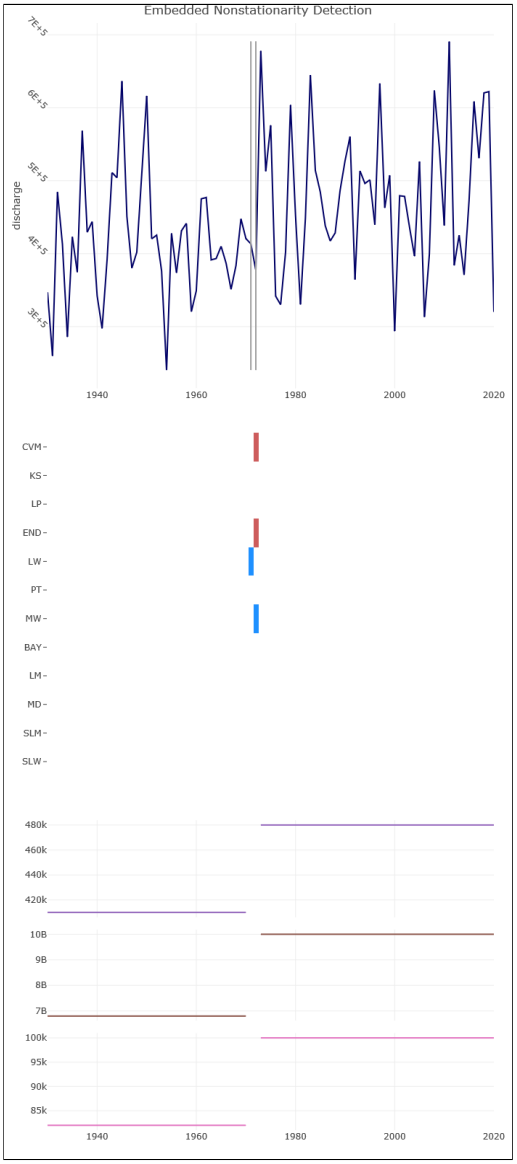

Figure C:6-26. Nonstationarity Detection Results for Annual Discharge Volume

6.4.5 Time Series Analysis

Time Series Analysis includes the determination of the appropriate time series model by using techniques that control for seasonality, trend, and nonstationarities. This tool includes linear, Auto Regressive Integrating Moving Average (ARIMA), and Exponential Smoothing (ETS) models. Time-series linear, ARIMA, and ETS models and diagnostic plots for Atchafalaya River estimated average monthly discharge are included in Figures C:6-27 through C:6-25. For all models, residuals appear to be homogenous (not increasing or decreasing over time). Residual autocorrelation plots and Box-Ljung test

p-values suggest autocorrelation for the ARIMA and ETS models. The models appear to suggest an increase in monthly average discharge over the period of record.

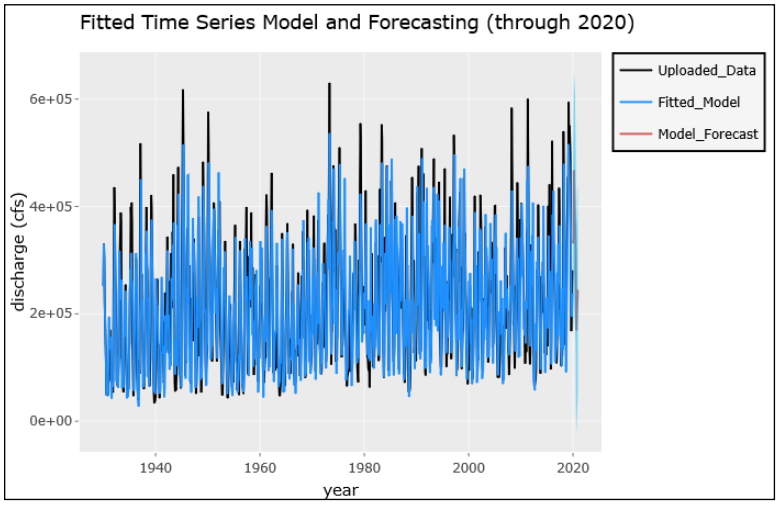

Figure C:6-27. Atchafalaya River Estimated Monthly Average Discharge Time Series Linear Model and Forecast

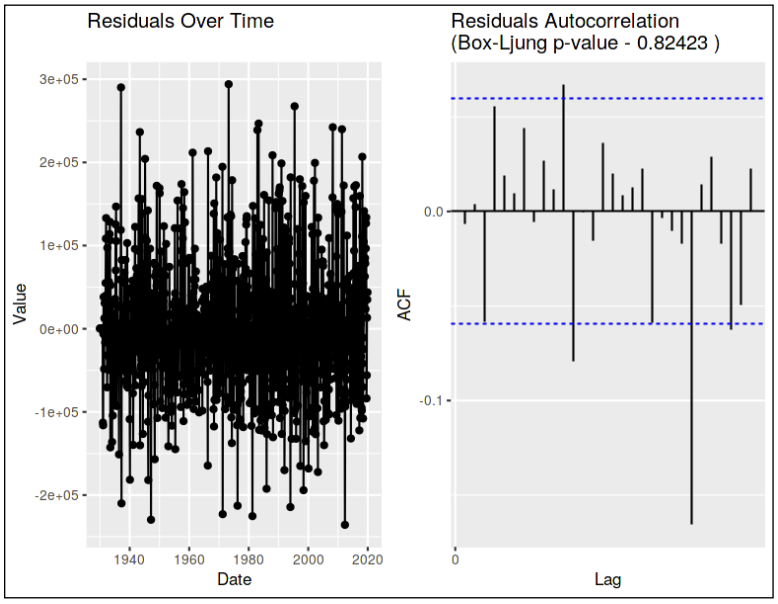

Figure C:6-28. Atchafalaya River Estimated Monthly Average Discharge Time Series Model Residual Plots

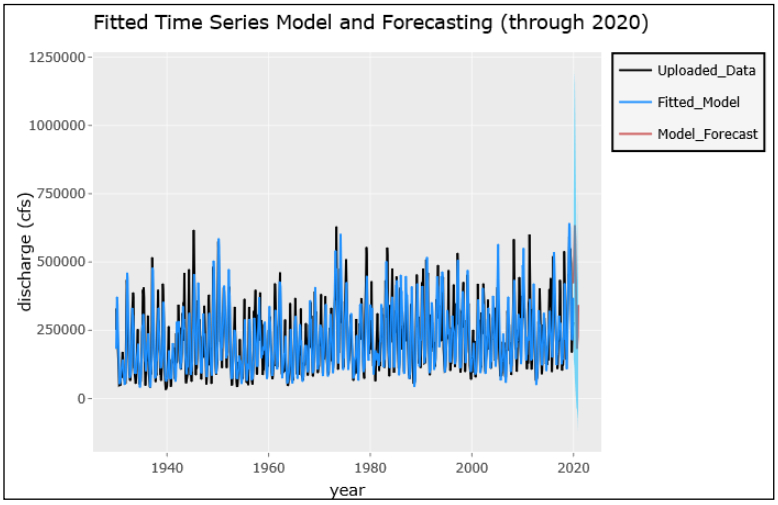

Figure C:6-29. Atchafalaya River Estimated Monthly Average Discharge ARIMA Model and Forecast

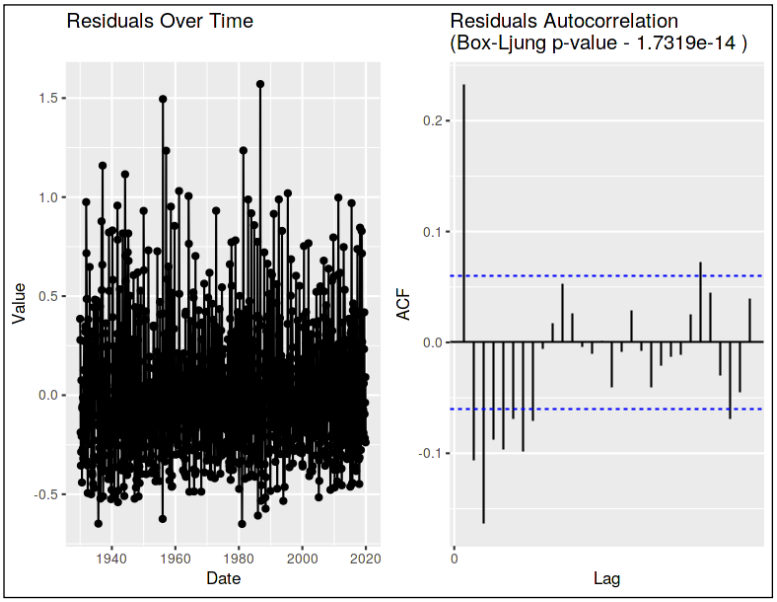

Figure C:6-30. Atchafalaya River Estimated Monthly Average Discharge ARIMA Residual Plots

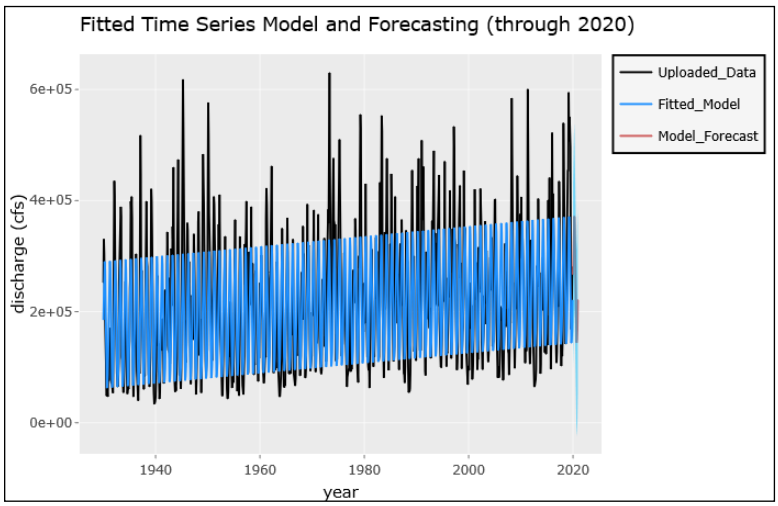

Figure C:6-31. Atchafalaya River Estimated Monthly Average Discharge ETS Model and Forecast

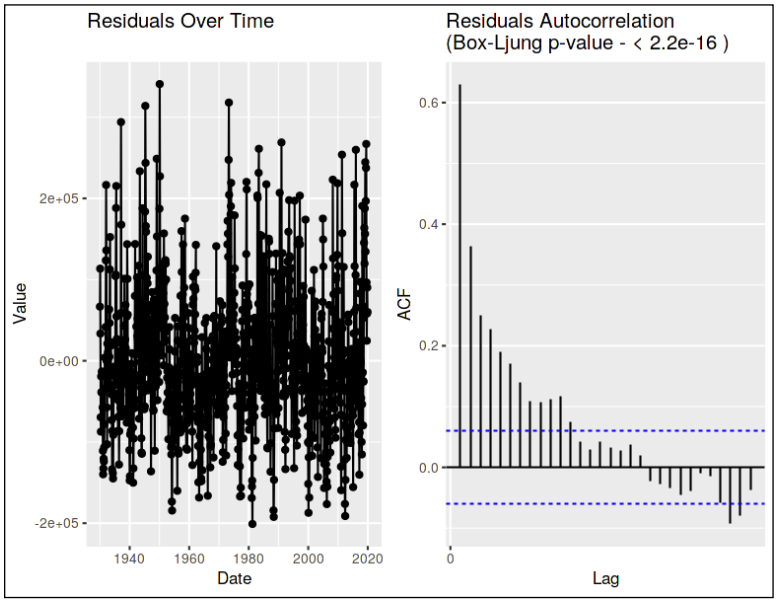

Figure C:6-32. Atchafalaya River Estimated Monthly Average Discharge ETS Residual Plots

Overall, the results of the Nonstationarity and Breakpoint Analyses suggest an increase in estimated Atchafalaya River flows and flow variability began around the mid-1960s/early 1970s.

6.4.6 VA Tool

The USACE Watershed Vulnerability Assessment Tool provides a screening-level assessment of future climate change vulnerability with regards to USACE functions for each fourth level watershed (level 4 HUCs using USGS delineations) in the continental United States (USACE 2016). The tool assesses vulnerability for two future time periods: 2035-2064 and 2070-2099, which are labeled '2050' and '2085', respectively, based on the midpoint of each time period. The tool also assesses two climate change scenarios, labelled 'wet' and 'dry.' These scenarios are based on annual precipitation forecasts for a suite of general circulation models (GCMs) for each second level watershed (level 2 HUCs). GCMs with annual precipitation above the median of all GCMs in the years 2050 and 2085 are used for modeling the 'wet' scenario for each respective time period, while those with annual precipitation below the median are used for modeling the 'dry' scenario. A key point to remember is that these distinctions are relative to each other, not to present climate. A 'wet' scenario, for example, may be wetter or drier than present climate so long as it is wetter than the median of all scenarios.

The assessment is performed with respect to USACE functions known as 'business lines', which include flood risk reduction, ecosystem restoration, recreation, regulatory, navigation, hydropower, water supply, and emergency management. Each business line includes a suite of 'indicators' which are parameters used to determine business line vulnerability (see Table C:6-4 for example). For each indicator within a business line, scores are determined based on the percentile of the rank among all fourth level watersheds of the difference between a future climate change scenario/time period combination as determined by GCMs and base conditions (the base conditions period of analysis varies by indicator), as well as indicator weight (which ranges between 1-2). The combined score of all indicators for a business line is the total score for that business line, known as a WOWA (Weighted Order Weighted Average) score. For a given future climate change scenario/time period/business line combination, watersheds with a WOWA score in the top 20th percentile are considered vulnerable to climate change.

Table C:6-4. Example Business Line Indicators

Business Line	Indicator Short Name	Importance Weight
Ecosystem Restoration	297_MACROINVERTEBRATE	2
	8_AT_RISK_FRESHWATER_PLANT	2
	277_RUNOFF_PRECIP	1.75
	221C_MONTHLY_COV	1.75
	156_SEDIMENT	1.5
	568C_FLOOD_MAGNIFICATION	1.5
	65L_MEAN_ANNUAL_RUNOFF	1.3
	568L_FLOOD_MAGNIFICATION	1
	700C_LOW_FLOW_REDUCTION	1

The assessment can also be performed using custom settings, which include the use of custom indicators and indicator weights, custom percentile thresholds for defining vulnerability, defining vulnerability based on the aggregate of all results (i.e. the top nth percentile of all combinations of watershed, climate change scenario, and time period), and by using a custom suite of watersheds. However, for the SCCL study, the "National Standard View" (no custom settings) was used.

The SCCL study is within the Louisiana Coastal watershed (level 4 HUC 0808). For each combination of climate change scenario and future time period, at least one business line has a WOWA score in the top 20th percentile, and therefore may be vulnerable to climate change risks (Table C:6-5) The business line most vulnerable according to the assessment tool is the ecosystem restoration business line, which had WOWA scores within the top 20th percentile for every combination of climate change scenario and future time period. The dry climate change scenario had three business lines with WOWA scores within the top 20th percentile for the 2085 time period.

Table C:6-5. Louisiana Coastal Watershed Business Line Vulnerability Summary

Time Period / Scenario	2050	2085
Dry	Ecosystem Restoration	Ecosystem Restoration, Recreation, Emergency Management
Wet	Ecosystem Restoration	Ecosystem Restoration

Table C:6-6 provides a summary of WOWA scores for each combination of business line, climate change scenario, and time period, while Table C:6-7 provides details concerning indicator scores. WOWA scores in the top 20th percentile are highlighted in yellow.

The ecosystem restoration business line, which is vulnerable to climate change risks for all future climate change scenarios and future time periods, is most affected by indicator scores for 8_AT_RISK_FRESHWATER_PLANT (percent of freshwater plant communities at risk) and 277_RUNOFF_PRECIP (percent change in runoff divided by percent change in precipitation), and 221C_MONTHLY_COV (short-term variability in hydrology, calculated as the 75th percentile of the annual ratios of the standard deviation of monthly runoff to the mean of monthly runoff), which are some of the most heavily weighted indicators for the business line. Indicator scores for HUC 0808 are generally similar to national average scores.

The emergency management business line, which is vulnerable to climate change risks for the dry climate change scenario for the 2085 future time period, is most affected by indicator scores for 447_DISABLED (percent of people disabled), 700C_LOW_FLOW_REDUCTION (change in low flow runoff conditions), and 130_FLOODPLAIN_POPULATION (population in the 500-year floodplain). These indicators are heavily weighted, with 130_FLOODPLAIN_POPULATION being the most heavily weighted indicator for the emergency management business line. Indicator scores for HUC 0808 are generally similar to national average scores.

The recreation business line, which is vulnerable to climate change risks for the dry climate change scenario for the 2085 future time period, is most affected by indicator scores for 700C_LOW_FLOW_REDUCTION, 570L_90PERC_EXCEEDANCE (changes in monthly runoff exceeded 90 percent of the time), and 95_DROUGHT_SEVERITY (drought severity index, or precipitation deficit). Despite being the most heavily weighted indicator, 95_DROUGHT_SEVERITY did not have the highest indicator score for either HUC 0808 or for the national average. Two indicators suggest drought conditions could be problematic under the dry climate change scenario for the 2085 future time period. The 2085 future time period in particular had relatively high indicator scores for 95_DROUGHT_SEVERITY compared to the national average for HUC 0808.

Table C:6-6. Louisiana Coastal Watershed WOWA Scores with Comparison to all Level 2 HUCs (WOWA Scores in the Top 20th Percentile are Highlighted in Yellow)

Business Line Name	Scenario	Epoch	WOWA Score		
				All HUCs	
			0808	Average	Range
Ecosystem Restoration	Base		72.6	68.3	56.3 - 80.6
	Dry	2050	73.3	69.2	55.9 - 81.7
		2085	73.3	69.4	55.8 - 81.9
	Wet	2050	74.4	70.0	55.6 - 89.8
		2085	74.1	70.7	54.7 - 89.4
Emergency Management	Base		67.7	65.0	57.9 - 76.6
	Dry	2050	67.9	65.9	58.3 - 75.0
		2085	70.1	66.9	57.0 - 77.4
	Wet	2050	66.7	65.0	56.6 - 79.4
		2085	66.2	65.6	56.6 - 75.9
Flood Risk Reduction	Base		46.0	45.3	37.3 - 70.9
	Dry	2050	46.3	46.7	35.1 - 70.1
		2085	49.5	47.3	35.7 - 69.1
	Wet	2050	54.6	53.3	39.8 - 92.8
		2085	52.5	55.1	40.9 - 86.7
Navigation	Base		63.5	63.0	54.7 - 74.8
	Dry	2050	65.8	65.3	54.9 - 75.2
		2085	69.9	67.3	55.2 - 77.5
	Wet	2050	69.9	67.0	56.4 - 84.3
		2085	68.1	69.0	57.9 - 84.4
Recreation	Base		61.7	62.9	55.2 - 72.2
	Dry	2050	64.9	65.7	57.1 - 74.4
		2085	75.4	67.5	57.4 - 82.2
	Wet	2050	64.5	66.0	57.7 - 85.6
		2085	62.7	66.5	56.7 - 83.6
Regulatory	Base		70.0	68.5	57.6 - 83.2
	Dry	2050	72.1	69.7	57.8 - 82.8
		2085	72.5	70.1	57.7 - 82.7
	Wet	2050	72.3	70.1	57.3 - 91.0
		2085	72.2	70.7	57.3 - 89.3

Table C:6-7. Lower Mississippi Watershed Business Line Indicator Scores with Comparison to all Level 4 HUCs

		WOWA Indicator Score								WOWA Indicator Percent of Business Line Total							
		HUC 0808						All HUCs		HUC 0808						All HUCs	
				2050		2085						2050		2085			
Business Line Name	Indicator Short Name	Average Score	Base	Dry	Wet	Dry	Wet	Average Score	Range of Score	Average Score	Base	Dry	Wet	Dry	Wet	Average Percent of Total	Range of Percent of Total
Ecosystem Restoration	8_AT_RISK_FRESHWATER_PLANT	28.6	28.7	28.8	28.4	28.8	28.4	26.7	17.7 - 30.0	38.9%	39.6%	39.3%	38.2%	39.3%	38.3%	38.5%	25.3% - 47.1%
	277_RUNOFF_PRECIP	13.9	14.3	14.7	14.6	11.3	14.4	11.0	2.1 - 20.1	18.9%	19.8%	20.0%	19.6%	15.4%	19.4%	15.8%	3.0% - 24.7%
	221C_MONTHLY_COV	11.7	10.5	11.2	10.8	14.9	11.0	9.4	1.3 - 20.4	15.9%	14.4%	15.3%	14.5%	20.3%	14.8%	13.5%	2.1% - 26.2%
	297_MACROINVERTEBRATE	8.0	8.0	8.0	7.9	8.0	7.9	8.8	3.2 - 30.0	10.8%	11.0%	10.9%	10.6%	10.9%	10.7%	12.6%	4.3% - 38.8%
	65L_MEAN_ANNUAL_RUNOFF	3.4	4.0	4.1	2.3	4.2	2.3	5.4	1.4 - 15.3	4.6%	5.6%	5.6%	3.1%	5.7%	3.2%	7.8%	2.1% - 21.6%
	568C_FLOOD_MAGNIFICATION	2.4	1.5	1.9	3.3	1.9	3.1	2.8	1.2 - 15.0	3.2%	2.1%	2.6%	4.5%	2.6%	4.3%	4.0%	1.6% - 20.3%
	700C_LOW_FLOW_REDUCTION	2.4	2.7	3.1	1.6	3.2	1.6	2.5	0.6 - 8.0	3.3%	3.7%	4.2%	2.2%	4.3%	2.2%	3.6%	0.9% - 12.0%
	156_SEDIMENT	2.3	2.0	0.5	4.4	0.1	4.3	2.0	0.0 - 17.3	3.1%	2.8%	0.6%	6.0%	0.1%	5.9%	2.8%	0.0% - 24.6%
	568L_FLOOD_MAGNIFICATION	0.9	0.8	1.0	1.0	1.0	1.0	0.9	0.6 - 3.1	1.3%	1.1%	1.4%	1.4%	1.3%	1.3%	1.4%	0.8% - 3.7%
Emergency Managemen	447_DISABLED	15.9	14.4	14.5	18.0	14.7	18.0	14.1	4.6 - 22.3	23.5%	21.2%	21.4%	26.9%	21.0%	27.1%	21.6%	6.4% - 32.7%
	700C_LOW_FLOW_REDUCTION	14.8	10.2	18.2	13.1	19.1	13.3	13.3	2.7 - 24.8	21.7%	15.0%	26.8%	19.7%	27.2%	20.0%	20.2%	4.6% - 32.1%
	130_FLOODPLAIN_POPULATION	12.3	20.1	10.6	10.5	10.4	10.2	8.9	0.0 - 26.4	18.2%	29.7%	15.6%	15.7%	14.8%	15.4%	13.4%	0.0% - 34.5%
	443_POVERTY_POPULATION	7.2	7.5	7.6	7.5	6.0	7.3	6.8	0.3 - 14.9	10.6%	11.1%	11.2%	11.3%	8.5%	11.0%	10.4%	0.4% - 20.5%
	700L_LOW_FLOW_REDUCTION	5.4	5.1	5.9	4.3	7.7	4.3	5.6	0.9 - 15.5	8.0%	7.5%	8.7%	6.4%	11.0%	6.5%	8.6%	1.5% - 20.1%
	448_PAST_EXPERIENCE	1.3	1.6	1.3	1.3	1.0	1.3	5.3	0.4 - 25.4	1.9%	2.3%	1.9%	1.9%	1.5%	1.9%	8.1%	0.5% - 35.8%
	568C_FLOOD_MAGNIFICATION	3.9	2.9	2.8	5.8	2.2	5.5	5.2	1.2 - 26.2	5.7%	4.3%	4.2%	8.8%	3.2%	8.4%	8.0%	1.6% - 33.0%
	277_RUNOFF_PRECIP	3.6	3.8	3.9	3.2	4.0	3.1	2.9	0.7 - 10.4	5.3%	5.6%	5.8%	4.7%	5.7%	4.7%	4.4%	1.0% - 14.9%
	450_FLOOD_INSURANCE_COMMUNITIES	1.0	1.3	1.0	1.0	0.8	1.0	1.9	0.2 - 10.6	1.5%	1.9%	1.5%	1.5%	1.2%	1.5%	2.8%	0.3% - 15.0%
	175C_ANNUAL_COV	1.5	1.0	1.7	1.6	1.4	1.7	1.3	0.4 - 18.2	2.2%	1.4%	2.5%	2.5%	2.0%	2.5%	1.9%	0.7% - 25.7%
	95_DROUGHT_SEVERITY	0.8	0.0	0.4	0.4	2.8	0.6	0.3	0.0 - 4.6	1.2%	0.0%	0.6%	0.6%	4.0%	0.9%	0.5%	0.0% - 6.2%
Flood Risk Reduction	568C_FLOOD_MAGNIFICATION	20.8	20.3	19.6	26.0	13.4	24.7	21.3	4.4 - 47.1	41.6%	44.2%	42.3%	47.7%	27.0%	47.1%	43.6%	6.5% - 57.6%
	568L_FLOOD_MAGNIFICATION	7.4	4.3	4.2	13.2	2.9	12.5	9.2	2.2 - 26.4	14.4%	9.4%	9.0%	24.1%	5.8%	23.8%	18.8%	3.3% - 43.3%
	277_RUNOFF_PRECIP	12.3	12.2	12.5	8.1	20.8	8.0	8.1	1.6 - 29.7	25.1%	26.6%	26.9%	14.8%	42.0%	15.2%	16.7%	2.8% - 47.3%
	590_URBAN_500YRFLOODPLAIN_AREA	6.3	6.7	7.4	4.8	8.0	4.7	6.8	0.0 - 43.5	12.9%	14.6%	16.0%	8.7%	16.1%	9.0%	12.8%	0.0% - 66.3%
	175C_ANNUAL_COV	2.9	2.4	2.7	2.6	4.5	2.6	4.2	1.2 - 37.3	5.9%	5.2%	5.8%	4.7%	9.1%	4.9%	8.2%	2.3% - 52.6%
Navigation	568C_FLOOD_MAGNIFICATION	12.2	8.0	7.8	20.5	5.6	19.1	14.4	4.0 - 29.5	18.0%	12.6%	11.9%	29.4%	8.0%	28.1%	21.8%	5.4% - 37.6%
	570C_90PERC_EXCEEDANCE	13.2	18.2	14.8	11.0	11.1	10.8	13.9	1.9 - 26.9	19.7%	28.6%	22.5%	15.8%	15.9%	15.9%	20.9%	2.6% - 36.2%
	700C_LOW_FLOW_REDUCTION	12.9	13.5	19.4	8.4	14.9	8.3	13.1	1.8 - 22.4	19.2%	21.2%	29.6%	12.0%	21.3%	12.1%	20.0%	2.5% - 33.9%
	277_RUNOFF_PRECIP	8.3	10.3	10.6	6.4	7.9	6.2	8.0	2.9 - 22.7	12.3%	16.2%	16.1%	9.1%	11.3%	9.1%	11.9%	4.7% - 30.4%
	156_SEDIMENT	7.0	5.5	0.9	14.5	0.2	13.9	6.2	0.0 - 22.8	10.3%	8.7%	1.3%	20.8%	0.2%	20.5%	9.4%	0.0% - 31.2%
	570L_90PERC_EXCEEDANCE	3.5	3.5	4.7	3.4	3.5	2.7	4.8	1.5 - 19.2	5.3%	5.5%	7.1%	4.9%	5.0%	3.9%	7.2%	2.2% - 29.1%
	95_DROUGHT_SEVERITY	5.7	0.0	1.6	1.1	22.2	3.6	2.1	0.0 - 28.5	8.2%	0.0%	2.4%	1.6%	31.8%	5.3%	3.0%	0.0% - 37.8%
	221C_MONTHLY_COV	2.5	1.9	3.4	2.5	2.6	2.0	2.0	0.8 - 4.6	3.6%	3.0%	5.1%	3.5%	3.7%	2.9%	3.0%	1.2% - 6.4%
	441_500YRFLOODPLAIN_AREA	2.1	2.5	2.5	1.9	1.9	1.5	1.4	0.0 - 7.4	3.1%	4.0%	3.9%	2.7%	2.7%	2.2%	2.1%	0.0% - 12.1%
	192_URBAN_SUBURBAN	0.1	0.1	0.1	0.1	0.1	0.1	0.5	0.0 - 7.3	0.2%	0.2%	0.2%	0.2%	0.2%	0.2%	0.7%	0.0% - 11.0%
Recreation	570L_90PERC_EXCEEDANCE	12.1	13.8	13.9	13.5	9.8	9.7	17.7	4.7 - 29.6	18.6%	22.4%	21.5%	20.9%	13.0%	15.5%	26.7%	7.9% - 43.8%
	700C_LOW_FLOW_REDUCTION	19.0	19.7	21.6	19.7	15.5	18.5	17.1	1.6 - 26.1	29.2%	32.0%	33.3%	30.5%	20.6%	29.5%	26.4%	2.6% - 39.6%
	221C_MONTHLY_COV	8.8	9.7	10.2	9.8	7.2	7.2	7.1	1.2 - 22.6	13.6%	15.8%	15.7%	15.2%	9.6%	11.5%	10.7%	2.1% - 31.5%
	571C_10PERC_EXCEEDANCE	5.7	6.9	6.7	5.3	4.6	4.9	6.7	1.4 - 20.6	8.7%	11.2%	10.3%	8.2%	6.2%	7.8%	10.4%	1.9% - 31.2%
	568C_FLOOD_MAGNIFICATION	3.6	3.3	2.4	6.9	2.1	3.6	5.3	1.8 - 27.5	5.6%	5.3%	3.6%	10.7%	2.7%	5.8%	8.0%	2.4% - 32.1%
	277_RUNOFF_PRECIP	4.0	5.0	5.0	3.9	3.5	2.7	4.8	1.2 - 12.7	6.2%	8.2%	7.7%	6.0%	4.6%	4.4%	7.3%	1.7% - 19.2%
	95_DROUGHT_SEVERITY	10.1	0.0	3.3	2.3	31.4	13.2	3.8	0.0 - 35.5	14.3%	0.0%	5.2%	3.6%	41.7%	21.1%	5.6%	0.0% - 46.1%
	568L_FLOOD_MAGNIFICATION	1.3	1.4	1.3	1.3	1.1	1.2	1.8	0.7 - 6.4	1.9%	2.2%	2.0%	2.1%	1.5%	1.9%	2.7%	1.1% - 7.9%
	156_SEDIMENT	1.1	1.8	0.4	1.8	0.1	1.6	1.4	0.0 - 20.8	1.8%	2.9%	0.6%	2.8%	0.1%	2.6%	2.2%	0.0% - 31.7%
Regulatory	8_AT_RISK_FRESHWATER_PLANT	25.1	25.1	25.2	25.1	25.2	25.0	23.8	15.8 - 26.8	35.0%	35.8%	35.0%	34.7%	34.8%	34.7%	34.1%	26.3% - 40.8%
	221C_MONTHLY_COV	13.1	12.4	13.3	12.9	13.6	13.2	9.3	1.1 - 18.4	18.2%	17.7%	18.5%	17.8%	18.8%	18.2%	13.2%	1.6% - 23.6%
	700C_LOW_FLOW_REDUCTION	8.0	6.7	9.6	6.9	9.9	7.0	8.4	0.8 - 16.1	11.2%	9.6%	13.3%	9.6%	13.7%	9.7%	12.2%	1.1% - 21.2%
	65C_MEAN_ANNUAL_RUNOFF	4.8	5.0	5.1	4.0	5.1	4.9	7.0	1.0 - 15.2	6.7%	7.1%	7.1%	5.5%	7.1%	6.8%	10.0%	1.3% - 20.2%
	297_MACROINVERTEBRATE	8.2	8.9	7.2	8.9	7.2	8.9	5.9	1.4 - 19.1	11.4%	12.7%	10.0%	12.3%	9.9%	12.3%	8.5%	1.7% - 25.0%
	65L_MEAN_ANNUAL_RUNOFF	2.3	2.7	2.8	1.7	2.8	1.7	4.6	1.2 - 13.1	3.3%	3.9%	3.8%	2.4%	3.9%	2.4%	6.6%	1.7% - 18.8%
	277_RUNOFF_PRECIP	4.2	3.9	4.0	5.0	4.0	3.9	3.2	0.7 - 11.7	5.8%	5.6%	5.5%	6.9%	5.5%	5.5%	4.7%	1.0% - 16.6%
	568C_FLOOD_MAGNIFICATION	2.1	1.6	1.5	3.1	1.5	3.0	3.0	1.0 - 16.2	2.9%	2.2%	2.1%	4.3%	2.0%	4.1%	4.3%	1.3% - 19.5%
	175C_ANNUAL_COV	1.8	1.9	2.2	1.4	2.2	1.4	2.1	0.5 - 17.7	2.5%	2.8%	3.0%	1.9%	3.1%	1.9%	2.9%	0.8% - 21.3%
	156_SEDIMENT	1.3	1.2	0.4	2.4	0.1	2.4	1.6	0.0 - 16.1	1.8%	1.7%	0.5%	3.3%	0.1%	3.3%	2.3%	0.0% - 22.7%
	568L_FLOOD_MAGNIFICATION	0.8	0.7	0.8	0.9	0.8	0.8	0.9	0.5 - 4.3	1.1%	1.0%	1.2%	1.2%	1.1%	1.2%	1.3%	0.7% - 5.6%

6.4.7 Climate Risk Table

Table 4. is a climate risk table that qualitatively describes future flood hazards and potential impacts on the tentatively selected plan. The current TSP is a non-structural plan that implements flood proofing and raises to the 2075 0.004 AEP total water level.

Table 2. Climate Risk Table for TSP Elements and Triggers

Feature or Measure	Trigger	Hazard	Harm	Qualitative Likelihood o Hazard Occurrence
Structural Raises	Increased extreme flow event frequency	Future flood volumes may be larger or longer-lasting than present	effects of large floods extend beyond existing MR&T protection	unlikely
Structural Raises	Increased extreme precipitation event frequency	Future precipitation events may be larger or longer-lasting than present	future precipitation events impact raised structures	unlikely
Structural Raises	RSLR	Subsidence and eustatic sealevel rise will result in higher surges and wave heights in the future	Structure elevations may become deficient beyond 2075	likely

6.4.8 Conclusion

Available academic literature is largely lacking in consensus about past trends in precipitation and temperature, with uneven cycles of warmer and cooler weather potentially obscuring longer-term changes, and natural variability in precipitation dominating changes in mean rainfall. Future changes described in the literature are expected to bring warmer temperatures, but varied effects for rainfall frequency and intensity. USACE Climate Tools were used to evaluate historical climate variables and future climate change vulnerabilities. The CHAT tool did not find a significant trend for 1995-2014 Lower Atchafalaya River at Morgan City annual peak flow, while climate change hydrology modeling for HUC 0808 suggests increases in annual maximum monthly streamflow and streamflow variability could occur, primarily under the wet climate change scenario. The Time Series Toolbox results for 1930-2019 estimated Atchafalaya River discharge suggest an increasing trend over the period of record and on a seasonal basis, and a step increase in flow and flow variability beginning in the mid-1960s/early 1970s. The Vulnerability Assessment tool suggests that the ecosystem restoration business line would be most vulnerable to climate change, and that the dry

climate change scenario and 2085 future time period would affect the greatest number of business lines. The results of the analysis indicate that the SCCL project is located in an area where the emergency management business line may be vulnerable in the future owing to the population within the 500 year floodplain, the projected prevalence of disabled individuals in the area, and the potential for changes to hydrology. Designers of the SCCL project and the residents of the project area should be aware of the potential for increased vulnerability in the future under an emergency management scenario.

Section 7
References

1. Carter, L.M., J.W. Jones, L. Berry, V. Burkett, J.F. Murley, J. Obeysekera, P.J. Schramm, and D. Wear. 2014: Ch. 17: Southeast and the Caribbean. Climate Change Impacts in the United States: The Third National Climate Assessment, J. M. Melillo, Terese (T.C.) Richmond, and G. W. Yohe, Eds., U.S. Global Change Research Program, 396-417. doi:10.7930/J0NP22CB. https://nca2014.globalchange.gov/downloads

2. Döll, P. and J. Zhang. 2010. Impact of climate change on freshwater ecosystems: a global-scale analysis of ecologically relevant river flow alterations. *Hydrol. Earth Syst. Sci. Discuss. 7:1305-1342*

3. Elguindi, N. and A. Grundstein. 2013. An integrated approach to assessing 21st century climate change over the contiguous U.S. using the NARCCAP RCM output. *Climatic Change 117:809-827*

4. Gao, Y., J S. Fu, J.B. Drake, Y. Liu, and J.F. Lamarque. 2012. Projected changes of extreme weather events in the eastern United States based on a high resolution climate modeling system. *Environmental Research Letters 7(4)*

5. Grundstein, A. 2009. Evaluation of climate change over the continental United States using a moisture index. *Climatic Change 93:103-115*

6. Hagemann, S., C. Chen, D.B. Clark, S. Folwell, S.N. Gosling, I. Haddeland, N. Hanasaki, J. Heinke, F. Ludwig, F. Voss, and A.J. Wiltshire. 2013. Climate change impact on available water resources obtained using multiple global climate and hydrology models. *Earth System Dynamics 4:129-144*

7. Jayakody, P., P.B. Parajuli, T.P. Cathcart. 2013. Impacts of climate variability on water quality with best management practices in sub-tropical climate of USA. Hydrological Processes.

8. Joetzjer, E., H Douvile, C. Delire, P. Ciais, B. Decharme, and S. Tyteca. 2013. Hydrologic benchmarking of meteorological drought indices at interannual to climate change timescales: a case study over the Amazon and Mississippi river basins. *Hydrol. Earth Syst. Sci. 17:4885-4895*

9. Kalra, A., T. Piechota, R. Davies, G. Tootle. 2008. Changes in U.S. Streamflow and Western U.S. Snowpack. *Journal of Hydrologic Engineering 13:156-163*

10. Kunkel, K.E., X.Z. Liang, and J Zhu. 2010. Regional climate model projections and uncertainties of U.S. summer heat waves. *Journal of Climate 23:4447-4458*

11. Li, W., L. Li, R. Fu, Y. Deng, H. Wang. 2011. Changes to the North Atlantic subtropical high and its role in the intensification of summer rainfall variability in the southeastern United States. *Journal of Climate 24:1499-1506*

12. Lindstedt, D.M. and E.M. Swenson. 2006. The Case of the Dying Marsh Grass. https://www.aphis.usda.gov/wildlife_damage/nwdp/pdf/Dying%20Marsh%20Grass.pdf

13. Liu, L, Y. Hong, J.E. Hocker, M.A. Shafer, L.M. Carter, J.J. Gourley, C.N. Bednarczyk, B. Yong, and P. Adhikari. 2012. Analyzing projected changes and trends of temperature and precipitation in the southern USA from 16 downscaled global climate models. *Theoretical and Applied Climatology 109:345-360*

14. Liu, Y., S.L. Goodrick, and J.A. Stanturf. 2013. Future U.S. wildfire potential trends projected using a dynamically downscaled climate change scenario. *Forest Ecology and Management 294:120-135*

15. McRoberts, D.B. and J.W. Nielsen-Gammon. 2011. A new homogenized climate division precipitation dataset for analysis of climate variability and climate change. *Journal of Applied Meteorology and Climatology 50:1187-1199*

16. National Oceanic and Atmospheric Administration (NOAA). 2019. State Climate Summaries 149-LA. https://statesummaries.ncics.org/chapter/la/#

17. NOAA. 2020. NOAA National Centers for Environmental Information Mapping Tool. https://gis.ncdc.noaa.gov/maps/ncei/

18. Pryor, S.C., J.A. Howe, and K.E. Kunkel. 2009. How spatially coherent and statistically robust are temporal changes in extreme precipitation in the contiguous USA? *International Journal of Climatology 29:31-45*

19. Scherer, M. and N. Diffenbaugh. 2014. Transient twenty-first century changes in daily-scale temperature extremes in the United States. *Climate Dynamics 42:1383-1404*

20. Small, D., S. Islam, and R.M. Vogel. 2006. Trends in precipitation and streamflow in the eastern U.S.: Paradox or perception? *Geophysical Research Letters 33*

21. Tebaldi, C. 2006. Going To The Extremes: An Intercomparison of Model-Simulated Historical and Future Changes in Extreme Events. *Climate Change 79:185-211*

22. U.S. Army Corps of Engineers (USACE). 2015. Recent Climate Change and Hydrology Literature Applicable to U.S. Army Corps of Engineers Missions – Lower Mississippi River Region 08. Civil Works Technical Report, CWTS-2015-01, USACE, Washington, DC. https://www.usace.army.mil/corpsclimate/Recent_CC_HydrologyLit_Applicable_USACE_Missions/

23. USACE. 2016. *US Army Corps of Engineers Vulnerability Assessment (VA) Tool User Guide (Version 1.1)*. Washington, DC: U.S. Army Corps of Engineers, Climate Preparedness and Resilience Community of Practice.

24. USACE. 2017. Guidance for Detection of Nonstationarities in Annual Maximum Discharges. Engineering Technical Letter No. 1100-2-3. https://www.publications.usace.army.mil/Portals/76/Publications/EngineerTechnicalLetters/ETL_1100-2-3.pdf

25. USACE. 2018. Guidance for Incorporating Climate Change Impacts to Inland Hydrology in Civil Works Studies, Designs, and Projects. Engineering and Construction Bulletin No. 2018-14. https://www.wbdg.org/ffc/dod/engineering-and-construction-bulletins-ecb/usace-ecb-2018-14

26. U.S. Environmental Protection Agency (USEPA). 2016. Climate Change Indicators in the United States, Fourth Edition. EPA 430-R-16-004. Washington, D.C.: EPA Office of Atmospheric Programs, Climate Change Division. https://www.epa.gov/climate-indicators

27. U.S. Global Change Research Program (USGCRP). 2017. Climate Science Special Report: Fourth National Climate Assessment, Volume 1. Washington, D.C.: U.S. Global Change Research Program. https://science2017.globalchange.gov/

28. USGCRP. 2018. Impacts, Risks, and Adaptation in the United States: Fourth National Climate Assessment, Volume II. Washington, D.C.: U.S. Global Change Research Program. https://nca2018.globalchange.gov/

29. Villarini, G., H.A. Smith, G.A. Vecchi. 2013. Changing Frequency of Heavy Rainfall over the Central United States. *Journal of Climate 26:351-357*

30. Wang, H., S. Schubert, M. Suarez, J. Chen, M. Hoerling, A. Kumar A, and P. Pegion. 2009. Attribution of the seasonality and regionality in climate trends over the United States during 1950-2000. *Journal of Climate 22:2571-2590*

31. Wang, J. and X. Zhang. 2008. Downscaling and projection of winter extreme daily precipitation over North America. *Journal of Climate 21:923-937*

32. Xu, X., Liu, W., Rafique, R., K. Wang. 2013. Revisiting Continental U.S. Hydrologic Change in the Latter Half of the 20th Century. *Water resources management 27: 4337-4348*

33. Westby, R.M., Y.Y. Lee, and R.X. Black. 2013. Anomalous temperature regimes during the cool season: Long-term trends, low-frequency mode modulation, and representation in CMIP5 simulations. *Journal of Climate 26, 9061-9076*

34. Zhang, C., H. Tian, Y. Wang, T. Zeng, Y. Liu. 2010. Predicting response of fuel load to future changes in climate and atmospheric composition in the Southern United States. *Forest Ecology and Management 260:556-564*